

THESIS ON MECHANICAL ENGINEERING E74

Environmental Aspects of Oil Shale Power Production

ALAR KONIST

TUT
PRESS

TALLINN UNIVERSITY OF TECHNOLOGY
Faculty of Mechanical Engineering
Department of Thermal Engineering

Dissertation was accepted for the defence of the degree of Doctor of Philosophy in Engineering on May 2, 2013

Supervisors:

Dr. Tõnu Pihu, Lead Research Scientist, Department of Thermal Engineering of TUT

Dr. Indrek Külaots, Senior Research Scientist, Department of Thermal Engineering of TUT / Senior Research Engineer and Lecturer, School of Engineering, Brown University, US

Opponents:

Dr. Jaan Tehver, EnPro Engineers Bureau Ltd, Project Manager, Estonia

Professor, Ron Zevenhoven, Department of Chemical Engineering, Thermal and Flow Engineering Laboratory, Åbo Akademi University, Turku Finland

Defence of the thesis: June 26, 2013 at 11:00
Room No.: VI-441
Tallinn University of Technology,
Ehitajate tee 5, Tallinn, Estonia

Declaration:

Hereby I declare that this doctoral thesis, my original investigation and achievement, submitted for the doctoral degree at Tallinn University of Technology has not been submitted for any academic degree.

Alar Konist

Copyright: Alar Konist, 2013
ISSN 1406-4758
ISBN 978-9949-23-489-9 (publication)
ISBN 978-9949-23-490-5 (PDF)

MEHCHANOTEHNIKA E74

**Põlevkivienergeetika
keskkonnatehnilised aspektid**

ALAR KONIST

CONTENTS

LIST OF ORIGINAL PUBLICATIONS	6
INTRODUCTION.....	7
NOMENCLATURE.....	9
1. LITERATURE REVIEW.....	10
1.1. Oil shale.....	10
1.2. Oil shale reserves.....	13
1.3. Commercial use of oil shales.....	15
1.4. Estonian oil shale.....	15
1.5. Oil shale combustion model.....	17
1.6. Estonian oil shale combustion.....	19
1.7. Environmental impact of Estonian oil shale based power production.....	21
2. EXPERIMENTAL METHODS.....	24
2.1. General.....	24
2.2. Oil shale and biomass co-combustion in a CFB boiler.....	24
2.3. Oil shale pulverized firing.....	25
2.4. Oil shale low-temperature vortex combustion.....	25
2.5. Emissions and trace metals from different combustion technologies.....	26
3. RESULTS AND DISCUSSION.....	28
3.1. Combustion of oil shale and wood chips.....	28
3.2. Chemical composition of ash.....	28
3.3. Ash balance.....	29
3.4. PF and CFB boiler heat balance.....	29
3.5. Flue gas.....	29
3.6. Specific consumption and emission of an energy unit.....	30
CONCLUSIONS.....	32
REFERENCES.....	34
LIST OF AUTHOR'S PUBLICATIONS.....	39
ABSTRACT.....	41
KOKKUVÕTE.....	42
ORIGINAL PUBLICATIONS.....	43
CURRICULUM VITAE.....	125
ELULOOKIRJELDUS.....	127

LIST OF ORIGINAL PUBLICATIONS

This thesis is based on the following papers, which are referred to in the text by their Roman numerals. The papers are reprinted by the generous permission of the publishers and presented at the end of the thesis:

- Paper I. **Konist, A.**, Pihu, T., Neshumayev, D., Külaots, I. *Low grade fuel – oil shale and biomass co-combustion in CFB boiler*. Oil Shale, 30/2S, 2013, xx - xx. Article in press.
- Paper II. **Konist, A.**, Pihu, T., Neshumayev, D., Siirde, A. *Oil shale pulverized firing: boiler efficiency, ash balance and flue gas composition*. Oil Shale, 30/1, 2013, 6 - 18.
- Paper III. Pihu, T., **Konist, A.**, Neshumayev, D., Loosaar, J., Siirde, A., Parve, T., Molodtsov, A. *Short-term tests on firing oil shale fuel applying low-temperature vortex technology*. Oil Shale, 29/1, 2012, 3 - 17.
- Paper IV. Parve, T., Loosaar, J., Mahhov, M., **Konist, A.** *Emission of fine particulates from oil shale fired large boilers*. Oil Shale, 28/1S, 2011, 152 - 161.
- Paper V. Loosaar, J., Parve, T., **Konist, A.** *Environmental impact of Estonian oil shale CFB firing*. Proceedings of the 20th International Conference on Fluidized Bed Combustion. Xi'an, China, May 18-20, 2009, 422-428.
- Paper VI. Arro, H., Pihu, T., Prikk, A., Rootamm, R., **Konist, A.** *Comparison of ash from PF and CFB boilers and behaviour of ash in ash fields*. Proceedings of the 20th International Conference on Fluidized Bed Combustion. Xi'an, China, May 18-20, 2009, 1054-1060.

Author's personal contribution

The contribution of the author to the papers included in the thesis is as follows:

- Paper I, II The main author of the paper. Participating in planning and conducting the experiments. Participating in interpretation of the results. Major role in writing.
- Paper III, IV Participating in planning and conducting the experiments. Participating in interpretation of the results and writing the paper.
- Paper V, VI Participating in planning and conducting the experiments. Participating in writing the paper.

INTRODUCTION

Energy is part of our everyday life. We depend on energy, but we rarely notice it. As long as there are no blackouts, we normally do not think about energy. Oil shale (OS) is Estonia's primary energy resource for achieving energy independence. Approximately 90% of the electricity consumed is produced from oil shale [1-3]. Estonian oil shale belongs to the low-grade fuel group. The total moisture content of the oil shale burned at power plants is 11–15%, and its heating value as received fuel is 8–11 MJ/kg (LHV) [4, 5, Paper III]. The ash content in oil shale can be above 50% [6]. Estonian oil shale is known as a difficult-to-burn fuel because of its specific nature. The high alkali and chlorine content of oil shale ash has caused significant corrosion and fouling problems in existing pulverized firing (PF) units, resulting in decreased availability of boilers. Gaseous emissions, such as CO₂, SO₂ and particulates, have been relatively high from these PF units. In 2004, the circulating fluidized bed (CFB) combustion technology was implemented for Estonian oil shale reducing significantly the above-mentioned problems and emissions. Still, the carbon dioxide emissions remained higher compared to conventional coal fired units. Therefore, until the beginning of the year 2011, oil shale was considered a fading energy resource in open markets.

The Daiichi nuclear power plant disaster in Fukushima has raised major questions regarding the future energy mix and the role of nuclear energy in many countries all over the world. In Europe, several countries have started to revise their energy policies. For example, Germany has made a decision to phase out nuclear power generation in the near future. The central pillars of the new energy policy will be renewable energy and energy efficiency with the additional emphasis on the maximum utilization of existing fossil fuel power plants. In the near future, there seems to be no good alternative to coal-based power for meeting the energy demand. The International Energy Agency noted in its recent report [7] that future energy perspectives and research activities should be focused on HELE (high efficiency low emissions) coal energy and on bioenergy production. Hence, coal and biomass co-combustion is one of the viable options [8]. Estonia has no coal reserves but has an unconventional fuel, namely, oil shale. Energy production from oil shale should be made more environmentally friendly by implementing new technologies. Therefore, it has to be known where technology development stands today and what the emissions and other factors concerning oil shale power production are.

Because fossil fuels are back in the power production business, numerous studies have focused on clean coal technologies, flue gas cleaning systems and co-combustion opportunities.

It is assumed that for Estonia biomass and oil shale, co-combustion can be the quickest, easiest and cheapest way to reduce the environmental impact of oil shale power production [9]. This statement was confirmed in Paper I. Estonia is applying two different combustion technologies for OS power production: PF and CFB technologies. Modification of PF technology for OS is essen-

tial. A recent study describing PF and vortex combustion (VC) technologies [10, 11] is presented in Papers II and III. Certain of the results concerning CFB technology and CFB boiler reliability are presented in the following articles [12-17].

The purpose of this thesis is to determine the existing situation at oil shale fired power plants by presenting the boiler efficiencies, ash flows, ash chemical compositions, specific emissions, fine particulates, trace metals and ash behavior in ash fields of the different combustion technologies [Papers I-VI]. This type of comparative and complex study for Estonian oil shale is unique. This thesis reviews the data from conducted in-situ tests and compares them with previous information. The chemical compositions of the ash formed by the different combustion technologies are compared. The changes in the emissions of all main polluting components in CFB firing compared to PF are analyzed and estimated. This analysis concerns the mass balance of trace metals in the initial fuel and in formed ash; the emissions of PCDD/F, PCB, PAH, and PM_{2.5/10}; and conventional air emissions as NO_x, SO₂, CO₂, CO, HCl, and TSP [Paper V].

The present work is based on in-situ experiments at full-scale OS firing boilers and at ash fields, where the ash is deposited. All analyses are based on international standards.

The objective of this thesis is to determine

- the efficiencies for different boiler types;
- the specific emissions and ash chemical compositions from different OS firing utility boilers;
- the fine particulates and emission levels from different OS firing industrial boilers;
- the trace metals from different OS firing utility boilers;
- the OS ash behavior at ash fields.

NOMENCLATURE

CFB	circulating fluidized bed (combustion technology)
FC	fixed carbon
HELE	high efficiency low emissions
HI	hydrogen index
IM	inert material
LHV	lower heating value, MJ/kg
MCR	maximum continuous rating
OI	oxygen index
OM	organic matter
OS	oil shale
PAH	polycyclic aromatic hydrocarbons
PCB	polychlorinated biphenyls
PCDD/F	dioxins and furans
PF	pulverized firing (combustion technology)
PM	particulate matter
PP	power plant
TOC	total organic carbon
TSP	total suspended particulates
VC	vortex combustion

Ash types:

BT	bottom/furnace ash
INTREX	internal heat exchanger ash
SH-RH	convective superheater and reheater ash
ECO	economizer ash
APH	air preheater ash
ESP I	electrostatic precipitator field No. 1 ash
ESP II	electrostatic precipitator field No. 2 ash
ESP III	electrostatic precipitator field No. 3 ash
ESP IV	electrostatic precipitator field No. 4 ash

Equations:

α	stoichiometric coefficient of oxidation
γ	stoichiometric coefficient of decarbonation
fr	quantity of carbon oxidized into CO and/or CO ₂
g	gas
k	iteration number
k_{CO_2}	extent of carbonate decomposition (ECD)
l	liquid

1. LITERATURE REVIEW

1.1. Oil shale

Oil shales are diverse fine-grained sedimentary rocks that contain a refractory organic material, commonly called kerogen that can be refined into higher calorific fuels or used for generating steam and electricity in direct combustion [5, 18-20]. Oil shales result from the contemporaneous deposition of fine-grained mineral debris and organic degradation products derived from the breakdown of biota. The conditions required for the formation of oil shales include the early development of anaerobic conditions, abundant organic productivity, and a lack of destructive organisms. Oil shales were most likely deposited in bodies of water that were either marine or fresh-water. The depositional environment is estimated to be lakes, deltaic swamps or isolated marine basins. The prevailing climate during deposition is similar to that favorable for coal formation. Oil shales can be classified as the “composites” of tightly bound organics and inorganics [21]. The general composition of oil shales is presented in Figure 1.

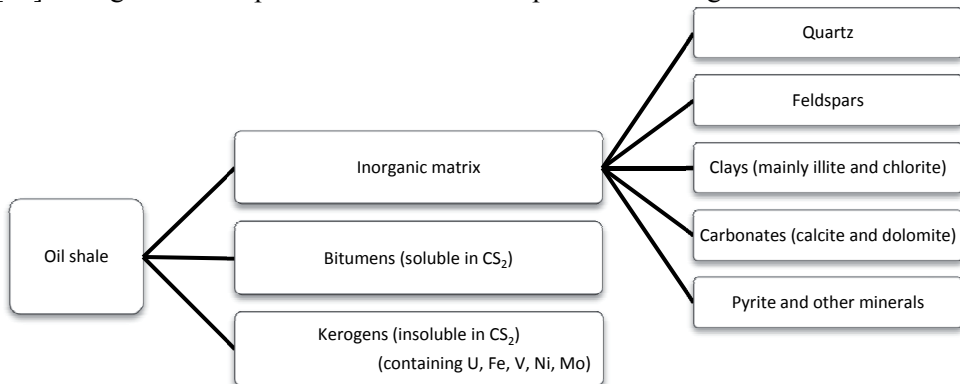


Figure 1. General composition of oil shales [21]

The organic matter in oil shale includes the remains of algae, spores, pollen, plant cuticle and the corky fragments of herbaceous and woody plants, and other cellular remains of lacustrine, marine, and land plants. These materials are essentially composed of nitrogen, hydrogen, carbon, oxygen, and sulfur. In certain type of oil shales, the organic matter is described as amorphous (bituminite). Most of the organic matter in oil shale is insoluble in organic solvents. Today, there is no lower limit on the sapropelic organic matter percentage for oil shales that has been unanimously accepted. The lower limit varies from 5 to 10% and the upper limit from 60 to 70% [22]. The organic matter of oil shale (which is the source of liquid and gaseous hydrocarbons) typically has a higher hydrogen and lower oxygen content than lignite and bituminous coal [23]. However, it has been shown that kerogen predominates in organic matter, and the chemical form or composition of the kerogen may vary extensively from deposit to deposit. This variation is observed because of changes in the amounts of oxygen, hydrogen and organic carbon. Oil shales can be classified according to their kerogen

type using the van Krevelen diagram [24, 25]. The van Krevelen graphic in Figure 2 A shows the kerogen type within a solid fossil fuel through thermal evolution paths as a function of the atomic H/C versus O/C ratios of the kerogen of the burial depths on the deposit. Thus, the kerogen type is classified as a function of the oxygen, carbon and hydrogen content of the fossil fuels [26]. The modified van Krevelen diagram in Figure 2 B with dispersed kerogen consists of hydrogen index (HI) versus oxygen index (OI) plots generated from the pyrolysis and TOC analysis of the whole rock [27].

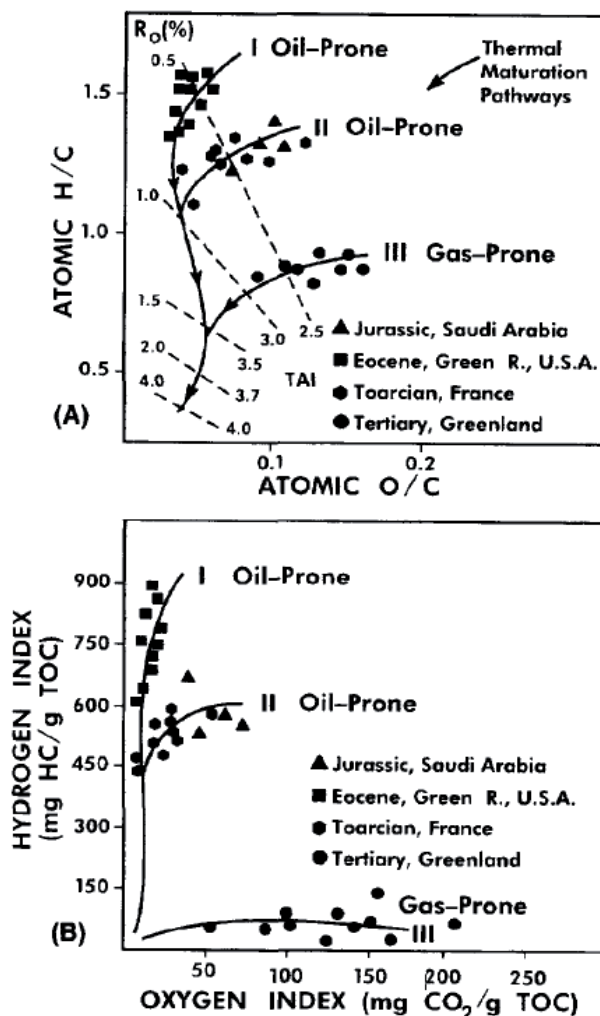


Figure 2. (A) Atomic H/C versus O/C diagram based on elemental analysis of kerogen and (B) HI versus OI diagram based on Rock-Eval pyrolysis of whole rock can be used to describe the type of organic matter in source rocks. TAI, thermal alteration index [28]. The type IV (inertinite) pathway is not shown.

The HI versus OI data can be generated more rapidly than the atomic H/C versus O/C data for van Krevelen diagrams. The relative hydrogen content in

kerogen (atomic H/C, HI) generally corresponds to the oil-generative potential. A higher hydrogen content corresponds to a higher oil yield. Oil and gas (CH₄) are more enriched in hydrogen compared to kerogen. During thermal maturation, the generation of these products causes the kerogen to become depleted in hydrogen and relatively enriched in carbon. During metagenesis and catagenesis, all kerogens approach graphite in composition (almost pure carbon) near the lower left portion of both diagrams in Figure 2 [27].

There are four principal types of kerogens found in coals and sedimentary rocks, which are defined using either atomic H/C versus O/C or HI versus OI diagrams (see Figure 2). These types are divided as follows [27]:

Type I

Immature type I kerogens are oil prone. These kerogens have high H/C (>1.5) and low O/C (<0.1) atomic ratios, as shown in Figure 2, and generally a low sulfur content. The type I kerogens yield a larger amount of extractable or volatile compounds upon pyrolysis. These kerogens are dominated by liptinite macerals. Vitrinites and inertinites can be present in lesser amounts. Type I kerogens appear to be derived from the extensive bacterial reworking of lipid-rich algal organic matter, though not always (e.g., Eocene Green River Formation). Major contributors to type I kerogens can be *Botryococcus* and similar lacustrine algae and their marine equivalents, such as *Tasmanites*.

Type II

Immature type II kerogens are oil prone (e.g., Jurassic of Saudi Arabia). They have high H/C (1.2-1.5) and low O/C atomic ratios compared to types III and IV. Type II kerogens generally have a higher sulfur content compared to other kerogens. Type II kerogens are also dominated by liptinite macerals [27]. Type II S kerogens (e.g., Miocene Monterey Formation) have a high sulfur content (e.g., 8-14 wt. %; atomic ratio S/C > 0.04) and seem to generate petroleum at a lower thermal maturity than other type II kerogens [29, 30].

Type III

Immature type III kerogens have low H/C (<1.0) and high O/C (<0.3) atomic ratios. These kerogens are gas prone because they yield some hydrocarbon gas but little oil during maturation. Type III kerogens yield less gas than types I and II. Type III kerogen is composed from liptinite macerals that may represent only a small portion of the kerogen. Some type III kerogen thick deltaic deposits have generated substantial oil (e.g., Mahakam Delta in Indonesia, U.S. Gulf Coast, and offshore West Africa).

Type IV

Type IV kerogen, also called "dead carbon," has very low H/C (approximately 0.5-0.6) and low to high O/C (<0.3) atomic ratios. Type IV kerogens are dominated by inertinite macerals that generate little to no hydrocarbons during maturation. Type IV kerogens can be derived from other kerogen types that have been reworked or oxidized [31].

Another option to characterize the kerogen types of oil shale is by their depositional history, including the organisms from which they were derived [32]. Major factors that determine the extent and nature of the organic and mineral

content and relative quality of any deposit are the age and depositional history [26].

Bitumen in oil shale is the fraction of the organic matter that is soluble in organic solvents. Most bitumen is generated by cracking (thermal dissociation) of the kerogen, but small amounts of bitumen originate from the lipid components in once-living organisms [27].

The mineral content of oil shales usually contains large amounts of inert mineral matter (60–90%). The mineral matter of some oil shales is composed of carbonates, including siderite, dolomite and calcite, with lesser amounts of aluminosilicate minerals. Silicates including quartz, feldspar, and clay minerals are dominant, and carbonates are a minor component in other types of oil shales, [23]. The extent and nature of the inorganic materials mainly depend on the depositional conditions and the characteristics of the host rock. For instance, the well-known Green River oil shale contains mainly carbonates with quartz, feldspars and illite, while typical oil shales contain primarily clay minerals [26].

1.2. Oil shale reserves

Oil shales are found in more than 44 countries [20]. There are over 600 known deposits [33], which range from early Palaeozoic to Cenozoic in age. The reserves of oil shale in the world are immense, exceeding the total resources of all other solid fuels (coal, lignite, brown coal). The most resources are found in the USA (72%), Brazil (5.4%), Jordan (4.2%), Morocco (3.5%) and Australia (2.1%) [22]. The estimated total world oil shale resource increased from 411 to 690 billion tons in 2010. This estimate should be taken as the lower limit because numerous deposits are still largely unexplored, and a number of countries are not reported [19, 34].

The properties of oil shale depend strongly on the deposit. It is difficult to find two analogous oil shales, mainly because of their extremely variable deposition conditions, as well as post-sedimentation alterations. Furthermore, the composition and quality of oil shales also vary within the limits of one deposit. Depending on the character of the deposit, there could be considerable variations among the results obtained by an analysis of different samples taken from the same deposit [22]. The typical properties of certain important oil shales are outlined in Table 1 [24]. These deposits are characterized by their age, the organic carbon of the organic matter, and the oil yield. The H/C atomic ratio of kerogen evaluates the quality of organic matter in source rocks.

Table 1. Properties of several important oil shale deposits [26]

Country	Location	Age	Oil shale		Kerogen (atomic ratio)		Retorting			Shale oil		
			Organic carbon, %	H/C	O/C	Oil yield, %	Conversion ratio, %	Density (15°C)	H/C (atomic)	N, %	S, %	
Australia	Glen Davis	Permian	40	1.6	0.03	31	66	0.89	1.7	0.5	0.6	
Australia	Tasmania	Permian	81	1.5	0.09	75.0	78					
Brazil	Irati	Permian		1.2	0.05	7.4		0.94	1.6	0.8	1.0-1.7	
Brazil	Tremembé-Taubaté	Permian	13-16.5	1.6		6.8-11.5	45-59	0.92	1.7	1.1	0.7	
Canada	Nova Scotia	Permian	8-26	1.2		3.6-19.0	40-60	0.88				
China	Fushun	Tertiary	7.9			3	33	0.92	1.5			
Estonia	Estonia Deposit	Ordovician	77	1.4-1.5	0.16-0.20	22	66	0.97	1.4	0.1	1.1	
France	Autun, St. Hilaire	Permian	8-22	1.4-1.5	0.03	5-10	45-55	0.89-0.93	1.6	0.6-0.9	0.5-0.6	
France	Crevenay, Severac	Toarcian	5-10	1.3	0.08-0.10	4-5	60	0.91-0.95	1.4-1.5	0.5-1.0	3.0-3.5	
S. Africa	Ermelo	Permian	44-52	1.35		18-35	34-60	0.93	1.6		0.6	
Spain	Puertollano	Permian	26	1.4		18	57	0.90		0.7	0.4	
Sweden	Kvamtorp	Lower Paleozoic	19			6	26	0.98	1.3	0.7	1.7	
UK	Scotland		12	1.5	0.05	8	56	0.88		0.8	0.4	
USA	Alaska	Jurassic	25-55	1.6	0.10	0.4-0.5	28-57	0.80				
USA	Colorado	Eocene	11-16	1.55	0.05-0.10	9-13	70	0.90-0.94	1.65	1.8-2.1	0.6-0.8	

¹ Conversion to oil based on organic carbon

The gross heating value of oil shales on a dry-weight basis ranges from 2.1 to 16.8 MJ/kg of rock. The high-grade kukersite oil shale of Estonia, which fuels several power plants, has a heating value of approximately 8.0 to 9.2 MJ/kg. By

comparison, the heating value of lignitic coal ranges from 14.7 to 19.3 MJ/kg on a dry, mineral-free basis [19].

1.3. Commercial use of oil shales

Today, five countries in the world are commercially mining oil shale. Estonia has an annual output of 15 million tons, China of 10 million tons, Brazil of 2.5 million tons, Russia of 1.3 million tons and Germany of 0.3 million tons. The total oil shale output amounts in Table 2 are given in millions of tons based on 2007/2008 data. Australia is left out because they have stopped oil shale utilization. The total amount of oil shale utilized in Australia from 1999 to 2003 was 1 million tons [20].

Table 2. World's total oil shale output until 2008 in millions of tons

Country	Estonia	China	Russia	Brazil	Germany	Total
Mining started	1916	1930	1934	1980	1943	
Cumulative	1026.0	630.0	227.3	49.5	11.3	1944.1

Estonia's oil shale output is the largest in the world. Most of the oil shale, approximately 12 million tons yearly, is used for power generation, and approximately 2 million tons are used for retorting to produce shale oil. Oil shale in China and Brazil is mainly utilized for retorting. German oil shale is utilized for power generation and for cement production.

1.4. Estonian oil shale

Estonian oil shale, kukersite, is a low-grade fuel, approximately 33% of which contains mainly kerogenous organic matter. The oil shale's chemical composition is presented in Table 3 [35].

Table 3. Average elemental composition of Estonian oil shale distributed between organic, sandy-clay and carbonate fractions, wt% (dry matter). Ca/S* is the molar ratio. The sandy-clay part is composed of clay minerals, quartz and feldspars [35]

Organic (%)		Sandy-clay (%)		Carbonate (%)	
C ^d	23.36	SiO ₂ ^d	15.16	CaO ^d	21.38
H ^d	2.93	CaO ^d	0.18	MgO ^d	2.94
S ^{d_o}	0.53	Al ₂ O ₃	4.08	FeO ^d	0.09
N ^d	0.10	Fe ₂ O ₃ ^d	0.71	CO ₂ ^d carbonate	20.06
Cl ^d	0.23	TiO ₂ ^d	0.18	Sum, K ^d	44.47
O ^d	3.02	MgO ^d	0.10		
Sum, R ^d	30.17	Na ₂ O ^d	0.20		
		K ₂ O ^d	1.60		
		FeS ₂ ^d	2.36		
		SO ₃ ^d	0.13		
		H ₂ O ^d	0.66		
		Sum, L ^d	25.36		
Average oil shale					
S _{total}					1.5
Ca _{carb}					13.6
Ca/S*					9.0

The oil shale deposits in Estonia are of national and regional importance, being the world's largest exploited deposit of oil shale. Mining started in 1916, and there has been continuous exploitation since 1919. The reserves of the deposit are completely explored. At present, approximately one billion tons of oil shale has been mined. According to the present assessment, the total amount of resources is five billion tons [36, 37]. The oil shale bed is not homogeneous but has a complicated structure that consists of oil shale layers of different qualities that lie alternately with limestone interlayers. The maximum bed thickness occurs in the Jõhvi–Kohtla-Järve area. To the west, south and east, the thickness of the oil shale layers, as well as the thickness of the entire bed, decrease. The total thickness of the payable bed in the Estonian field is 2.5–3.2 m; oil shale layers account for 1.8–2.6 m, and limestone layers account for 0.6–0.7 m. The payable oil shale layers in the Estonian field are located to the east of Kadrina, extending to the Narva River. Further to the east, the total thickness of the oil shale bed in the Leningrad field is 1.6–1.9 m, of which 1.0–1.3 m is oil shale. On the northern coast of Estonia, the oil shale layers outcrop onto the earth's surface. To the south, in the direction of Peipsi Lake, the depth of the bed increases by 3.5 m/km [38, 39]. Figure 3 shows the general profile of the Estonian oil shale field and the average heating values of the layers. The capital letters mark the oil shale layers, beginning with the lowest layer. The payable layers are A–F [39].

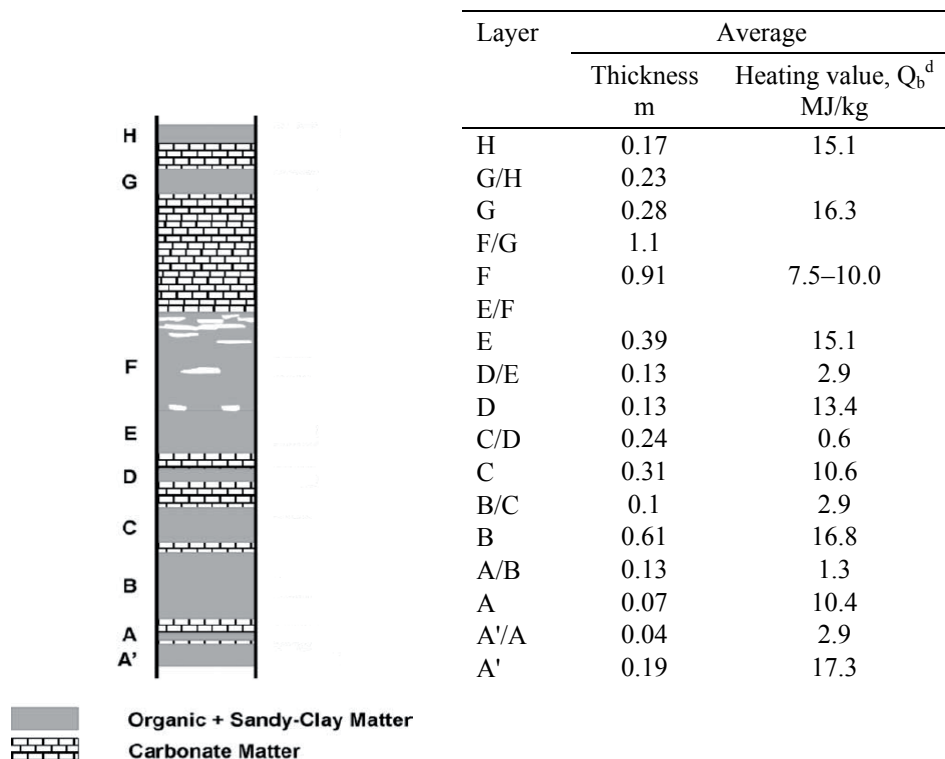


Figure 3. Profile of Estonian oil shale bed and the characteristics of oil shale layers [39]

Estonian kukersite oil shale seams contain organic matter, carbonate and clastic materials in various proportions. The carbonate material consists mainly of pore-filling micritic carbonate mud together with a variable content of fine to coarse skeletal debris. The carbonate content (mainly calcite) ranges in different kukersite seams from 20 to 70%, and the organic matter content varies from 10–15% to 50–60%. The clastic matrix is composed mainly of silt-size quartz and illite, and the minor clastic minerals are feldspars and chlorite. Pyrite is a rather common authigenic mineral in kukersite oil shale [40]. The organic matter of Estonian oil shale (kerogen) represents a mixture of high-molecular poly-functional organic compounds, the detailed structure of which is still being studied [36]. The molar ratio of Ca to S is typically greater than 5 and can be as high as 10. This property means that the fuel itself contains the excess Ca needed to capture the SO₂ that evolves during firing. As a disadvantage, the ash content remaining after power generation is approximately 45% on a dry mass basis. Today, approximately 5–7 million tons of oil shale ash is produced annually, and more than 90% of the same ash is wet deposited in the ash fields next to the oil shale fired power plants.

In fact, Estonia has two different oil shales: kukersite and graptolitic argillite, also known as Dictyonema argillite or Dictyonema shale. The latter is a dark, blackish- or greyish-brown fine grained radioactive claystone with a low organic matter content (15 to 20%) and heating value (4.2–6.7 MJ/kg). Argillite is the thickest shale (more than 4 m), and there are an estimated 60 billion tons of it [41]. Argillite contains several rare elements, including molybdenum (up to 600 g/t), vanadium (up to 1,200 g/t) and uranium (up to 300–400 g/t). From 1948 to 1977, uranium ore was processed at Sillamäe in NE Estonia for the production of uranium [42]. Some 250,000 tons of ore were unearthed, and more than 60 tons of uranium compounds were produced. This processing waste still poses a threat to environment. Later, the Sillamäe plant switched to processing imported raw material [22].

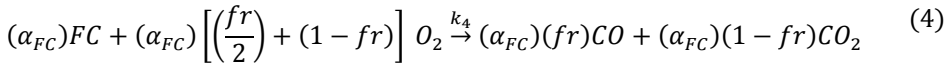
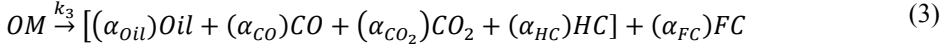
1.5. Oil shale combustion model

Despite oil shale's complex chemical composition and kinetic behavior, experimental evidence suggests that a mechanism consisting of only a few global reactions would capture the most important characteristics of the combustion process [43]. A six-step mechanism for oil shale is suggested to describe the thermal decomposition [44]. The presence of a wide variety of minerals in the oil shale matrix significantly complicates its thermal behavior. As a consequence, a variety of reactions is brought about by the application of heat under an oxidative atmosphere on the oil shale samples. In general, the following reactions can potentially exist for oil shale [43]:

- water vaporization;
- dry matter volatilization – conversion of organic matter into volatile matter and fixed carbon;
- volatile matter dissociation into bitumen and gases;

- volatile matter oxidation;
- fixed carbon oxidation;
- carbonate mineral decomposition into solid residue and gases.

Based on research results presented in [44], a four-step mechanism for oil shale combustion is proposed [43] and is shown in Eqs. (2)–(5). The overall reaction is given in Eq. (1). Inert materials that are present in the kinetic mechanisms are not taken into consideration in the estimation process.



The three main constituents of OS that decompose are organic matter, fixed carbon and carbonates. Consequently, the major breakdown mechanism in OS is the scission of the atomic bonds available in their compounds. The devolatilization reaction of organic matter (OM), Eq. (3), releases oil (bitumen), CO, CO₂, and light hydrocarbons represented by HC, leaving fixed carbon (FC) in the solid matrix. In the oxidation reaction, Eq. (4), the FC is oxidized, releasing CO and CO₂. In Eq. (5), the decarbonation reaction, the carbonate considered is essentially CaCO₃, which decomposes into quick lime and additional CO₂. The process of drying is described by the approach that represents a heterogeneous reaction between liquid water and vapor, Eq. (2). Solid residue remains as an inert material (IM), Eq. (6) [43].

The combustion behavior of oil shale shifts from homogeneous to heterogeneous during the entire combustion process. During the low-temperature stage, the combustible matter is made up of volatiles. In the high-temperature stage, the combustible matter includes fixed carbon and residual volatiles [45].

- *Homogeneous combustion stage (280 – 500 °C)*

In a mathematical model of OS homogeneous combustion, the following assumptions are made:

(a) During combustion stage, large amounts of mineral matter may help the particles of oil shale maintain their original size [46].

(b) The diffusion rates and combustion volatiles within OS are infinite. The combustion reaction is controlled by the pyrolysis rate of the volatile matter.

(c) The distribution of the volatile matter within a particle is uniform.

(d) The Nusselt number of convective heat transfer between the solid phase and the gas phase is equal to 2 according to the experimental results of [47-49].

The homogeneous combustion process has been mathematically modeled on the basis of these assumptions, where the model includes four equations: the energy equation of the gas phase, the energy equation of the solid phase, the kinetic

equation and the particle density equation [50]. The pyrolytic heat value of volatile matter is also considered in the energy equation because of the high content of volatile matter [45].

- *Heterogeneous combustion stage (620 – 730 °C)*

In a mathematical model of OS heterogeneous combustion, the following assumptions are made:

(a) During combustion, large proportions of ash may help the particles of oil shale maintain their original size [46].

(b) Volatile matter and carbonates pyrolytic heat is negligible.

(c) CO₂ should be the main product of carbon combustion because the temperature is not high. It is assumed that the heterogeneous reaction is of first order and that the combustion form of char is described as $C + O_2 = CO_2$.

(d) The temperature distribution inside the solid particle is uniform.

(e) The solid particles are heated only by the reaction heat from the volatile combustion.

The heterogeneous combustion process has been modeled on the basis of these assumptions, where the heterogeneous combustion model includes four equations: the kinetic equation of a heterogeneous reaction, the kinetic equation of a homogeneous reaction, the energy equation of a solid phase and the particle density equation [50]. The inner surface area of a fuel particle is notably important for char combustion based on previous experimental results [51] because the devolatilization in the low-temperature stage makes an OS particle multiporous. Therefore, the inner area of particle, as one of the reaction interfaces, should be considered in the kinetic equation of a heterogeneous reaction [45].

1.6. Estonian oil shale combustion

Oil shale volatile matter and char combustion can occur concurrently in a system consisting of particles of different size because the particle size influences the heating rate and the release intensity of volatiles. Oil shale burning in the pulverized oil shale flame requires no more than 15 to 20 percent of the total burning-out time, despite the high volatile matter content. The remainder of the time is required for char combustion. Approximately 80 to 90 percent of the total heat in fuel is released in the zone of volatile matter combustion. Oil shale char burns in a kinetically controlled low-temperature regime. The density of combustible matter is uniform in a particle, and oxygen has free access to the inside of a particle. The particle size does not affect the combustion kinetic rate. The combustion rate decreases over time because of changes in the active pore sizes within the particle [5].

Oil shale burned in power plants has the following proximate characteristics: $W_i^f = 11\text{--}13\%$, $A^f = 45\text{--}57\%$, $CO_2 = 16\text{--}19\%$, and $Q_i^f = 8.3\text{--}8.7$ MJ/kg [6].

There are three common combustion technologies that have been used for the combustion of oil shale: (1) grate firing, (2) pulverized firing and (3) fluidized bed combustion [5]. Fluidized bed combustion is typically divided into three modes: (a) bubbling fluidized bed, (b) circulating fluidized bed and (c) pressurized fluidized bed. During the 1980s, an attempt was made for modified low-

temperature pulverized firing called Vortex combustion, which was tried again in year 2010, but this technique did not give the presumed results [Paper III].

Long-term experience in oil shale usage has proven that [18]

1. Regardless of the combustion technology, a special boiler has to be designed and constructed for oil shale combustion.
2. The direct combustion of OS for power production is more reasonable.
3. Low-temperature combustion is a preferable technology for oil shale-based power production. CFB combustion at atmospheric pressure is a good example.

Initially, Estonian oil shale was used as a fuel in locomotives. Thereafter, more and more lump oil shale was burned in industrial boilers [6, 52].

The utilization of oil shale for power production in Estonia started at the beginning of the 1920s, when the first lump oil shale was fired on grate. The key problem with firing oil shale rich in volatile matter is ensuring soot-free combustion. This issue was successfully solved by designing a special type of grate. Soon, the exploitation of fine oil shale started as well [18]. An important milestone in the history of the oil shale power industry was the start of oil shale firing at the Tallinn Power Plant in 1924. The electrical capacity of the Tallinn Power Plant was 23 MW. This year can be considered the start of the oil shale power industry. The latest designs of oil shale grate-fired boilers were characterized by a furnace completely covered with waterwall tubes; evaporator tube bundles with large heat-delivery surface areas were located at the tubes' exits. Grate firing lost its importance because of its limited capacities and low steam parameters [5].

The next stage was the introduction of oil shale PF technology. The first power plant using oil shale PF technology was the Kohtla-Järve Power Plant. This plant was commissioned in 1949 and had the designed electrical capacity of 48 MW. The Ahtme Power Plant began operation in 1951 and had an electrical capacity of 75.5 MW. Steam boilers at these power plants were slightly modified because the medium-pressure boilers were initially designed for the PF of coal or brown coal combustion [6].

From 1959 to 1965, the first high-pressure PF boilers, TP-17, were launched at the Balti Power Plant (BPP). They were specially designed for firing oil shale. TP-17 was equipped with four direct flow corner burners. The steam pressure was 9.8 MPa and the steam production 190 t/h. TP-17 was soon followed by TP-67, in which front wall-fixed turbulent burners were used. The steam pressure was 13.8 MPa and the steam production 280 t/h [18]. The designed electrical capacity of the BPP was 1624 MW. The first power unit at the Eesti Power Plant (EPP) was inaugurated in 1969 and had a steam pressure of 13.8 MPa and a steam production of 320 t/h [18]. The designed capacity of the power plant was 1610 MW. In Estonia, a total of 42 PF oil shale boilers, including TP-17, TP-67 and TP-101, were launched at oil shale power plants in 1959-1973 [53]. During the PF of oil shale, the temperature in the furnace can reach 1350 to 1400 °C [Paper III].

Oil shale-fired pulverized furnaces and grate-fired furnaces have high-temperature corrosion, environmental pollution and slag-bonding problems [54].

Oil shale-fired bubbling fluidized beds have scale-up problems regarding the boiler capacity and a high carbon content in the fly ash. Several specialists recommend burning oil shale in a CFB boiler, which produces a satisfactory combustion efficiency and low NO_x and SO₂ emissions [45].

Based on previous research, at the beginning of 2004, a power unit with an electrical capacity of 215 MW with two CFB boilers was put into operation at the EPP. Months later, a power unit of the same type was put into operation at the BPP. The units are designed to produce 90 kg/s of superheated steam at a pressure of 13.1 MPa and a temperature of 540 °C and reheat steam at 2.7 MPa pressure. The load range is from 40 to 100% of the maximum continuous rating (MCR) [55]. During CFB firing, the temperatures are lower compared to PF. The temperature in the furnace during fluidized bed combustion is between 750 and 850 °C, and the typical temperature is below 800 °C.

1.7. Environmental impact of Estonian oil shale based power production

Today, approximately 5–7 million tons of oil shale ash is formed annually by PF and CFB combustion boilers. Currently, less than 10% of the oil shale ash has a beneficial utilization in the construction material industry (e.g., making Portland cement and gas-concrete), in the road construction industry (stabilization of roadbeds) and in agriculture (e.g., liming of acid soils). The relatively high calcium sulfate content in CFBC ash limits its utilization in the construction material industry and in road construction. The rest of the oil shale ash is wet deposited in the ash fields next to the power plants. In total, more than 280 million tons of ash has been deposited in ash fields since the 1950s. The transport and deposition of these large amounts of ash are managed hydraulically at low ash-water ratios of approximately 1:20. The total area of settling ponds and open return flow channels of the ash handling systems is 1,312,000 m² BPP and 3,014,000 m² EPP [56]. Experience with ash field exploitation has indicated that the ash binds water at approximately 0.6–0.7 m³ per ton of ash. The water in the ash fields is lost because of evaporation but is also gained because of precipitation. The average atmospheric precipitation in Estonia is 550–750 mm per year. Approximately half of it is lost because of evaporation [35].

The properties of the PF ash stored at ash fields have been investigated in [57, 58]. The changes in the properties of moistened PF ash in laboratory conditions have been investigated in [59]. The results of XRD analyses show in X-ray spectra the peaks belonging to the portlandite, α -quartz, calcite and ettringite. The ash field material also contains small extents of several silicates, Ca-aluminates and other minerals. The differences in the CFB and PF ash properties have been investigated earlier. It was found that ashes formed in boilers operating by different combustion technologies differ significantly by their chemical and phase composition as well as by their surface properties [60]. The introduction of CFB combustion has caused several important changes in the mineralogical composition and properties of oil shale ash. The reason is that the CFB boiler furnace firing temperature is approximately 600 °C lower than in the PF coun-

terpart, resulting in weaker fuel mineral decomposition and lower novel mineral formation intensity during combustion. In this case, the ash sintering tendency is substantially weaker than that observed in PF ash. The measured compressive strength of oil shale ash from the CFB boiler ESP is 4.4 N/mm^2 . The compressive strength of oil shale ash from the PF boiler ESP is approximately fourfold higher – 15.3 N/mm^2 . The corresponding specific surface areas (Blaine method) were $4,533\text{--}9,806 \text{ cm}^2/\text{g}$ and $707\text{--}3,966 \text{ cm}^2/\text{g}$ [Paper VI].

The ash properties and behavior at the ash fields have changed because of the low combustion temperature in the CFB boiler. The formation of novel minerals with binding properties in CFB ash is much lower compared to PF ash, in which solidification is low. Because of lower temperatures compared to PF boilers, the fuel mineral decomposition and novel mineral formation occurs at a lower rate in CFB boilers. Furthermore, the CFB ash contains less $\beta\text{-}2\text{CaO}\cdot\text{SiO}_2$ and CaO in free form and in less of a glassy phase. The low activity of the CFB ash might be the main reason for the inefficient solidification processes in the ash fields. The obtained data confirmed that if the share of PF ash decreases, there is a need to alter the ash storage technology/methods [Paper VI]. Dry handling of ash in powerplants is the key to find the future utilization markets for this vast amount of ash still landfilled in Estonia. Wet removal of ash poses a threat to Estonian environment and removes the ability to beneficially use this, perhaps valuable, byproduct of power generation

In these ash fields, the highly alkaline wet ash and ash transportation water continue to absorb CO_2 from the atmosphere. Therefore, these OS ash fields act as CO_2 sponges by capturing some of the released CO_2 back from the atmosphere. This process is independent of power plant load. The dynamics and the extent of CO_2 capture from the atmosphere by OS ashes formed in PF and CFBC boilers were investigated in [56]. The baseline data for the further calculations were taken from the sampling and determination of the CO_2 content in the ash field material. The chemical analysis results of ash samples drilled out at the site are normalized to water- and CO_2 -free ash content. The difference of the CO_2 content (ΔCO_2) in the ash field material from the total boiler ash CO_2 content shows the amount of CO_2 captured from the surrounding atmosphere [56].

The emitted quantities of CO_2 from the PF and CFB boilers were estimated based on an average heating value of 8.45 MJ/kg . The CO_2 absorption coefficients in the ash field in the case of CFB technology have been calculated to be 0.07 t and in the case of PF technology 0.03 t per ton of fuel. On the ash field, the ash of the CFB boiler binds 8.1% and the PF boiler ash 3.2% from the emitted CO_2 . The tests of CO_2 absorption by alkali water showed that the total surface of settling ponds can absorb up to 50 thousand tons of CO_2 annually. Considering the share of the PF and CFB firing technologies used in the Estonian oil shale power plants and taking into account the total surface area of the sediment ponds, the quantity of CO_2 that could be absorbed is approximately $5\text{--}6\%$ of the emitted CO_2 [56, 61].

Besides CO_2 , the main air pollutants formed during the combustion of oil shale are sulfur dioxide (SO_2), nitrogen oxides (NO_x) and solid particles. Never-

theless, the most substantial greenhouse gas emitted to atmosphere is carbon dioxide (CO₂). The concentration of air pollutants in flue gas depends primarily on the combustion technology and the burning regime, while the emission of solid particles is determined by the efficiency of fly ash capturing devices.

One of the biggest environmental impacts of oil shale PF is a high SO₂ emission (despite the high calcium to sulfur [Ca/S] molar ratio in the fuel). The molar ratio of Ca to S is typically greater than 5 and can be as high as 10. This means that the fuel itself contains the excess Ca needed to capture all the SO₂ that is emitted during firing [35]. The flue gas of the typical oil shale PF boiler contains more than 1,500 mg/Nm³ of SO₂ in spite of the binding of 80% of fuel sulfur by the ash in the boiler. The sulfur captured by the ash depends on the following parameters: the composition of the fuel, particle size distribution, the temperature regime (i.e., temperature profile in the gas pass of the boiler, combustion technology), the oxygen partial pressure in the flue gas and the duration of the sulphation process [62]. A high SO₂ emission in a PF boiler is mainly caused by the formation of calcium compounds of low reactivity in the high temperature medium in the furnace. These sintered compounds, which contain calcium oxide (CaO), have a low sulfur capturing capability [5]. The average particulate content in flue gas is approximately 1,500–2,000 mg/Nm³. Currently, the power plants are equipped with new electrostatic precipitators, and the particulate content in flue gas is under 100 mg/Nm³ [39]; with fabric filters, the content of particulates is less than 2 mg/Nm³. The NO_x content in flue gas is between 300–400 mg/Nm³ for the PF technology.

The environmental impact of CFB is lesser than that of PF. A lower temperature in oil shale CFB firing favors the capturing of sulfur. The concentration of SO₂ in the flue gas is almost negligible because almost 100% of the sulfur is bound by the free CaO in the ash [13]. Therefore, there is no need to add sorbent (limestone) into the fluidized bed for sulfur capture. This reaction is one of the key advantages of oil shale CFB combustion [5].

A comparative study of the fly ash originating from CFB combustion and the PF technology conducted by Kahru and Põllumaa showed that CFB fly ash was less toxic than that of PF [33]. Thus, a complete transfer to CFB technology will reduce (a) the atmospheric emission of hazardous trace elements and (b) the fly ash toxicity to aquatic organisms compared to PF technology [63].

Oil shale combustion in the circulating fluidized bed entails further opportunities for development. Reducing CO₂ emissions requires looking for new solutions. CFB combustion allows the burning of oil shale together with coal, wood chips and peat without a major modification of the boiler. The BPP has achieved success in the co-combustion of oil shale and wood chips. The new 300 MW power unit under construction will enable co-burning oil shale with up to 50% biomass [18].

2. EXPERIMENTAL METHODS

2.1. General

Full-scale experiments were conducted on high-pressure CFB and PF boilers. Tests were conducted according to international standards. The major goal of the tests was to determine the boiler efficiencies, flue gas composition, solid particulates and chemical composition of the ashes from different types of boilers.

Because many modifications have been made to the PF boiler flue gas cleaning systems during the last decade, the ash distribution data at different ash discharge ports were obtained. This enables the chemical composition of the total ash flow going to the ash fields to be evaluated.

2.2. Oil shale and biomass co-combustion in a CFB boiler

The major goal of OS and biomass co-combustion in CFB boiler tests was to perform the analyses of ash and flue gas as well as to determine the boiler efficiency. The tests were carried out with the following fuel shares (as the thermal input): 85% OS and 15% wood chips.

During the tests, analyses of the fuel, ash and flue gas were performed. Fuel samples were taken on a daily basis. The ash samples were taken from several ports located in the furnace chamber, INTREX, super-/reheater (SH, RH), economizer (ECO), air preheater (APH) and from all four fields of the electrostatic precipitator (ESP). The sampling points are shown in Figure 4. The ash was taken from the dry flow to ensure the representativeness of samples. To determine the mass division (total suspended particulates PM10 and PM2.5), samples of fly ash were taken after the ESP. The samples were used to determine the detailed chemical composition of the ash.

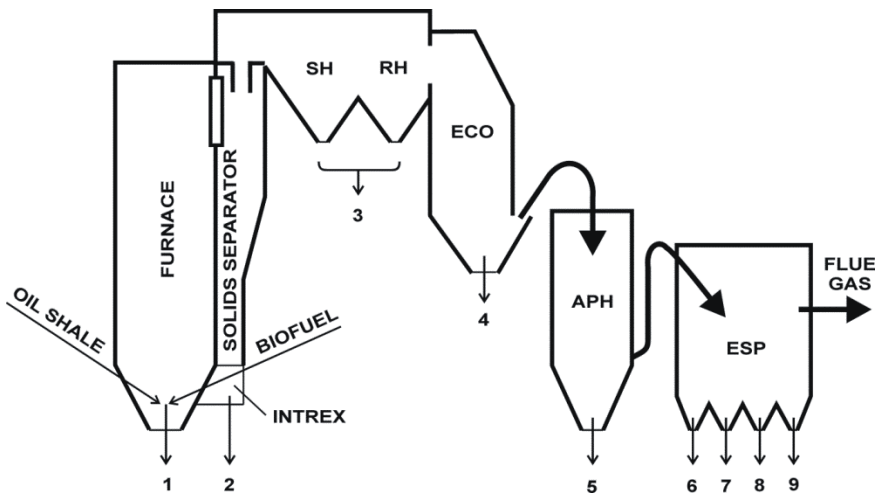


Figure 4. Schematic diagram of CFB boiler system with sampling points [Paper I]

In the tests, the boiler efficiency was calculated. The temperature and composition of the flue gas were measured before the ESP.

2.3. Oil shale pulverized firing

During pulverized firing, the major goal of the tests was to perform analyses of the ash and the flue gas, as well as to verify the data of the flue gas composition, ash balance and boiler efficiency obtained in the 1980s. The essential auxiliaries of the energy unit were registered. During the tests, analyses of the fuel, ash and flue gas were performed. Fuel samples were taken on a daily basis. The ash samples were taken from several ports located in the furnace chamber, SH, ECO and cyclone and from all three fields of the ESP. To determine the mass division (TSP PM10 and PM2.5), samples of the fly ash were taken before the induced draft (ID) fan. The sampling points are shown in Figure 5. The results of the sample analyses were averaged to reach a representative estimate. Furthermore, during the tests, the major process parameters of the boiler and unit as a whole were recorded using the plant's standard data acquisition system to determine the unit's electricity self-consumption. The temperature and composition of the flue gas were measured before the ID fan on both sides of the boiler. The analysis of the combustion gas was carried out from the ports behind the ESP. The same ports were used for taking fly ash samples to determine the division of the finest particles in the flue gas.

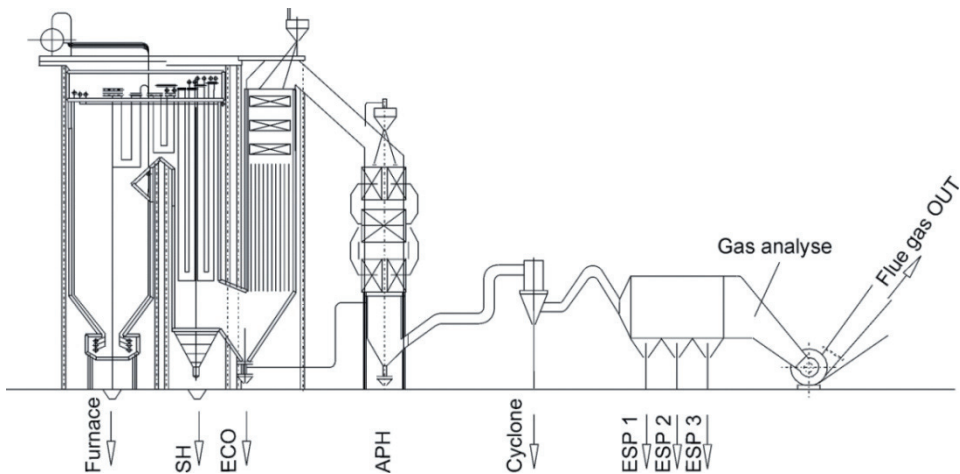


Figure 5. Schematic of PF boiler TP-101 with sampling points [Paper II]

The composition of the flue gas was determined applying an FTIR type analyzer for wet gas at a temperature of 180 °C. The flue gas moisture content was also determined by a FTIR spectrometer.

2.4. Oil shale low-temperature vortex combustion

The full-scale experiments were carried out on a high-pressure boiler, TP-67, at the BPP. For the generation of a low-temperature horizontal vortex motion in the combustion chamber, a set of modifications were made for the tests. The modifications included replacing the vortex burners that were located on the boiler wall at the lower row with direct-flow burners with a downward slope. The opening

of the combustion chamber throat along the entire width of the lower forced draft was performed by mounting two-stage deflection-nozzle devices.

The main parameters of the boiler were as follows: a boiler load (live steam) of 280 t/h, a live steam pressure of 13.8 MPa and a temperature of 515 °C.

During the experiments, samples of the bottom ash and fly ash from the inertia dust collectors after the SH and ECO and from the ESP first and second fields were taken from both the left and the right sides of the boiler. The sampling points are depicted in Figure 6.

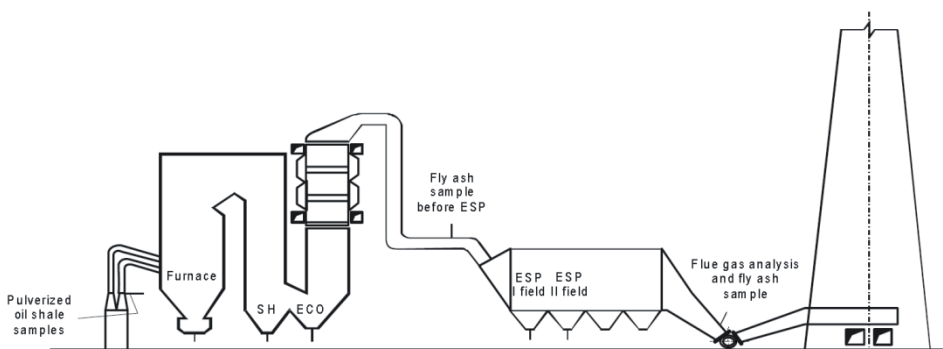


Figure 6. Schematic of PF boiler TP-67 with sampling points (Paper III)

To determine the modified boiler ash balance, the ash mass flow rates in the ash discharge ports were found experimentally. The ash mass flow of the dust collectors located under the SH and ECO were determined by a slurry method that consisted of measuring the time required to fill the calibrated volume with slurry and measuring the slurry mass. The mass flow of the fly ash entering the ESP was obtained by measuring the fly ash content in the flue before the ESP. The flue gas analysis was performed after the ESP using the FTIR type gas analyzer.

2.5. Emissions and trace metals from different combustion technologies

Samples to determine PAH, PCDD/F, and trace metals were collected following the respective standards, CEN 1948:1999, parts 1-3; CEN 14385:2004. A quantitative determination of PCDD/PCDF, PCB and PAH was provided by the laboratory of Ecochem a.s. in Prague.

Fine particulate (PM_{2.5/10}) emissions were measured at the PF and CFB boiler types. There were no former data about these emissions from oil shale fired boilers. The high health risks related to the fine particulates in the air are well known, and stricter requirements on the control and reduction of these emissions are introduced at present. PM_{2.5/10} emissions were determined with a Johnas II type cascade impactor system from Paul Gothe GmbH. Sampling standards CEN 13284-1 and VDI 2066 were followed. Samples were fed into circular 50 mm quartz fiber filters of type MK 360 of Munktell (catching efficiency of 99.998 % at a cutsize of 0.3 µm).

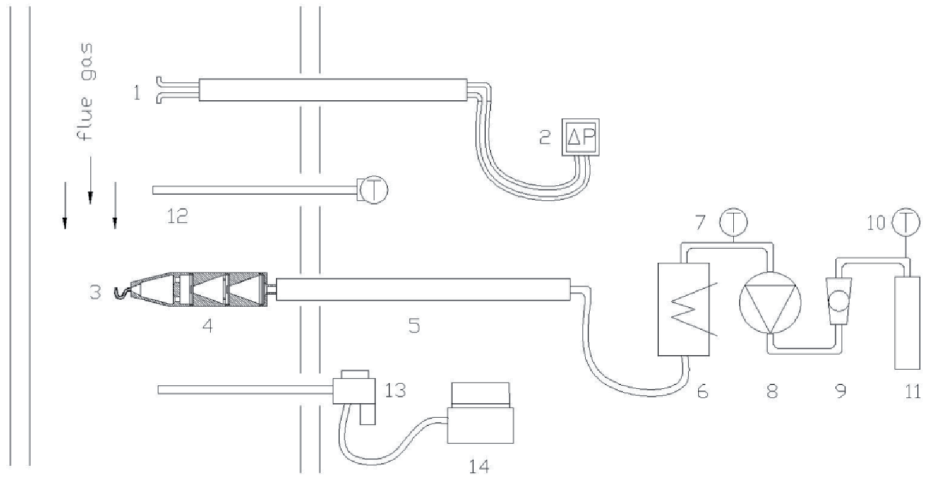


Figure 7. General measuring setup (Paper IV).

1 – S-type Pitot tube, 2 – differential manometer, 3 – nozzle, 4 – Johnas II cascade impactor, 5 – heated sample probe, 6 – condensator, 7 – thermometer, 8 – suction pump, 9 – flow meter, 10 – thermometer, 11 – O₂ analyzer, 12 – thermocouple, 13 – gas analysis probe, 14 – FTIR gas analyzer.

The general measuring setup is shown in Figure 7. The sampling was performed from one point of the flue gas cross-section, which was chosen based on the flue gas velocity field determined beforehand for the whole cross-section [Paper V].

3. RESULTS AND DISCUSSION

3.1. Combustion of oil shale and wood chips

Typical Estonian oil shale and wood chips were used for tests. The fuel samples were analyzed in laboratories of the Department of Thermal Engineering (DTE) of Tallinn University of Technology and in power plant accredited laboratories. The fuel characteristics during different tests were averaged, and the results in Papers I-III are presented in Table 4. The variations in the OS composition confirm that OS is not a homogeneous fuel.

Table 4. Estonian oil shale and wood chips fuel characteristics

	Wood chips	Oil shale
W_i^r , moisture, as received fuel (%)	43.5	11.6 - 14.9
Q_b^d , heating value, dry fuel in calorimetric bomb (MJ/kg)	20.2	10.3 - 13.9
Q_i^r , heating value, as received fuel (MJ/kg)	9.6	8.1 - 10.8
A^r , ash content, as received fuel (%)	1.6	42.6 - 49.1
$(CO_2)_m^r$, carbonate CO_2 content, as received fuel (%)	–	15.2 - 18.2

To obtain representative data and mean values, the duration of the full-scale tests should be as long as possible to minimize the fluctuations in the flue gas and the variations in the ash chemical composition.

3.2. Chemical composition of ash

The chemical composition of the ashes from different combustion technologies are presented in Table 3 in Papers I and II and in Tables 5 and 6 in Paper III. Comparing the ashes from different combustion technologies, a significant difference in the CO_2 and CaO_{free} content in the PF and CFB ash samples was observed. The extent of carbonate mineral decomposition was partial in the case of the CFB. The tests on the PF boiler indicated that the extent of carbonate decomposition (k_{CO_2}) at full load was in the range of 0.92–0.97. At partial load, the decomposition was somewhat lower in the ashes of the super heater and economizer, 0.85 and 0.87, respectively, and was substantially lower in the bottom ash, 0.59 [Paper II]. The tests on the CFB boiler indicated that the k_{CO_2} was in the range of 0.74–0.88 in the convective part of the boiler and 0.51 in the bottom ash [Paper I]. This result confirms the impact of the combustion temperature on the decomposition of carbonate minerals. There was also a significant difference in the CaO content bound into novel minerals. The CaO bound by novel minerals was significantly higher in the PF ashes than in the CFB ashes. At considerably higher furnace temperatures, approximately more than two times more CaO was bound into different ash minerals [Paper VI].

3.3. Ash balance

The ash balance for CFB can be estimated according to [2], where studies were conducted with conventional and enriched OS. The OS and biomass co-combustion ash balance in a CFB boiler should be the same as with the enriched OS because the ash input with fuel decreases. The ash balance for a PF boiler is presented in Fig. 2 in Paper II. The total share of ash from the furnace, SH and ECO is 51%. The results differ from those reported in [5] because four old ESPs have been replaced with three new ones. Furthermore, the pre-precipitator chamber before the cyclone has been removed. The VC ash balance is shown in Fig. 5 in Paper III. The figure shows that in spite of the coarsening of the ash particles, the share of the ash streams captured in the furnace (bottom ash) was smaller than expected compared to previous experiments on medium-pressure boilers. The bottom ash stream was approximately 23% of the total ash flow rate.

3.4. PF and CFB boiler heat balance

The heat balance and thermal efficiency estimations of the considered full-scale experimental study of the PF and CFB boilers were performed on the basis of the standard [64], applying the indirect method that takes into account the peculiarity of the oil shale as a fuel. The amount of heat released, the ash content and the amount of flue gas during the combustion of 1 kg of oil shale depend strongly on the endothermic and exothermic processes in the mineral part of the fuel [5]. These processes include the decomposition of calcite and dolomite, the oxidation of FeS_2 , the sulfating of CaO and the formation of new minerals. A more detailed description on the calculation of the amount of heat and the ash content is presented in [4]. It was found that the gross thermal efficiencies of the PF and CFB boiler were 86.4% and 88.8%, respectively [Paper I and II].

3.5. Flue gas

The flue gas analyses for PF and VC were performed behind the ESP before the induction of a draft fan. The results are presented in Table 7 in Paper III and in Table 10 in Paper II. Retrofitting the boiler to use VC technology did not result in a reduction of SO_2 emissions, indicating an even weaker process of binding sulfur oxides in this furnace compared to PF. According to the test results presented in Table 10 in Paper II, the share of the flue gas components depends on the boiler load changes. At partial load, the oxygen content in the flue gas is twice larger than at full load. At full load, the content of the other components in flue gas is substantially higher compared to that at partial load. For example, the content of SO_2 at full load is approximately twice that at partial load. The mass division of fly ash after the ESP was determined in three tests at both boiler loads in Figure 3 in Paper II. As predicted, the content of the finest ash particles ($<2.5 \mu\text{m}$) is higher at a nominal load. The results are in agreement with the results obtained in Paper IV.

The composition of the flue gas during biomass and OS co-combustion in a CFB boiler was determined before the ESP. The values of the average concentration of the flue gas are given in Table 7 in Paper I, where the OS and biomass firing test results are compared with the ones in [1]. We can conclude that co-combustion reduces CFB boiler emissions. The mass division of the fly ash after the ESP was determined in three parallel tests, shown in Figure 2 in Paper I. The content of the finest ash particles remained in the same limits when firing OS with biomass compared to pure OS firing, as shown in Fig. 5 in Paper IV. The significant influence of the oil shale firing mode on the shape of the fine ash particles was noticed from the SEM pictures of PM_{2.5} fractions at oil shale PF and CFB combustion in Figure 3 in Paper V. The ash particles from PF (<1400 °C) are overburnt (melted) and nicely round. Because of the much lower furnace temperatures in the CFB boiler (<850 °C), the ash particles have an irregular shape [Paper V].

The trace metal emission and distribution at OS PF and CFB firing are presented in Table 1 in Paper V. The emissions were remarkably lower in CFB compared to PF. One of the reasons is the more efficient ESP-s installed at the CFB units, which decreased the trace element release with solid particles about twofold. Because of a similar temperature distribution at the tail of the CFB boiler, the emission of trace elements in the gaseous phase was at the same level as for PF.

Ten times lower level of Hg content in flue gases from CFB boiler if compared to PF system was unexpected. At flue gas temperature (~160 °C) most of the Hg is in elemental form (Hg⁰) in gas phase and the results for CFB and PF should be comparable. The reason for this discrepancy may be caused by different temperature regime and oxygen content. Hg reacts with oxygen and forms HgO. The HgO is bound by carbon contained in ash. Carbon content in the CFB boiler ash is higher compared to PF and therefore the Hg content in the flue gas is less, because Hg is bound with ash.

The elements' relative enrichment factors were different from the former results [65], which could be explained by the changes in the fly ash size distribution. As usual, the enrichment occurs towards finer ashes. The enrichment factor is highest for the Cd and also for the PF ashes [Paper V].

3.6. Specific consumption and emission of an energy unit

The specific indicators of the fuel consumption and ash emission for PF and CFB, both per useful heat (MWh_{th}) and gross electricity production (MWh_e^{br}), are given in Table 5. The specific indicators of the fuel and ash were obtained experimentally for the first boiler of the energy unit. The results were assumed to be applicable for the second boiler as well. The specific indicators of the CO₂, CO and SO₂ emissions per gross electricity (kg/MWh_e^{br}) are in Table 6. There are two values of the CO₂ emission, one based on the sample measurements and the other calculated based on the fuel composition [Paper I and II].

The heat rate of the CFB unit, firing biomass with a thermal share of 15%, was 2.36 MWh_{th}/MWh_e^{br}, corresponding to a gross energy efficiency of 42.37%.

The heat rate of the PF unit was $2.49 \text{ MWh}_{\text{th}}/\text{MWh}_{\text{e}}^{\text{br}}$, corresponding to a gross energy efficiency of 40.16%.

Table 5. Specific indicators of the fuel consumption and ash emissions for PF and CFB

Indicator	Firing technology		
	PF	CFB*	CFB (OS+BIO)
Oil shale consumption per useful heat, $\text{kg}/\text{MWh}_{\text{th}}$	489	441	375
Biomass consumption per useful heat, $\text{kg}/\text{MWh}_{\text{th}}$	-	-	56
Ash formation per useful heat, $\text{kg}/\text{MWh}_{\text{th}}$	223	217	182
Oil shale per electricity (gross), $\text{kg}/\text{MWh}_{\text{e}}^{\text{br}}$	1 219	1160	882
Biomass per electricity (gross), $\text{kg}/\text{MWh}_{\text{e}}^{\text{br}}$	-	-	132
Ash formation per electricity (gross), $\text{kg}/\text{MWh}_{\text{e}}^{\text{br}}$	555	570	428

* According to [1] with a power unit efficiency of 0.38 and an OS heating value of 8.4 MJ/kg.

Table 6. Specific emission indicators

Pollutant per electricity (gross), $\text{kg}/\text{MWh}_{\text{e}}^{\text{br}}$	PF	CFB	CFB (OS+BIO)
CO_2 ¹	974	872	788
CO_2 ²	1 066	923	927
CO	0.111	0.083	0.111
SO ₂	11.89	0	0

¹ – calculation based on the measured percentage of CO₂ with the calculated volume of dry gas;

² – calculation based on the fuel composition.

The test with a biomass thermal share of 15% indicated that the specific emissions of SO₂, CO and NO_x remained the same or slightly decreased compared to [2], where only OS was fired with an LHV of 8.5 MJ/kg. The ash content decreased by 16%, and the CO₂ emissions were 14.6% lower. The specific emission of the SO₂ in PF was 11.89 $\text{kg}/\text{MWh}_{\text{e}}^{\text{br}}$, and for CFB, it is considered as zero [Papers I and II].

CONCLUSIONS

Full scale experiments and in-situ studies were conducted in EPP, BPP and at ash fields. The obtained results are summarized. Based on the tests, we can make the following conclusions:

- VC technology did not result in the reduction of SO₂ emissions. SO₂ emissions during the experiments at the full boiler load varied within the range of 2,715–3,344 mg/Nm³, exceeding emissions of SO₂ for the existing PF technology and indicating an even weaker process of binding sulfur oxides in the furnace. Analysis of the bottom ash chemical composition showed considerable increase in the amounts of unburned carbon. Therefore, the retrofitting of PF units to VC was stopped.
- The gross thermal efficiency of the PF boiler TP-101 was 86.4%. The specific consumption of oil shale per useful heat and gross electricity production was 0.489 t/MWh_{th} and 1.219 t/MWh_e^{br}, respectively. The same indicators for ash formation were 0.223 t/MWh_{th} and 0.555 t/MWh_e^{br}, respectively. The heat rate of the unit was 2.49 MWh_{th}/MWh_e^{br}, which corresponds to a gross energy efficiency of 40.16%. The average concentration of the NO_x and SO₂ emissions at stable load varied insignificantly. The tests at partial and full loads showed that the specific emissions of SO₂, CO₂, CO, NO and HCl at full load were higher, e.g., the content of SO₂ was almost twice that at partial load.
- During OS and biomass co-combustion, the gross thermal efficiency of the CFB boiler was 88.8%. The ash content decreased by 16%, and CO₂ emissions were 14.6% lower. The content of the fine particles (<2.5 μm) of the ash after the ESP remained in the same limits as those in Paper IV. The specific consumption of oil shale per useful heat and gross electricity was 0.375 t/MWh_{th} and 0.882 t/MWh_e^{br}, respectively. The specific consumption of biomass per useful heat and gross electricity was 0.056 t/MWh_{th} and 0.132 t/MWh_e^{br}, respectively. The same indicators for the total ash formation were 0.182 t/MWh_{th} and 0.428 t/MWh_e^{br}, respectively. The heat rate of the unit was 2.36 MWh_{th}/MWh_e^{br}, corresponding to a gross energy efficiency of 42.37%.
- It was found that in the case of oil shale CFB firing, the relative share of very small (<2.5 μm) particulates is higher because of the very efficient milling effect of the relatively soft minerals of oil shale in the CFB furnace. To study the emission, the mass distribution of the CFB boiler ash between different separation points along the flue gas duct (ash mass balance) was determined, and analyses of the sampled ashes were provided.
- With the introduction of CFB firing at Estonian oil shale power plants, the environmental impact of oil shale power production decreased significantly. There was a decrease not only in conventional air pollutants but also trace metals, PAH and dioxins/furans. Therefore, the content of

toxic compounds is not limiting the possible utilization of CFB ash in agriculture and the industry.

- The relative enrichment of trace metals towards smaller ash fractions (flying ash versus landfilled total ash) takes place, as was found in former studies.
- The PAH concentrations in the flue gas of the CFB boiler are at least several times lower than in PF boilers. The benzo(a)pyrene content remains below 11 ng/Nm³ (6% O₂) in CFB firing. The PCDD/F and PCB air emissions of oil shale firing CFB boilers are very low, that is, below 20 mg per year.
- The PM10 relative content in the emissions of oil shale boilers (PF and CFB) is significant, forming over 80% TSP. The PM2.5 share from TSP is higher in the case of the CFB boiler, exceeding 50%. The absolute values are lower for the CFB boilers.
- The share of solid particles with a size over 10 µm tends to increase in correlation with the TSP content.
- Today, the sediment ponds and ash field of oil shale power plants absorb approximately 5–6% of the emitted CO₂.

REFERENCES

1. Plamus, K., Soosaar, S., Ots, A., Neshumayev D. *Firing Estonian oil shale of higher quality in CFB boilers - environmental and economic impact*. Oil Shale, 2011, vol. 28, no. 1S, pp. 113-126.
2. Plamus, K., Ots, A., Pihu, T., Neshumayev, D. *Firing Estonian oil shale in CFB boilers - ash balance and behaviour of carbonate minerals*. Oil Shale, 2011, vol. 28, no. 1, pp. 58-67.
3. Raukas, A., Siirde, A. *New trends in Estonian oil shale industry*. Oil Shale, 2012, vol. 29, no. 3, pp. 203-205.
4. Kuusik, R., Uibu, M., Kirsimäe, K., Mõtsep, R., Meriste, T. *Open-air deposition of Estonian oil shale ash: formation, state of art, problems and prospects for the abatement of environmental impact*. Oil Shale, 2012, vol. 29, no. 4, pp. 376-403.
5. Ots, A. *Oil Shale Fuel Combustion*. Tallinn: Tallinn University of Technology, 2006, 833 p.
6. Ots, A. *Estonian oil shale properties and utilization in power plants*. Energetika, 2007, vol. 53, no. 2, pp. 8-18.
7. International Energy Agency (IEA), *Technology roadmap: high-efficiency, low-emissions coal-fired power generation*. IEA, Paris, 2012, 42 p.
8. Lüschen, A., Madlener, R. *Economic viability of biomass cofiring in new hard-coal power plants in Germany*. Biomass and Bioenergy, 2013, In Press.
9. Roos, I., Soosaar, S., Volkova, A., Streimikene, D. *Greenhouse gas emission reduction perspectives in the Baltic States in frames of EU energy and climate policy*. Renewable and Sustainable Energy Reviews, 2012, vol. 16, no. 4, pp. 2133-2146.
10. Konist, A., Pihu, T., Neshumayev, D., Siirde, A. *Oil shale pulverized firing: boiler efficiency, ash balance and flue gas composition*. Oil Shale, 2013, vol. 30, no. 1, pp. 6-18.
11. Pihu, T., Konist, A., Neshumayev, D., Loosaar, J., Siirde, A., Parve, T., Molodtsov, A. *Short-term tests on firing oil shale fuel applying low-temperature vortex technology*. Oil Shale, 2012, vol. 29, no. 1, pp. 3-17.
12. Arro, H., Prikk, A., Pihu, T. *Combustion of Estonian oil shale in fluidized bed boilers, heating value of fuel, boiler efficiency and CO₂ emissions*. Oil Shale, 2005, vol. 22, no. 4S, pp. 399-406.
13. Hotta, A., Parkkonen, R., Hiltunen, M., Arro, H., Loosaar, J., Parve, T., Pihu, T., Prikk, A., Tiikmaa, T. *Experience of Estonian oil shale combustion based on CFB technology at Narva Power Plants*. Oil Shale, 2005, vol. 22, no. 4S, pp. 381-398.

14. Pihu, T., Arro, H., Prikk, A., Rootamm, R., Konist, A. *Corrosion of air preheater tubes of oil shale CFB boiler*. Oil Shale, 2009, vol. 26, no. 1, pp. 5-12.
15. Suik, H., Pihu, T., Molodtsov, A. *Wear of fuel supply system of CFB boilers*. Oil Shale, 2008, vol. 25, no. 2, pp. 209-216.
16. Suik, H., Pihu, T. *Warranty reliability of CFB boiler burning oil shale*. Oil Shale, 2009, vol. 26, no. 2, pp. 99-107.
17. Parve, T., Loosaar, J., Mahhov, M., Konist, A. *Emission of fine particulates from oil shale fired large boilers*. Oil Shale, 2011, vol. 28, no. 1S, pp. 152-161.
18. Talumaa, R. *Developments of oil shale combustion technologies for power production in Estonia*. Oil Shale, 2012, vol. 29, no. 4, pp. 303-305.
19. Dyni, J. R. *Geology and resources of some world oil-shale deposits*. Oil Shale, 2003, vol. 20, no. 3, pp. 193-252.
20. Qian, J., Yin, L., Wang, J., Han, F., Li, S., He, Y. *Oil shale – petroleum alternative*. Beijing: China Petrochemical Press, 2010, 625 p.
21. Yen, T. F., Chilingar, G. V. *Chapter 1 Introduction to Oil Shales*. Developments in Petroleum Science, 1976, vol. 5, pp. 1-12.
22. Raukas, A., Punning, J.-M. *Environmental problems in Estonian oil shale industry*. Energy & Environmental Science, 2009, vol. 2, pp. 723-728.
23. Dyni, J. R. *Geology and resources of some world oil-shale deposits*: Scientific Investigation Report 2005-5294, U.S. Geological Survey. Reston, Virginia, 2006, 42 p.
24. Tissot, B. P., Welte, D. H. *Petroleum formation and occurrence*. New York: Springer-Verlag, 1984, 699 p.
25. Forsman, J. P. *Geochemistry of kerogen*. Organic Chemistry. New York, Pergamon Press, 1963, pp. 163-172.
26. Altun, N. E., Hiçyilmaz, C., Hwang, J.-Y., Suat Bağcı, A., Kök, M. V. *Oil shales in the world and Turkey: Reserves, current situation and the future prospects: A review*. Oil Shale, 2006, vol. 23, no. 3, pp. 211-227.
27. Peters, K. E., Cassa, M. R. *Applied Source Rock Geochemistry*. The petroleum system – from source to trap. L. B. Magoon and W. G. Dows, Eds., AAPG Memoir, 1994, no. 60, pp. 93-120.
28. Jones, R. W., Edison, T. A., *Microscopic observations of kerogen related to geochemical parameters with emphasis on thermal maturation*. Low temperature metamorphism of kerogen and clay minerals. SEPM Pacific Section, Los Angeles. 1978, pp. 1-12.
29. Baskin, D. K., Peters, K. E. *Early generation characteristics*. AAPG Bulletin, 1992, vol. 76, pp. 1-13.
30. Orr, W. L. *Kerogen/asphaltene/sulfur relationships in sulfur-rich Monterey oils*. Organic Geochemistry, 1986, vol. 10, pp. 499-516.

31. Demaison, G. J., Holck, A. J., Jones, R. W., Moore, G. T. *Predictive source bed stratigraphy; a guide to regional petroleum occurrence*. Proceedings of the 11th World Petroleum Congress, London, 1983, pp. 17-29.
32. Hutton, A. C. *Classification, organic petrography and geochemistry of oil shale*. Proceedings of the 1990 Eastern Oil Shale Symposium, Lexington, 1991, pp. 163-172.
33. Kahru, A., Põllumaa, L. *Environmental hazard of the waste streams of oil shale industry: an ecotoxicological review*. Oil Shale, 2006, vol. 23, no. 1, pp. 53-93.
34. World Energy Council, *Survey of Energy Resources 2010. Oil Shale*, World Energy Council, London, 2010, 608 p.
35. Pihu, T., Arro, H., Prikk, A., Rootamm, R., Konist, A., Kirsimäe, K., Liira, M., Mõtlep, R. *Oil shale CFBC ash cementation properties in ash fields*. Fuel, 2012, vol. 93, pp. 172-180.
36. Veiderma, M. *Estonian oil shale - Resources and usage*. Oil Shale, 2003, vol. 20, no. 3S, pp. 295-303.
37. Teedumäe, A., Raukas, A. *The possibility of integrating sustainability into legal framework for use of oil shale reserves*. Oil Shale, 2006, vol. 23, no. 2, pp. 119-124.
38. Aarna, A. *Oil Shale* (in Estonian). Tallinn: Valgus, 1989, 144 p.
39. Arro, H., Prikk, A., Pihu, T. *Calculation of qualitative and quantitative composition of Estonian oil shale and its combustion products. Part 1. Calculation on the basis of heating value*. Fuel, 2003, vol. 82, pp. 2179-2195.
40. Bauert, H., Kattai, V. *Kokersite oil shale*. Geology and mineral resources of Estonia. A. Raukas, A. Teedumäe, Eds., Tallinn, Estonian Academy Publishers, 1997, pp. 313-327.
41. Petersell, V. *Dictonema argillite*. Geology and mineral resource of Estonia. A. Raukas, A. Teedumäe, Eds., Tallinn, Estonian Academy Publishers, 1997, pp. 327-331.
42. Barnekow, U., Jakubick, A. T., Paul, M. *Stabilization and decommissioning of the Sillamae Radioactive Tailings Pond*. Tailings and mine waste 2003, Vail, 2003, pp. 487-496.
43. Bazelatto Zanoni, M.-A. B., Massard, H., Martins, M. F. *Formulating and optimizing a combustion pathways for oil shale and its semi-coke*. Combustion and Flame, 2012, vol. 159, no. 10, pp. 3224-3334.
44. Martins, M. F., Salvador, S., Thovert, J.-F., Debenest, G. *Co-current combustion of oil shale – Part 2: Structure of the combustion front*. Fuel, 2010, vol. 89, no. 1, p. 133–143.
45. Jiang, X. M., Han, X. X., Cui, Z. G. *Progress and recent utilization trends in combustion of Chinese oil shale*. Progress in Energy and Combustion Science, 2007, vol. 33, p. 552–579.

46. Al-Otoom, A. Y., Shawabkeh, R. A., Al-Harashseh, A. M., Shawaqfeh, A. T. *The chemistry of minerals obtained from the combustion of Jordanian oil shale*. Energy, 2005, vol. 30, no. 5, pp. 611-619.
47. Hayhurst, A. N. *The mass transfer coefficient for oxygen reacting with a carbon particle in a fluidized or packed bed*. Combustion and Flame, 2000, vol. 121, no. 4, pp. 679-688.
48. Imai, T., Murayama, T., Ono, Y. *Estimation of convective heat transfer coefficients between a spherical particle and fluid at lower Reynolds number*. Journal of Iron and Steel Research, International, 1995, vol. 35, no. 12, pp. 1438-1443.
49. Sheng, C. D., Yuan, J. W., Xu, M. H., Ma, Y. Y. *Ignition model of pulverized-coal cloud heated by radiation*. Journal of Combustion Science Technology, 1996, vol. 2, no. 1, pp. 38-45.
50. Han, X. X., Jiang, X. M., Cui, Z. G. *Mathematical model of oil shale particle combustion*. Combustion Theory Model, 2006, vol. 10, no. 1, pp. 145-154.
51. Zajdlík, R., Jelemensky, L., Remiarova, B., Markos, J. *Experimental and modelling investigations of single coal particle combustion*. Chemical Engineering Science, 2001, vol. 56, no. 4, pp. 1355-1361.
52. Kattai, V., Saarde, T., Savitski, L. *Estonian oil shale: geology, resources, mining* (in Estonian), Tallinn: Akadeemia Trükk, 2000, 248 p.
53. Pihu, T., Arro, H., Prikk, A., Parve, T., Loosaar, J. *Combustion experience of Estonian oil shale in large power plants*. International conference on Oil Shale: Recent trends in oil shale, Amman, 2006, pp. 1-13.
54. Paist, A. *Present and future of oil shale based energy production in Estonia*. Oil Shale, 2011, vol. 28, no. 1S, pp. 85-88.
55. Jantti, T., Eriksson, T., Hotta, A., Hyppä, T., Nuortimo, K. *Circulating Fluidized-Bed Technology Toward Zero CO₂ Emissions*. Foster Wheeler Ltd., Varkaus, 2007, 21 p.
56. Pihu, T., Arro, H., Prikk, A., Konist, A., Uibu, M., Kuusik, R. *Reducing of carbon dioxide emissions at oil shale ash deposition*. International Oil Shale Symposium, Tallinn, 2009, pp. 49-50.
57. Arro, H., Prikk, A., Pihu, T. *Research of Balti Power Plant's ash fields* (in Estonian), Tallinn University of Technology, Tallinn, 2002, 84 p.
58. Kespre, T. *Mineralogy of Eesti Power Plant's oil shale ash plateau sediments* (In Estonian), University of Tartu, Tartu, 2004, 46 p.
59. Kuusik, R., Paat, A., Veskimäe, H., Uibu, M. *Transformations in oil shale ash at wet deposition*. Oil Shale, 2004, vol. 21, no. 1, pp. 27-42.
60. Kuusik, R., Uibu, M., Kirsimäe, K. *Characterization of oil shale ashes formed at industrial-scale CFBC boilers*. Oil Shale, 2005, vol. 22, no. 4S, pp. 407-419.

61. Konist, A., Pihu, T. *Reducing CO₂ emissions with oil shale circulating fluidized bed boiler ash*. The 21st international conference on Fluidized Bed Combustion, Naples, 2012, pp. 1117-1122.
62. Ots, A. *Formation and emission of compounds affecting environment*. Oil Shale, 2005, vol. 22, no. 4S, pp. 499-535.
63. Blinova, I., Bityukova, L., Kasemets, K., Ivask, A., Käkinen, A., Kurvet, I., Bondarenko, O., Kanarbik, L., Sihtmäe, M., Aruoja, V., Schvede, H., Kahru, A. *Environmental hazard of oil shale combustion fly ash*. Journal of Hazardous Materials, 2012, Vols. 229-230, pp. 192-200.
64. EVS-EN 12952-15:2003, Water-Tube Boilers and Auxiliary Installations. Part 15. Acceptance Tests.
65. Aunela-Tapola, L., Frandsen, F., Häsänen, E. *Trace metal emissions from the Estonian oil shale fired power plant*. Fuel Processing Technology, 1998, vol. 57, no. 1, pp. 1-24.

LIST OF AUTHOR'S PUBLICATIONS

1. **Konist, A.**, Pihu, T., Neshumayev, D., Külaots, I. *Low grade fuel – oil shale and biomass co-combustion in CFB boiler*. Oil Shale, 30/2S, 2013, xx - xx. Article in press.
2. **Konist, A.**, Pihu, T., Neshumayev, D., Siirde, A. *Oil shale pulverized firing: boiler efficiency, ash balance and flue gas composition*. Oil Shale, 30/1, 2013, 6 - 18.
3. Pihu, T., Arro, H., Prikk, A., Rootamm, R., **Konist, A.**, Kirsimäe, K., Liira, M., Mõtlep, R. *Oil shale CFBC ash cementation properties in ash fields*. Fuel, 93, 2012, 172 - 180.
4. **Konist, A.**, Pihu, T. *Reducing CO₂ emissions with oil shale CFB boiler ash*. Proceedings of the 21th International Conference on Fluidized Bed Combustion. Naples, Italy, June 3-6, 2012.
5. Pihu, T., **Konist, A.**, Neshumayev, D., Loosaar, J., Siirde, A., Parve, T., Molodtsov, A. *Short-term tests on firing oil shale fuel applying low-temperature vortex technology*. Oil Shale, 29/1, 2012, 3 - 17.
6. Parve, T., Loosaar, J., Mahhov, M., **Konist, A.** *Emission of fine particulates from oil shale fired large boilers*. Oil Shale, 28/1S, 2011, 152 - 161.
7. Suik, H., Pihu, T., **Konist, A.** *Catastrophic wattage of tubes in fluidized bed boiler*. Oil Shale, 28/1S, 2011, 162 - 168.
8. Pihu, T., Arro, H., Prikk, A., Rootamm, R., **Konist, A.** *Corrosion of air preheater tubes of oil shale CFB boiler. Part I. Dew point of flue gas and low-temperature corrosion*. Oil Shale, 26/1, 2009, 5 - 12.
9. Arro, H., Pihu, T., Prikk, A., Rootamm, R., **Konist, A.** *Comparison of ash from PF and CFB boilers and behaviour of ash in ash fields*. Proceedings of the 20th International Conference on Fluidized Bed Combustion. Xi'an, China, May 18-20, 2009, 1054-1060.
10. Loosaar, J., Parve, T., **Konist, A.** *Environmental impact of Estonian oil shale CFB firing*. Proceedings of the 20th International Conference on Fluidized Bed Combustion. Xi'an, China, May 18-20, 2009, 422-428.
11. Loosaar, J., Parve, T., **Konist, A.** *Emissions from Estonian oil shale PF and CFB firing*. In: Book of abstracts: International Oil Shale Symposium. Tallinn, Estonia, June 8-11, 2009.
12. Pihu, T., Arro, H.; **Konist, A.**, Kuusik, R., Prikk, A., Uibu, M. *Reducing of carbon dioxide emissions at oil shale ash deposition*. In: Book of abstracts: International Oil Shale Symposium. Tallinn, Estonia, June 8-11, 2009.
13. **Konist, A.**, Parve, T., Loosaar, J. *Tallinnan TKK Lämpötekniikan laitoksen Päästömittaukset 2006*. In: XVI Valtakunnalliset Päästömittaajapäivät, Lahhti, Finland, April 12-13, 2007, 1 - 11.

ACKNOWLEDGEMENTS

The thesis is based on the work carried out at the Department of Thermal Engineering of Tallinn University of Technology and also at the Eesti and Balti Power Plants. Financial support for the research was provided by the Eesti Energia Narva Power Plants, the Estonian Ministry of Education and Research (SF0140024s07) and the Estonian Science Foundation (Grant No 8782).

I would like to express my deepest gratitude to the supervisors PhD Tõnu Pihu and PhD Indrek Külaots for their guidance and valuable advice. Especially to Tõnu who dealt with my thesis in our extremely tight time schedule. Also, I am grateful to Professor Andres Siirde who has taught me that simply words won't do your research work. Special thanks to PhD Jüri Loosaar, PhD Dmitri Neshumayev, Teet Parve and Maaris Nuutre for their time and help. I am most grateful to Sulev Soosaar who has improved the linguistical quality of the thesis. Also, I am most grateful for Toomas Tiikma scholarship.

I would like to thank my family – Kaspar and Reelika for their constant support and encouragement during my thesis writing.

ABSTRACT

Oil shale is Estonia's primary energy resource for achieving energy independency. Approximately 90% of the electricity consumed is produced from oil shale. Oil shale is the primary contributor to air pollution and waste. To reduce the environmental impact of oil shale power production and to increase the reliability of boilers, different combustion technologies have been introduced and modified at various times. Different combustion technologies – pulverized firing (PF) and circulating fluidized bed (CFB), are currently utilized at oil shale-fired power plants. An attempt was made to use vortex combustion (VC) technology, but this effort did not result in success. The present work is based on in-situ experiments at full-scale oil shale firing boilers and at ash fields, where the ash is deposited. All analyses are based on international standards.

The goal of this thesis is to analyze the existing situation at Estonian oil shale fired power plants by determining the boiler efficiencies, ash flows, ash chemical compositions, specific emissions, fine particulates, trace metals and ash behavior in ash fields of different combustion technologies. The thesis presents a detailed review of the data obtained from the conducted in-situ tests and compares it with previous results. The chemical compositions of the ash formed by different combustion technologies are compared. An analysis and an estimation of the changes in the emission of all of the primary polluting components in CFB firing compared to PF are presented. This analysis includes the mass balance of the trace metals in the initial fuel and in formed ash; the emissions of PCDD/F, PCB, PAH, and PM_{2.5/10}; and conventional air emissions, such as NO_x, SO₂, CO₂, CO, HCl, and TSP.

It was found that the heat rate of the CFB unit, firing biomass with a thermal share of 15%, was 2.36 MWh_{th}/MWh_e^{br}, corresponding to a gross energy efficiency of 42.37%. The heat rate of the PF unit was 2.49 MWh_{th}/MWh_e^{br}, corresponding to a gross energy efficiency of 40.16%.

The test with a biomass thermal share of 15% showed that the specific emission of SO₂, CO and NO_x remained the same or decreased slightly compared to the conventional firing of OS with an LHV of 8.5 MJ/kg. The ash content decreased by 16%, and the CO₂ emissions were 14.6% lower.

The specific emission of SO₂ in PF was found to be 11.89 kg/MWh_e^{br}, and for CFB, it is considered as zero. The PAH concentrations in the flue gas of the CFB boiler were at least several times lower than in PF boilers. The ash of the CFB boiler at the ash field bound 8.1% of the emitted CO₂, and the PF boiler ash bound 3.2% of the emitted CO₂.

With the introduction of CFB firing at Estonian oil shale power plants, the environmental impact of oil shale power production has decreased significantly, not only in terms of conventional air pollutants but also with trace metals, PAH and dioxins/furans and ash as a CO₂ absorber. The co-combustion of oil shale with biomass in a CFB boiler decreases the environmental footprint of OS power production even more.

KOKKUVÕTE

Üle 90% Eestis tarbitavast elektrienergiast toodetakse põlevkivist. Põlevkivi on madala kütteväärtusega tuharikas kütus, mida kasutatakse nii tolmpõletus- kui ka ringleva keevkihiga kateldes. Põletustehniliselt erinevad need katlad üksteisest märgatavalt. Erinevad põlemistemperatuurid ja kütuse ettevalmistus erinevates katlatüüpides on ühed olulisemad tegurid, mis mõjutavad tekkiva tuha ja suitsugaaside koostist.

Käesoleva doktoritöö eesmärk on uurida erinevatel põletustehnoloogiatel tekkivaid õhu- ja tuhaheitmeid ning tuha käitumist tuhaväljal. Selleks teostati tööstuslikud katsed erinevat tüüpi kateldel ja viidi läbi uuringud tuhaväljadel. Saadud tulemuste põhjal saab hinnata põlevkivienergeetika keskkonnamõju ja erinevate põletustehnoloogiate jätkusuutlikkust pidevalt karmistuvates keskkonnaningimustes.

Doktoritöö peamised tulemused on järgnevad:

- Tolmpõletuskatla rekonstrueerimine madalatemperatuurse keeriskoldega katlaks ei anna vajalikke tulemusi. Vääveldioksiidi heitmed pigem isegi suurenevad.
- Tolmpõletuskatla TP-101 kasutegur oli 86,4% ning kütuse- ja tuha erikuld olid vastavalt 1,219 t/MWh_e^{br} ja 0,555 t/MWh_e^{br}.
- Ringleva keevkihiga katla kasutegur põlevkivi ja biokütuse koospõletusel oli 88,8% ning kütusekulud olid vastavalt põlevkivi kulu 0,882 t/MWh_e^{br} ja biokütuse kulu 0,132 t/MWh_e^{br} ning tuha eriteke oli 0,428 t/MWh_e^{br}.
- Ülipeente tuhaosakeste (<2,5 µm) osakaal keevkihtpõletusel on võrreldes tolmpõletuskatlagaga suurem, kuna ringluse tõttu hõõrduvad tuhaosakesed omavahel.
- Raskemetallide osakaal on keevkihtpõletusel võrreldes tolmpõletusega märgatavalt vähenenud ega põhjusta tuhakasutusele piiranguid.
- Polüaromaatsete süsivesinike kontsentratsioon keevkihtkatlas on võrreldes tolmpõletuskatlagaga märgatavalt vähenenud.
- Ülipeente tuhaosakeste PM10/2,5 summaarne osakaal on keevkihtpõletusel võrreldes tolmpõletusega väiksem.
- Elektrifiltrite efektiivsus mõjutab otseselt ülipeente tuhaosakeste kontsentratsiooni.
- Tuhaväljad seovad 5–6% elektrijaamade emiteeritavast süsihappegaasist.

ORIGINAL PUBLICATIONS

PAPER I

LOW GRADE FUEL - OIL SHALE AND BIOMASS CO-COMBUSTION IN CFB BOILER

ALAR KONIST^{(a)*}, TÕNU PIHU^(a),
DMITRI NESHUMAYEV^(a), INDREK KÜLAOTS^(b)

^(a) Department of Thermal Engineering, Tallinn University of Technology
Kopli 116, 11712 Tallinn, Estonia

^(b) School of Engineering, Brown University, 182 Hope Street, Providence
Rhode Island, USA 02912

Abstract. Estonia has two of the world's largest oil shale firing circulating fluidized bed (CFB) units with a designed electrical capacity of 215 MW each. The units are based on double boiler CFB technology provided by Foster Wheeler Energia OY. The units are located at Eesti and Balti power plants (EPP and BPP). The paper presents analyses of data obtained from tests of oil shale and biomass co-combustion in the full-scale CFB boiler located at BPP. The tests were conducted at nominal boiler load: 100% (314 t/h), with a biomass thermal input of 15%. During the experiments ash samples from the furnace chamber (bottom ash), INTREX, super-/reheater (SH, RH), economizer (ECO), and air preheater (APH), and from all four fields of the electrostatic precipitator (ESP) were taken. Samples of fly ash for determining the mass division (total suspended particulates PM10 and PM2.5) were taken after the ESP. The gas analysis was performed at the ESP inlet. Analysis of the chemical composition of ash was carried out. The specific consumption of oil shale per useful heat and gross electricity were found and other techno-economic characteristics determined.

It was found that oil shale and biomass co-combustion reduced CO₂ emission by 14.6% and ash formation by 16% when compared with conventional oil shale CFB combustion. The SO₂ emissions remained in the limits of 20–30 mg/Nm³. Total suspended particulates PM10 and PM2.5 did not change compared to conventional oil shale CFB firing. The CFB boiler efficiency even increased slightly, when it is known that in case of coal and biomass co-combustion it decreases. Therefore, oil shale and biomass co-combustion can be considered as a viable option and near-term solution for reducing the environmental impact of oil shale-based power production.

Keywords: oil shale, biomass, co-combustion, TSP PM 10/2.5, ash composition, CO₂ emission reduction.

* Corresponding author: e-mail alar.konist@ttu.ee

1. Introduction

Estonian oil shale (OS) is a very difficult-to-burn fuel due to its unique properties. The high alkali and chlorine content of OS ash has caused significant corrosion and fouling problems in pulverized firing (PF) units, resulting in decreased availability. Gaseous emissions, especially SO₂ and particulate emission, have been high. Since in Estonia almost 90% of electricity is produced from OS [1, 2], the co-combustion of biomass and OS can be the quickest, easiest and cheapest way to reduce the environmental impact of OS-based power production [3, 4].

Estonia is implementing two different combustion technologies for OS-based power production: PF and circulating fluidized bed (CFB) technologies. A recent study describing PF and vortex combustion technologies are presented in [5, 6]. Some of the results of tests on CFB technology and CFB boiler reliability are presented in [7–12].

In the OS CFB boilers, fouling and corrosion problems in the convective superheaters have been prevented by a careful choice of the steam temperature for each superheating stage and by using effective heat surface cleaning methods. INTREX superheaters are used as the last super/reheating stage, and refractory lined separators as the second superheating stage, allowing lower steam temperature to be used in convective super/reheater (SH, RH) sections where the risk of high-temperature corrosion is the highest. The existing CFB boilers use pneumatic fuel feeding with many feeding points, resulting in good fuel mixing and providing favorable conditions for sulfur binding in the lower furnace. SO₂ emission is considerably reduced due to the inherent limestone content of oil shale ash, which favors sulfur capture in CFB conditions. SO₂ and NO_x emissions are reduced by 99% and 30%, respectively, while particulate emission decreased significantly compared to the old PF units with lower efficiency electrostatic precipitators (ESP). The improved efficiency and decreased carbonate decomposition in CFB has decreased the CO₂ emission per produced power unit by nearly 24% [8].

The careful CFB boiler design has resolved problems related to oil shale combustion, and no signs of significant fouling or corrosion of heat exchangers have occurred in the CFB boilers at Narva Power Plants. Still, air pre-heater corrosion has been noticed in CFB units, but it has been caused by too low temperatures at the air preheater (APH) inlet, which has been an operational fault [9].

Improved availability, lower maintenance costs and higher efficiency of CFB units have significantly improved the unit's economics. According to the performance tests, the net efficiency of CFB units is 38–39%, whereas in the PF units it is in the range of 29–30%.

Higher efficiency was obtained by implementing higher live and reheat steam temperature, reducing flue gas heat losses by applying better control of excess air and reducing the flue gas temperature at the outlet.

Another significant part of efficiency improvement comes from the lower carbonate decomposition and higher sulfation rate during CFB combustion, the effect of which is about 0.4 MJ/kg or 5% compared with those in PF reported by Hotta et al. [8].

Recent studies point out that utilization of biomass fuels in CFB boilers may cause operational problems, such as agglomeration, deposit formation, and corrosion [13–17]. However, such problems can be limited with proper boiler design, suitable boiler operation, alternative bed materials or additives, and most effectively by co-combustion with coal or peat that can capture problematic elements from biomass/wastes. Since OS powered CFB units have been carefully designed to avoid such operational problems, OS and biomass co-combustion in CFB seems the most promising option to reduce the environmental impact of OS-based power production.

The current paper deals with the study of OS and biomass co-combustion in a CFB boiler with 15% of biomass thermal contribution. Previous studies on coal and biomass co-combustion point out that 20% is the optimum amount, which can be burnt in a CFB boiler without following drawbacks. If the biomass contribution is higher, the boiler thermal efficiency decreases, NO_x and other flue gas components exceed the allowed environmental legislation limits and there have been noticed problems with heating surface fouling [18]. The aim of this paper is to investigate the effect of OS and biomass co-combustion on CFB boiler thermal efficiency, emissions, distribution of particulate matter, ash chemical composition and CO_2 reduction.

2. Experimental set-up

The major goal of tests was to carry out analyses of ash and flue gas, as well as to determine the boiler efficiency. The tests were performed with the following fuel shares (as of thermal input): 85% of OS and 15% of wood chips. OS was of class P3 (particle size 0–40 mm) from the screening before enrichment from Aidu open-pit mine. Wood chips from stem wood and branches were used as the biomass fuel. The main characteristics of the fuels used are presented in Table 1.

The main characteristics of the boiler during the tests are given in Table 2. The variations of steam pressure and mass flow during all tests are shown as well. It can be seen that the variations are smaller than the marginal values given in the standard EN 12952-15 (2003) [19].

Table 1. Fuel characteristics

	Wood chips	Oil shale
W_i^r , moisture, as received fuel, %	43.5	12.6
Q_b^d , heating value, dry fuel in calorimetric bomb, MJ/kg	20.2	11.3
Q_i^r , heating value, as received fuel, MJ/kg	9.6	8.9
A^r , ash content, as received fuel, %	1.6	49.1
$(\text{CO}_2)_m^r$, carbonate CO_2 content, as received fuel, %	–	18.2

Table 2. Boiler characteristics at nominal load

Boiler load, MW _{th}	245.7
Electrical load of unit, MW _e	197.9
Steam temperature (live/superheated), °C	534.2/535.7
Steam pressure (live/superheated), MPa	12.82/2.16
Pressure variation of live steam, %	0.8
Steam mass flow (live/superheated), kg/s	86.95/76.2
Mass flow variation of live steam, %	2.6
Flue gas temperature (after ESP), °C	178

During the tests the analyses of fuel, ash and flue gas were carried out. The location of ports (1–9) for collecting samples is shown in Fig. 1. Fuel samples were taken on daily average basis. The ash samples were taken from several ports located in the furnace chamber, INTREX, super-/reheater (SH, RH), economizer (ECO), and air preheater (APH), and from all four fields of the electrostatic precipitator (ESP). Samples of fly ash for determining the mass division (total suspended particulates PM10 and PM2.5) were taken after the ESP. The samples were used for determining a detailed chemical composition of ashes. In the frame of the tests the boiler efficiency was calculated as well.

The results of sample analyses were averaged to reach a representative estimate. Also, during the tests the major process parameters of the boiler and unit as a whole were recorded using the plant's standard data acquisition system. The temperature and composition of flue gas were measured before the ESP.

The total of 9 ash samples were taken from several ports located in the furnace, INTREX, super heater, ECO, and APH, and from all four fields (ESP1, ESP2, ESP3 and ESP4) of the ESP. The ash was taken from the dry flow to ensure the representativeness of samples.

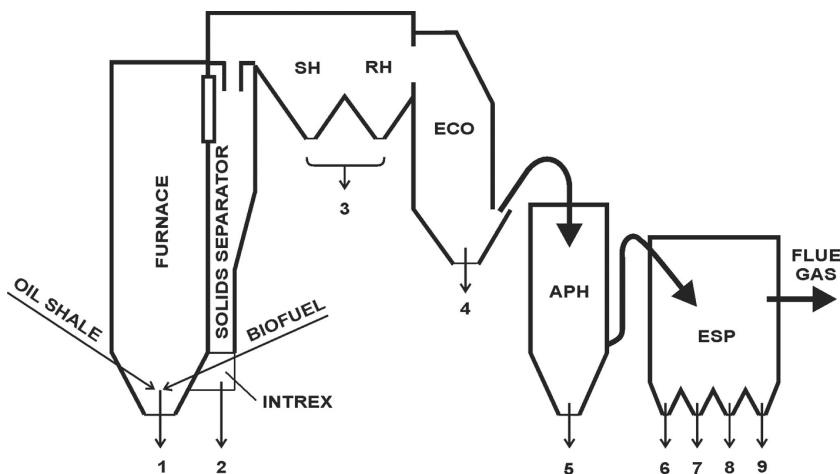


Fig. 1. CFB boiler sampling points.

The analysis of flue gas was carried out from the sampling ports before the ESP. The composition of flue gas was determined applying an FTIR type analyzer for wet gas, at a temperature of 180 °C. The flue gas moisture content was also determined by a FTIR spectrometer.

Fly ash samples were taken after the ESP to determine the division of finest particles (PM10 and PM2.5) in flue gas.

3. Results and discussion

3.1. Fuel – oil shale

The oil shale samples were analyzed in the laboratories of the Department of Thermal Engineering (DTE) of Tallinn University of Technology and BPP. The local laboratory of BPP determined the daily average heating value and moisture content (W_i^f) of the OS used. The DTE laboratory performed the ultimate and proximate analyses of wood chips and OS. Table 1 presents the heating values determined in a calorimetric bomb (Q_b^d) and as received fuel (Q_i^f) calculated by general moisture content.

3.2. The chemical composition of ash samples

The samples were taken at nominal (100%) boiler load (steam flow rate about 314 t/h). The composition of ash (at 815 °C) is presented in Table 3. The nitrogen content in ash samples was below detection limit.

Table 3. Chemical composition of ash, %

	Furnace	INTREX	SH	ECO	APH	ESP 1	ESP 2	ESP 3	ESP 4
CO ₂	21.03	5.54	5.09	4.69	4.33	4.49	4.22	3.76	7.13
C (CO ₂)	5.74	1.51	1.39	1.28	1.18	1.22	1.15	1.03	1.94
C _{elem}	5.93	1.50	1.39	1.33	1.19	1.26	1.17	1.10	1.92
S _{elem}	3.99	7.38	3.84	3.09	4.14	2.23	2.36	2.33	2.59
SO ₃ total	9.98	18.65	9.60	7.73	10.35	5.6	5.98	5.83	6.48
S _{sulphate}	3.37	7.04	3.51	2.90	3.84	2.20	2.29	2.30	2.60
SO ₃ sulphate	8.43	17.60	8.78	7.24	9.61	5.50	5.73	5.75	6.50
S _{sulphide}	0.62	0.34	0.33	0.19	0.30	0.03	0.07	0.03	-0.01
SiO ₂	7.21	10.27	28.82	32.09	27.62	34.56	35.37	36.18	30.43
Fe ₂ O ₃	2.76	3.21	4.43	4.78	4.82	4.97	4.93	5.30	5.30
Al ₂ O ₃	3.12	3.87	9.26	8.48	7.17	9.69	10.72	11.60	11.38
CaO	53.20	58.16	42.67	36.23	40.10	31.68	31.85	30.21	30.35
CaO _{free}	15.65	26.93	16.06	14.84	17.44	13.79	12.52	10.30	3.60
MgO	1.21	1.79	0.81	4.34	3.42	3.64	3.57	4.00	3.24
K ₂ O	0.52	0.95	2.58	3.19	2.45	3.67	3.76	4.06	3.45
Na ₂ O	0.17	0.13	0.23	0.47	0.25	0.28	0.3	0.29	0.27
Cl	0.16	0.24	0.35	0.47	0.36	0.45	0.44	0.71	1.44
Loss on ignition _{815 °C}	21.2	6.10	5.20	5.10	4.30	4.60	4.40	4.40	10.0

The extent of carbonate minerals decomposition in various ash samples is presented in Table 4 and the results are compared with those of a previous CFB study [2].

Table 4. The extent of carbonate minerals decomposition (k_{CO_2})

Sampling point Fuel	Furnace	INTREX	SH-RH	ECO	APH	ESP 1	ESP 2	ESP 3	ESP 4
BIO + OS	0.51	0.88	0.85	0.86	0.88	0.84	0.85	0.86	0.74
OS 8.5	0.47	0.97	0.79	0.80	0.85	0.82	0.83	0.84	0.81
OS 11.1	0.68	0.97	0.82	0.83	0.88	0.82	0.83	0.85	0.70

The tests indicated that the extent of carbonates decomposition (k_{CO_2}) at the nominal load is in the range of 0.51–0.88. The weighted average is between 0.72–0.75 when using ash balance data obtained by Plamus et al. [2]. When firing OS with biomass or firing OS with higher heating value, the extent of carbonates decomposition increases.

For characterizing ashes the bulk densities were determined. Table 5 presents the bulk densities determined for ashes from the furnace, INTREX, superheater, economizer, air preheater and ESP 1–4. For comparison, previous results of CFB firing tests, where OS with a heating value of 8.5 and 11.1 MJ/kg was used, are also given [2].

Table 5. Bulk density of ash flows, g/cm^3

Sampling point Fuel	Furnace	INTREX	SH-RH	ECO	APH	ESP 1	ESP 2	ESP 3	ESP 4
BIO + OS	1.503	1.286	0.908	0.791	0.919	0.698	0.681	0.543	0.412
OS 8.5	1.483	1.28	0.787	0.668	0.841	0.652	0.666	0.564	0.431
OS 11.1	1.647	1.3	0.758	0.71	0.841	0.598	0.565	0.515	0.447

3.3. Boiler heat balance

The heat balance and thermal efficiency estimations of the considered full-scale experimental study of the CFB boiler were performed on the basis of the standard [19] by the indirect method taking into account the specific nature of oil shale as a fuel. The amount of heat released, ash content and flue gas amount during combustion of 1 kg of oil shale depends strongly on the endothermic and exothermic processes taking place in the mineral part of the fuel [5]. These processes include the decomposition of calcite and dolomite, oxidation of FeS_2 , sulfating of CaO and formation of new minerals. A more detailed description of the calculation of heat amount and

ash content can be found in [20]. Combustion flue gas mass and volume were calculated. Flue gas content (dry gas), kg/kg, was found as follows:

$$\mu_{\text{God}} = 12.5122\gamma_{\text{C}} + 26.3604\gamma_{\text{H}} - 3.3212\gamma_{\text{O}} + 1.0\gamma_{\text{N}} \\ + \left[(1 - \eta_{\text{S}}) 1.9953 + 3.2947 \right] \gamma_{\text{S}} + k_{\text{CO}_2} \gamma_{\text{CO}_2},$$

where η_{S} is desulfurization efficiency (p. 8.3.5 in [19]); k_{CO_2} is the extent of carbonate mineral decomposition [21]; γ_{C} , γ_{H} , γ_{O} , γ_{N} , γ_{S} , γ_{CO_2} are carbon, hydrogen, oxygen, nitrogen, sulfur and carbonate carbon dioxide contents in fuel, respectively, kg/kg.

Flue gas volume (dry gas), m³/kg, was calculated as follows:

$$V_{\text{God}} = 8.8930\gamma_{\text{C}} + 20.9724\gamma_{\text{H}} - 2.6424\gamma_{\text{O}} + 0.7997\gamma_{\text{N}} \\ + \left[(1 - \eta_{\text{S}}) 0.68172 + 2.6325 \right] \gamma_{\text{S}} + 0.509\gamma_{\text{CO}_2} k_{\text{CO}_2}.$$

Carbon dioxide content (dry gas), kg/kg, was found as follows:

$$\mu_{\text{CO}_2} = 3.6699\gamma_{\text{C}} + 0.0173\gamma_{\text{H}} - 0.0022\gamma_{\text{O}} \\ + \left[(1 - \eta_{\text{S}}) 0.001 + 0.0017 \right] \gamma_{\text{S}} + k_{\text{CO}_2} \gamma_{\text{CO}_2}.$$

All calculations for heat balance were made for normal conditions: $t_{\text{r}} = 0$ °C, $p_{\text{r}} = 101\,325$ Pa. The boiler efficiency at nominal load according to the EN standard was 88.8% (Table 6).

Table 6. Boiler efficiency

Item	Value	
	kW	%
Heat input		
Heat from fuel combustion	266 654	96.0
Physical heat of fuel	1118	0.4
Input heat of combustion air	10 133	3.6
Total	277 905	100.0
Useful heat capacity	245 689	
Loss with flue gas	25 620	9.3
Loss due to unburned fuel (CO)	5	0.0
Bottom ash loss	3605	1.3
Fly ash loss	913	0.3
Loss due to radiation	854	0.3
Total	30 997	11.2
Heat efficiency		88.8

3.4. Flue gas

The composition of flue gas was determined before the ESP. The values of average concentration of major emission gases are given in Table 7, presenting for comparison also OS and biomass firing test results obtained by

Plamus et al. [1]. We can conclude that co-combustion reduces CFB boiler emissions.

Table 7. Concentration of main pollutants in flue gas before ESP (6% O₂)

Fuel used	CO ₂ , %	CO, mg/Nm ³	NO _x , mg/Nm ³	SO ₂ , mg/Nm ³
OS+BIO	13.8	20–30	140–200	0
OS 8.5	14.4	20–45	200	15.0
OS 11.1	11.2	20–45	200	15.0

The content of finest particles of fly ash together with its mass division (PM_{10/2.5}) after the ESP is an important indicator of flue gas composition. The fly ash cannot be caught by the final section of the ESP and as a result, it is emitted into the ambient air.

The mass division of fly ash after the ESP was determined in three parallel tests (Fig. 2). The content of finest ash particles remained in the same limits when firing OS with biomass compared to pure OS firing [12].

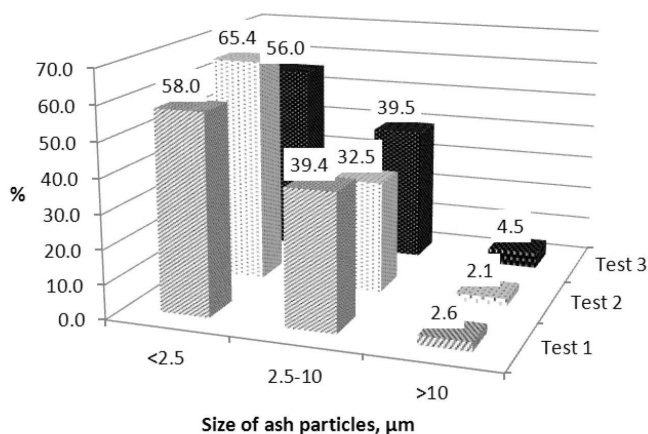


Fig. 2. Fly ash mass distribution after ESP.

3.5. Specific consumption and emission of the energy unit

Specific mass flow indicators of fuel and ash, CO₂, CO and SO₂ emissions both per useful heat (MWh_{th}) and gross electricity production (MWh_e^{br}) are given in Table 8. The specific indicators of fuel and ash per production unit obtained experimentally for the first boiler of the energy unit were assumed to be applicable to the second boiler as well. In Table 9 there are two values of CO₂ emission – based on sample measurements, and calculated on the basis of fuel composition.

The heat rate of the unit was 2.36 MWh_{th}/MWh_e^{br}, corresponding to the gross energy efficiency of 42.37%.

Table 8. Specific indicators of fuel consumption and ash emissions

Indicator	Unit	Value
Oil shale consumption per useful heat	g/kWh _{th}	375
Biomass consumption per useful heat	g/kWh _{th}	56
Ash formation per useful heat	g/kWh _{th}	182
Oil shale per electricity (gross)	g/kWh _e ^{br}	882
Biomass per electricity (gross)	g/kWh _e ^{br}	132
Ash emission per electricity (gross)	g/kWh _e ^{br}	428

Table 9. Specific emission indicators

Pollutant	Per useful heat, kg/MWh _{th}	Per electricity (gross), kg/MWh _e ^{br}
CO ₂ ¹	334	788
CO ₂ ²	393	927
CO	0.045	0.111
SO ₂	0	0

¹ – calculation based on measured percentage of CO₂ with calculated volume of dry gas;

² – calculation based on fuel composition.

4. Conclusions

The data from experimental tests conducted on CFB boiler indicate that the thermal gross efficiency of the boiler is 88.8%. Regarding emission into air, the average concentration of CO, NO_x and SO₂ at stable load varied insignificantly. The test with biomass thermal share of 15% showed that the specific emission of SO₂, CO and NO_x remained the same or slightly decreased compared with the values reported by Plamus et al. in [2] where only OS was fired with LHV of 8.5 MJ/kg. The ash content was decreased by 16% and CO₂ emissions were 14.6% lower. The content of fine particles (< 2.5 μm) of ash after the ESP remained in the same limits compared to the results obtained by Parve et al. [12].

The specific consumption of oil shale per useful heat and gross electricity was 0.375 t/MWh_{th} and 0.882 t/MWh_e^{br}, respectively. The specific consumption of biomass per useful heat and gross electricity was 0.056 t/MWh_{th} and 0.132 t/MWh_e^{br}, respectively. The same indicators for total ash formation were 0.182 t/MWh_{th} and 0.428 t/MWh_e^{br}, respectively.

The heat rate of the unit was 2.36 MWh_{th}/MWh_e^{br}, corresponding to the gross energy efficiency of 42.37%.

The test results encouraged OS and biomass co-combustion in a CFB boiler. Therefore additional biomass feeding system has been installed which allows increasing biomass share up to 50% of thermal input. Preliminary test results indicate that there is no effect on fouling, however, boiler efficiency may decrease, but it mainly depends on fuel moisture content (based on unpublished data by T. Pihu et al.).

Acknowledgements

The authors are grateful to the staff of Narva Power Plants and especially to Mr. Rain Veinjärv, Development Manager. Without his support this project could not have been carried out.

REFERENCES

1. Plamus, K., Soosaar, S., Ots, A., Neshumayev, D. Firing Estonian oil shale of higher quality in CFB boilers – environmental and economic impact. *Oil Shale*, 2011, **28**(1S), 113–126.
2. Plamus, K., Ots, A., Pihu, T., Neshumayev, D. Firing Estonian oil shale in CFB boilers – ash balance and behaviour of carbonate minerals. *Oil Shale*, 2011, **28**(1), 58–67.
3. Lüschen, A., Madlener, R. Economic viability of biomass cofiring in new hard-coal power plants in Germany. *Biomass and Bioenergy*, vol. in Press, 2013.
4. Roos, I., Soosaar, S., Volkova, A., Streimikene, D. Greenhouse gas emission reduction perspectives in the Baltic States in frames of EU energy and climate policy. *Renew. Sust. Energ. Rev.*, 2012, **16**(4), 2133–2146.
5. Konist, A., Pihu, T., Neshumayev, D., Siirde, A. Oil shale pulverized firing: boiler efficiency, ash balance and flue gas composition. *Oil Shale*, 2013, **30**(1), 6–18.
6. Pihu, T., Konist, A., Neshumayev, D., Loosaar, J., Siirde, A., Parve, T., Molodtsov, A. Short-term tests on firing oil shale fuel applying low-temperature vortex technology. *Oil Shale*, 2012, **29**(1), 3–17.
7. Arro, H., Prikk, A., Pihu, T. Combustion of Estonian oil shale in fluidized bed boilers, heating value of fuel, boiler efficiency and CO₂ emissions. *Oil Shale*, 2005, **22**(4S), 399–406.
8. Hotta, A., Parkkonen, R., Hiltunen, M., Arro, H., Loosaar, J., Parve, T., Pihu, T., Prikk, A., Tiikma, T. Experience of Estonian oil shale combustion based on CFB technology at Narva Power Plants. *Oil Shale*, 2005, **22**(4S), 381–398.
9. Pihu, T., Arro, H., Prikk, A., Rootamm, R., Konist, A. Corrosion of air preheater tubes of oil shale CFB boiler. Part I. Dew point of flue gas and low-temperature corrosion. *Oil Shale*, 2009, **26**(1), 5–12.
10. Suik, H., Pihu, T., Molodtsov, A. Wear of the fuel supply system of CFB boilers. *Oil Shale*, 2008, **25**(2), 209–216.
11. Suik, H., Pihu, T. Warranty reliability of CFB boiler burning oil shale. *Oil Shale*, 2009, **26**(2), 99–107.
12. Parve, T., Loosaar, J., Mahhov, M., Konist, A. Emission of fine particulates from oil shale fired large boilers. *Oil Shale*, 2011, **28**(1S), 152–161.
13. Hupa, M. Interaction of fuels in co-firing in FBC. *Fuel*, 2005, **84**(10), 1312–1319.
14. Vamvuka, D., Pitharoulis, M., Alevizos, G., Repouskou, E., Pentari, D. Ash effects during combustion of lignite/biomass blends in fluidized bed. *Renew. Energ.*, 2009, **34**(12), 2662–2671.

15. Doshi, V., Vuthaluru, H. B., Korbee, R., Kiel, J. H. A. Development of a modeling approach to predict ash formation during co-firing of coal and biomass. *Fuel Process. Technol.*, 2009, **90**(9), 1148–1156.
16. Basu, P., Butler, J., Leon, M. A. Biomass co-firing options on the emissions reduction and electricity generation costs in coal-fired power plants. *Renew. Energ.*, 2011, **36**(1), 282–288.
17. Aho, M., Envall, T., Kauppinen, J. Corrosivity of flue gases during co-firing Chinese biomass with coal at fluidised bed conditions. *Fuel Process. Technol.*, 2013, **105**, 82–88.
18. Pronobis, M. The influence of biomass co-combustion on boiler fouling and efficiency. *Fuel*, 2006, **85**(4), 474–480.
19. EVS-EN 12952-15:2003: *Water-Tube Boilers and Auxiliary Installations. Part 15. Acceptance Tests.*
20. Neshumayev, D., Ots, A., Parve, T., Pihu, T., Plamus, K., Prikk, A. Combustion of Baltic oil shales in boilers with fluidized bed combustion. *Power Technology and Engineering*, 2011, **44**(5), 382–385.
21. Arro, H., Prikk, A., Pihu, T. Calculation of qualitative and quantitative composition of Estonian oil shale and its combustion products. Part 1. Calculation on the basis of heating value. *Fuel*, 2003, **82**(18), 2179–2195.

Presented by

Received

PAPER II

OIL SHALE PULVERIZED FIRING: BOILER EFFICIENCY, ASH BALANCE AND FLUE GAS COMPOSITION

ALAR KONIST*, TÕNU PIHU, DMITRI NESHUMAYEV,
ANDRES SIIRDE

Department of Thermal Engineering, Tallinn University of Technology
116 Kopli St., 11712 Tallinn, Estonia

Abstract. *The paper presents analyses of data obtained from oil shale pulverized firing tests carried out at the Eesti Power Plant (EPP) that is part of an Estonian power company Narva Power Plants (NPP) owned by a state company Eesti Energia AS. The tests were conducted at two boiler loads: 50% (158 t/h) and 100% (320 t/h) in the TP-101 boiler. During experiments samples of bottom and fly ashes from inertia dust collectors after the super heater (SH) and economizer (ECO), as well as fly ash from the electrostatic precipitator (ESP) of the first, second and third fields were taken. Analysis of the gas sample taken at the ESP exit was performed. The ash distribution at different ash discharge ports was obtained. Analysis of the ash chemical composition was carried out. The specific consumption of oil shale per useful heat and gross electricity production was found and other techno-economic characteristics were determined. The tests at partial and nominal loads showed that the emission of SO₂, CO₂, CO, NO and HCl at nominal load were essentially higher. The content of fine ash particles (<2.5 μm) after the ESP was higher at nominal load.*

Results of analysis can serve as a basis for future research and development projects. Also, they can be used to decide whether to continue operation of PF units.

Keywords: *oil shale, pulverized firing, boiler efficiency, ash balance, flue gas composition.*

1. Introduction

Eesti Energia AS is Estonia's leading and one of the most significant power generating companies in the Baltic region. The company owns two power plants in the vicinity of Narva city – the Balti Power Plant (BPP) and the Eesti Power Plant (EPP), which are the biggest oil shale fired power plants

*Corresponding author: e-mail alar.konist@ttu.ee

in the world [1]. Most of power plants units are based on pulverized firing (PF) technology which has been applied since the 1960s. In the year 2004 the circulating fluidized bed (CFB) technology was successfully implemented for oil shale combustion. Since then a lot of studies have been conducted to describe this technology and determine the positive and negative aspects regarding oil shale combustion. Some of the results concerning the CFB technology and boiler reliability are presented in [2–15]. Even though CFB is the best available technology, the use of the PF technology is still needed to meet the energy demand during the period of transition from PF to CFB. At the same time, due to stricter environmental requirements there is a need to install equipment to reduce sulphur and nitrogen emissions.

Despite the fact that numerous theoretical and experimental studies described in [16] have been devoted to the oil shale PF technology, still a lot of valuable information is missing. In addition to PF and CFB combustion technologies of oil shale also an attempt was made to apply the vortex combustion (VC), which consists in the generation, in the lower part of the furnace, of a circulatory motion of the gas relative to the horizontal axis (the horizontal vortex) by rearranging the geometry of the combustion air injection and the fuel feeding into the combustion chamber. A detailed description of the effort to apply the VC to oil shale can be found in [17].

To compare CFB and PF technologies, including the efficiencies of desulphurization, the present situation with PF boiler emissions, ash balance and boiler efficiency had to be determined in detail, both at partial and nominal loads. In the frame of the research oil shale firing tests were performed on the boiler TP-101 of the EPP's energy unit No. 5. In the energy unit with a capacity of 200 MW_e the pulverized combustion technology is applied. The TP-101 boiler has four flues and its steam output is 320 t/h with parameters of 14 MPa and 540/540 °C. Some of the characteristics that are attributed to this technology include temperatures as high as 1350–1400 °C within the combustion chamber, the occurrence of reducing atmosphere zones in the furnace and the fine particle fraction of the ground fuel, but also significant features of the thermal conversion of the mineral part of oil shale.

2. Experimental set-up

The major goal of tests was to carry out the analyses of ash and flue gas, as well as verify data obtained in the 1980s – flue gas composition, ash balance and boiler efficiency. The tests were conducted with the oil shale of class P3 (particle size 0–40 mm) from the screening before enrichment from Estonia and Viru mines, and P4 (0–300 mm) fuel from the Estonia mine.

The main characteristics of the boiler during the tests are given in Table 1. The variations of steam pressure and mass flow during all tests are presented as well. It can be seen that the variations are smaller than the marginal values given in the standard EVS-EN 12952-15 (2003) [18].

Table 1. Boiler characteristics

Item	Partial load	Nominal load
Boiler load, MW _{th}	131.0	235.4
Electrical load of unit, MW _e	100.02	192.54
Steam temperature (live/superheated), °C	514.0/509.8	508.9/510
Steam pressure (live/superheated), MPa	12.76/1.02	12.91/2.06
Pressure variation of live steam, %	0.8	0.2
Steam mass flow (live/superheated), kg/s	44.26	85.08/74.93
Mass flow variation of live steam, %	4.2	1.5
Flue gas temperature (after the ESP), °C	181	190

During the tests the essential auxiliaries of the energy unit were registered. The total electricity use of the auxiliary equipment of the unit was 12.23 MW (12.2%) at partial load and 15.47 MW (8.0%) at nominal load.

During the tests the analyses of fuel, ash and flue gas were carried out. The location of ports for collecting samples is shown in Fig. 1. Fuel samples were taken on daily average basis. Ash samples were taken from several ports located in the furnace chamber, super heater (SH), economizer (ECO) and cyclone, and from all three fields of the electrostatic precipitator (ESP). Samples of fly ash for determining the mass division (total suspended particulates PM10 and PM2.5) were taken before the flue-gas fan. All ash samples were taken from both sides (A – left and B – right) of the boiler. The samples were used for determining a detailed chemical composition of cyclone and ESP ashes, including the content of CaO_{free} and CO_{2carbonate}. During the tests the electricity use of the auxiliary equipment of the unit and boiler efficiency were calculated as well.

The results of sample analyses were averaged to reach a representative estimate. Also, during the test the major process parameters of the boiler and unit as a whole were recorded using the plant's standard data acquisition

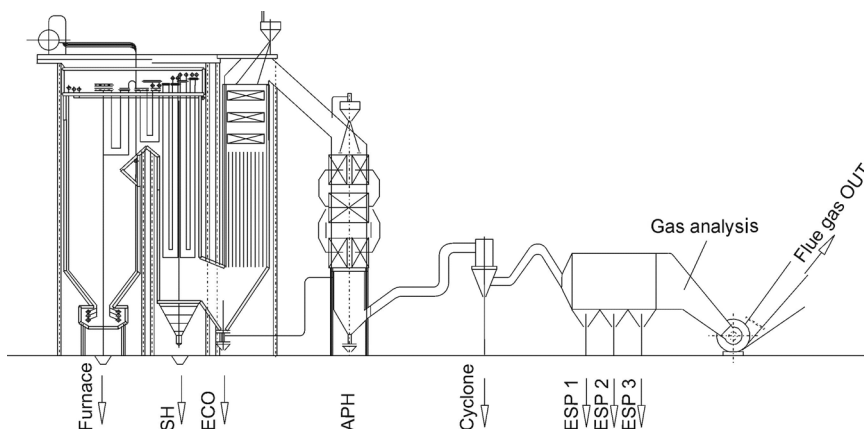


Fig. 1. Boiler TP-101 – sampling points.

system enabling to determine the unit's electricity self-consumption. The temperature and composition of flue gas were measured before the flue gas exhaust fan on both sides of the boiler.

The test at partial (50%; ~158 t/h of primary steam) boiler load was conducted firing oil shale from the Viru mine. During the nominal (100%; ~310 t/h) load test three varieties of oil shale supplied from Viru and Estonia mines were used.

The samples of bottom and fly ash from both boiler sides were taken at nominal and partial loads. The total of 16 ash samples were taken from several ports located in the furnace, super heater, economizer and cyclone, and from all three fields of the electrostatic precipitator (ESP1, ESP2 and ESP3). The ash was taken from the dry flow to ensure representative samples.

2.1. Composition of flue gas

The analysis of combustion gas was carried out at both loads and the sample was taken from the ports behind the ESP. The flow of combustion gas from the boiler is divided into two passes and directed into two ESPs (filters A (right) and B (left)). Gas samples for analyses were taken from both sides of the boiler as the composition of flue gas and ash mass flows in these ducts are different, as a rule. The measurements in both passes were made during 15 minutes. Also, the flow speed was measured periodically and temperature continuously.

The same ports were used for taking fly ash samples to determine the division of the finest particles (PM10 and PM2.5) in flue gas. The composition of flue gas was determined applying an FTIR type analyzer for wet gas, at a temperature of 180 °C. The flue gas moisture content was also determined by a FTIR spectrometer.

3. Results and discussion

3.1. Fuel – oil shale

The oil shale samples were analyzed in laboratories of the Department of Thermal Engineering (DTE) of Tallinn University of Technology and EPP. The local laboratory of EPP determined the daily average heating value and moisture content W_i^r . The DTE laboratory made the ultimate and proximate analysis of the same samples. Table 2 presents the heating values determined

Table 2. Oil shale characteristics

	Partial load	Nominal load
W_i^r , %	12.7	11.6
Q_b^d , MJ/kg	10.9	10.3
Q_i^r , MJ/kg	8.5	8.1
A^r , %	44.3	45.8
$(CO_2)_c^r$, %	16.7	17.2

in a calorimetric bomb (Q_b^d) as well as calculated by general moisture content (Q_i^r). The heating values determined in both laboratories are practically the same.

3.2. The chemical composition of ash samples

The samples were taken at two boiler loads: nominal (100%; ~310 t/h) and partial (50%; ~158 t/h). The composition of fuel and ash (at 815 °C) is presented in Table 3. The nitrogen content in ash samples was below detection limit.

Table 3. Chemical composition of ash, %

	Load, t/h	Furnace	SH	ECO	Cyclone	ESP 1	ESP 2	ESP 3
CO ₂	158	18.71	7.36	5.91	1.92	1.60	1.40	0.93
	310	2.67	1.10	2.87	1.08	1.68	1.46	1.18
C (CO ₂)	158	5.10	2.01	1.61	0.52	0.44	0.38	0.25
	310	0.73	0.30	0.78	0.29	0.46	0.40	0.32
C _{elem}	158	5.71	2.03	1.58	0.31	0.34	0.25	0.18
	310	0.72	0.21	0.68	0.19	0.35	0.25	0.16
S _{elem}	158	1.09	1.75	1.72	1.42	2.51	2.88	3.70
	310	0.83	1.53	1.79	0.98	2.37	2.75	3.42
SO ₃ total	158	2.73	4.38	4.30	3.56	6.28	7.20	9.25
	310	2.08	3.83	4.48	2.45	5.93	6.88	8.55
S _{sulphate}	158	1.02	1.75	1.74	1.44	2.44	2.76	3.65
	310	0.79	1.51	1.77	0.94	2.27	2.66	3.24
SO ₃ sulphate	158	2.55	4.38	4.35	3.60	6.10	6.90	9.13
	310	1.98	3.76	4.41	2.35	5.67	6.64	8.09
SiO ₂	158	12.99	16.25	20.01	23.77	34.41	36.02	41.32
	310	24.58	28.34	26.42	28.74	35.55	37.03	37.98
Fe ₂ O ₃	158	4.66	3.58	4.00	1.58	1.30	1.47	1.16
	310	3.85	4.05	4.17	4.11	3.93	4.08	3.97
Al ₂ O ₃	158	5.98	9.73	11.54	14.45	18.01	21.24	20.34
	310	14.70	8.50	6.85	7.59	9.22	8.89	11.33
CaO	158	57.74	59.08	58.54	57.21	36.04	33.46	28.01
	310	53.38	46.76	45.75	45.70	33.37	28.96	24.67
CaO _{free}	158	16.41	25.07	19.45	23.40	12.28	10.53	6.82
	310	19.79	14.35	15.00	17.31	10.35	9.63	6.28
MgO	158	0.90	2.95	1.04	2.02	1.45	1.09	2.04
	310	5.30	5.27	6.42	6.81	3.36	4.36	3.10
K ₂ O	158	1.16	1.69	1.73	1.93	4.10	5.51	7.49
	310	1.90	2.21	2.19	1.95	5.25	5.54	7.19
Na ₂ O	158	0.24	0.18	0.18	0.21	0.34	1.89	0.56
	310	0.24	0.24	0.22	0.19	0.38	0.41	0.47
Cl	158	0.22	0.16	0.16	0.16	0.22	0.40	0.54
	310	0.10	0.14	0.13	0.18	0.42	0.33	0.50
Loss on ignition, 815 °C	158	19.00	7.90	6.20	2.00	1.40	1.70	1.80
	310	3.00	1.25	2.90	0.90	1.80	1.60	1.70

Table 4. Carbon content in ash samples

Sampling point	Boiler load, t/h	Chemical analysis, %		Calculated, %	
		CO ₂	C _{elem}	CO _{carb}	C _{org}
Furnace	158	18.71	5.71	5.10	0.61
	310	2.67	0.72	0.73	0.01
Super heater	158	7.36	2.03	2.01	0.02
	310	1.10	0.21	0.30	0.07
Economizer	158	5.91	1.58	1.61	–
	310	2.87	0.68	0.78	–
Cyclone	158	1.92	0.31	0.52	–
	310	1.08	0.19	0.29	–
ESP 1	158	1.60	0.34	0.44	–
	310	1.68	0.35	0.46	–
ESP 2	158	1.40	0.25	0.38	–
	310	1.46	0.25	0.40	–
ESP 3	158	0.93	0.18	0.25	–
	310	1.18	0.16	0.32	–

The content of organic carbon in ash samples is given in Table 4 and the extent of carbonate minerals decomposition in various ash samples is presented in Table 5.

Table 5. The extent of carbonate minerals decomposition (k_{CO_2})

Boiler load	Furnace	SH	ECO	Cyclone	ESP 1	ESP 2	ESP 3
Partial	0.59	0.85	0.87	0.96	0.95	0.95	0.96
Nominal	0.94	0.97	0.92	0.97	0.95	0.95	0.96

The content of free lime (CaO_{free}) in ash samples taken from various fields of the ESP was 6–12%. Considering the filter balance the content was 10.1% at full load and 11.8% at partial load. The content of organic carbon is low as is typical of the pulverized combustion of oil shale.

The tests indicated that the extent of carbonate minerals decomposition (k_{CO_2}) at the nominal load is in the range of 0.92–0.97. At the partial load the decomposition is somewhat lower in ashes of the super heater and economizer – 0.85 and 0.87, respectively, and is substantially lower in bottom ash (0.59).

The size distribution of ash is presented in Table 6. The residue R₂₀₀₀ of the bottom ash on the sieve with an aperture of 2000 μm at the partial load was only 0.05%.

There are no significant differences in composition between ashes from tests at normal and partial loads. Still, the higher variability of the ash from the partial load test can be noticed. Also, the median size of the ash samples taken from the furnace, super heater and economizer at the full load is larger compared to the partial load ash.

Table 6. The size distribution of ash, % of cumulative oversize

Residue, R(x)	Boiler load, t/h	Furnace	Super heater	Economizer	Cyclone
0.500	158	14.44	7.62	1.02	–
	310	14.33	1.11	0.44	–
0.355	158	26.02	5.86	2.07	0.04
	310	27.46	17.99	3.02	0.14
0.180	158	57.92	39.90	24.26	4.83
	310	61.79	50.98	18.06	6.68
0.125	158	69.84	62.21	47.35	17.19
	310	75.62	66.89	33.69	22.35

For characterizing ashes and for drawing up an ash balance the bulk and aggregate densities of ashes were determined. Table 7 presents the aggregate densities determined for ashes from the super heater, economizer, cyclone and ESP 1. In order to obtain pure ash samples and exclude the falling of ash deposits from heating surfaces after automatic cleaning when ash sampling was performed, the ash samples were sieved using a 3 mm sieve before determination of density. The mass share of the sieved particles was 2–16%.

Table 7. Aggregate density of ash

Sampling point	Density, ρ , g/cm ³
Super heater	2.57
Economizer	2.60
Cyclone	2.71
ESP 1	2.63

The aggregate densities were used to estimate the ash mass flow. There was no variation of aggregate density at different boiler loads. Therefore, the average densities are presented by ash type (Table 7). The bulk densities determined by the DTE laboratory are given in Table 8.

Table 8. Bulk density of ash flows, g/cm³

Sampling point	Partial	Nominal
Furnace (bottom ash)	1.230	1.128
Super heater	1.201	1.209
Economizer	1.274	1.335
Cyclone	1.420	1.546
ESP 1	1.086	1.120
ESP 2	0.945	0.953
ESP 3	0.817	0.794

3.3. Ash balance

The method based on pulp (a mix of ash and water) was applied to determine the mass flow of ash from the super heater, economizer, cyclone and ESP

fields 1 to 3. The method described in detail in [17] includes the determination of ash flow rate by measuring pulp volume and mass.

The ash mass flows were determined for samples taken from under the super heaters, economizers and cyclone, and from ESP fields 1 to 3 at partial and nominal loads. The samples were taken twice at both loads and the mass flow was determined in every sample point three times. Therefore, the calculated value of the flow is the mean of six measurements. The results were used for drawing up the ash balance. The ash input into the boiler was calculated on the basis of the fuel flow by applying an indirect balance method. The amount of furnace ash was calculated subtracting the total volume of ash of super heaters, economizers, cyclone and all three fields of ESP from the volume of boiler input ash.

The ash balance at nominal load is presented in Fig. 2. The total share of ash from the furnace, super heaters and economizers is 51%. The results differ from those reported in [16] because four old ESPs have been replaced with three new ones. Also, the pre-precipitator chamber has been removed before the cyclone.

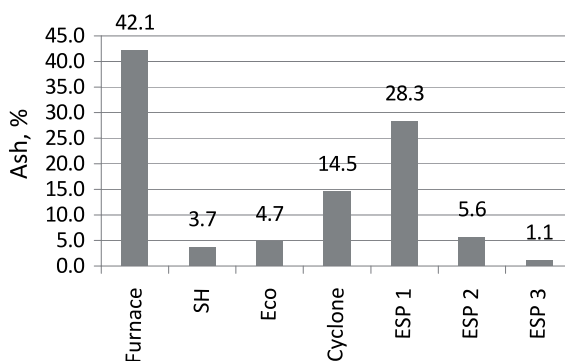


Fig. 2. Ash balance at nominal load.

3.4. Boiler heat balance

In the full-scale experimental study heat balance and thermal efficiency estimations of the TP-101 boiler were made on the basis of the standard [18] by using the indirect method taking into account the specific characteristics of oil shale as a fuel. The amount of heat released, ash content and flue gas amount during combustion of oil shale depend strongly on the endothermic and exothermic processes taking place in the mineral part of the fuel [16]. These processes include the decomposition of calcite and dolomite, oxidation of FeS_2 , sulfation of CaO and formation of new minerals. A more detailed description of the calculation of heat amount and ash content can be found in [7]. Combustion flue gas mass and volume and carbon dioxide ratio to fuel mass were calculated. For calculations the following equations were used:

1) flue gas mass (dry gas), kg/kg:

$$\mu_{\text{God}} = 12.5122\gamma_{\text{C}} + 26.3604\gamma_{\text{H}} - 3.3212\gamma_{\text{O}} + 1.0\gamma_{\text{N}} \\ + \left[(1 - \eta_{\text{S}}) 1.9953 + 3.2947 \right] \gamma_{\text{S}} + k_{\text{CO}_2} \gamma_{\text{CO}_2},$$

where γ_{C} , γ_{H} , γ_{O} , γ_{N} , γ_{S} , γ_{CO_2} are carbon, hydrogen, oxygen, nitrogen, sulfur and carbonate carbon dioxide contents in fuels, respectively, kg/kg; η_{S} is the efficiency of desulfurization (p. 8.3.5 in [18]); k_{CO_2} is the extent of carbonate mineral decomposition [19];

2) flue gas volume (dry gas), m³/kg:

$$V_{\text{God}} = 8.8930\gamma_{\text{C}} + 20.9724\gamma_{\text{H}} - 2.6424\gamma_{\text{O}} + 0.7997\gamma_{\text{N}} \\ + \left[(1 - \eta_{\text{S}}) 0.68172 + 2.6325 \right] \gamma_{\text{S}} + 0.509\gamma_{\text{CO}_2} k_{\text{CO}_2}.$$

3) carbon dioxide content ratio to fuel mass (dry gas), kg/kg:

$$\mu_{\text{CO}_2_0} = 3.6699\gamma_{\text{C}} + 0.0173\gamma_{\text{H}} - 0.0022\gamma_{\text{O}} \\ + \left[(1 - \eta_{\text{S}}) 0.001 + 0.0017 \right] \gamma_{\text{S}} + k_{\text{CO}_2} \gamma_{\text{CO}_2}.$$

All heat balance calculations were made for normal conditions: $t_{\text{r}} = 0$ °C, $p_{\text{r}} = 101\,325$ Pa. According to the above-mentioned EVS-EN standard the boiler efficiency at nominal load was 86.4% (Table 9).

Table 9. Boiler efficiency

Item	Value	
	kW	%
Heat input		
Heat from fuel combustion	264 599	97.2
Physical heat of fuel	846	0.3
Input heat of combustion air	6 431	2.4
Electrostatic precipitator	432	0.2
Total	272 308	100.1
Useful heat capacity	235 233	
Loss with flue gas	32 360	11.9
Loss due to unburned fuel (CO)	30	0.0
Bottom ash loss	2 979	1.1
Fly ash loss	0	0.0
Loss due to radiation	1 707	0.6
Total	37 076	13.6
Heat efficiency		86.4

3.5. Flue gas

The composition of flue gas was determined after the ESP (see Fig. 1). Additionally, the EPP personnel measured the flue gas oxygen content after the air preheater. The average concentration of major emission gases are given in Table 10.

The series of four tests were performed at both nominal and partial load. The test results (Table 10) indicate that the share of flue gas components depending on boiler load changes. At partial load the oxygen content in flue gas is twice that at full load. At full load the content of other components in flue gas is substantially higher as compared to that at partial load. For example, the content of SO₂ at full load is approximately twice that at partial load.

Table 10. Concentration of main pollutants in flue gas after the ESP (6% O₂)

Boiler load	O ₂ , %	CO ₂ , %	CO, ppm	NO, ppm	SO ₂ , ppm	HCl, ppm
Partial	12.5	12.9	17.2	145.6	938.3	55.9
Nominal	6.1	12.7	22.7	109.7	1059.1	60.2

The content of finest particles of fly ash together with its mass division (PM_{10/2.5}) after the ESP is an important indicator of flue gas composition. This is the fly ash that cannot be caught by the final section of the ESP and, as a result, is emitted into the ambient air.

The mass division of fly ash after the ESP was determined in three tests at both boiler loads (Fig. 3). As predicted, the content of finest ash particles (<2.5 μm) is higher at nominal load.

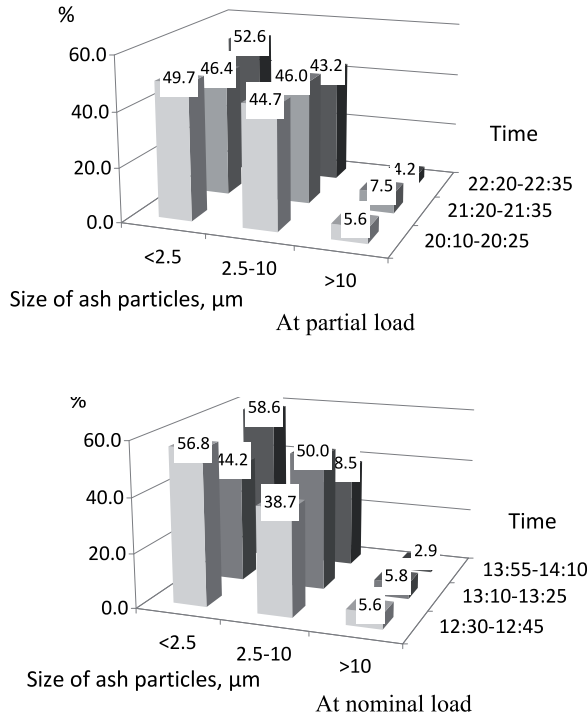


Fig. 3. Fly ash mass distribution after ESP.

3.6. Specific consumption and emission of the energy unit

Specific mass flow indicators of fuel and ash, CO₂, CO and SO₂ emissions both per useful heat (MWh_{th}) and gross electricity production (MWh_e^{br}) are given in Table 11. The specific indicators of fuel and ash per production unit obtained experimentally for the first boiler of the unit were assumed to be applicable for the second boiler as well. In Table 12 there are two values of the CO₂ emission – based on sample measurements, and calculated on the basis of fuel composition.

The heat rate of the unit was 2.49 MWh_{th}/MWh_e^{br}, corresponding to the gross energy efficiency of 40.16%.

Table 11. Specific indicators of fuel consumption and ash emissions

Indicator	Unit	Value
Oil shale consumption per useful heat	g/kWh _{th}	489
Ash formation per useful heat	g/kWh _{th}	223
Oil shale per electricity (gross)	g/kWh _e ^{br}	1219
Ash emission per electricity (gross)	g/kWh _e ^{br}	555

Table 12. Specific emission indicators

Pollutant	Per useful heat, kg/MWh _{th}	Per electricity (gross), kg/MWh _e ^{br}
CO ₂ ¹	391	974
CO ₂ ²	428	1066
CO	0.045	0.111
SO ₂	4.77	11.89

¹ Calculation based on measured percentage of CO₂ with calculated volume of dry gas.

² Calculation based on fuel composition.

4. Conclusions

The data from the experimental tests conducted on the high-pressure PF boiler TP-101 indicate that the gross thermal efficiency of the boiler is 86.4%. Regarding emission into air, the average concentration of NO_x and SO₂ emissions at stable load varied insignificantly. The test at partial and nominal loads showed that the specific emission of SO₂, CO₂, CO, NO and HCl at full load was essentially higher, e.g. the content of SO₂ was almost twice that at partial load. Also, the content of fine particles (<2.5 μm) of ash after the ESP was higher at nominal load.

During the test, the distribution of the ash amount at different boiler locations was experimentally obtained. The bottom and ESP ashes are the main contributors to the ash flow. The experimental results show that the present situation differs from the designed one as four old ESPs have been

replaced with three new ones and the pre-precipitator chamber has been removed before the cyclone.

The specific consumption of oil shale per useful heat and gross electricity production was 0.489 t/MWh_{th} and 1.219 t/MWh_e^{br}, respectively. The same indicators for ash formation were 0.223 t/MWh_{th} and 0.555 t/MWh_e^{br}.

The heat rate of the unit was 2.49 MWh_{th}/MWh_e^{br}, which corresponds to the gross energy efficiency of 40.16%.

The results of analysis are a good basis for future research and development projects. Also, they can be used to decide on the future operation of PF units at Narva PP.

Acknowledgements

The authors are grateful to the staff of Narva PP, and especially to Mr. Rain Veinjärv, Development Manager, for support in carrying out this project.

REFERENCES

1. Siirde, A. Oil shale – Global solution or part of the problem? *Oil Shale*, 2008, **25**(2), 201–202.
2. Arro, H., Loosaar, J., Ots, A., Pihu, T., Prikk, A., Rusheļjuk, P., Hiltunen, M., Hotta, A., Parkkonen, R., Peltola, K. Firing Estonian oil shale in CFB boilers. In *Proc. 19th FBC Conference*, May 21–24, 2006, Vienna, Austria, Part II.
3. Arro, H., Prikk, A., Pihu, T. Calculation of CO₂ emission from CFB boilers of oil shale power plants. *Oil Shale*, 2006, **23**(4), 356–365.
4. Arro, H., Prikk, A., Pihu, T. Combustion of Estonian oil shale in fluidized bed boilers, heating value of fuel, boiler efficiency and CO₂ emissions. *Oil Shale*, 2005, **22**(4S), 399–406.
5. Arro, H., Pihu, T., Prikk, A., Rootamm, R., Konist, A. Comparison of ash from PF and CFB boilers and behaviour of ash in ash fields. In *Proc. 20th International Conference on Fluidized Bed Combustion*, May 18–20, 2009, Xian City, China, 2010, Part 7, 1054–1060.
6. Hotta, A., Parkkonen, R., Hiltunen, M., Arro, H., Loosaar, J., Parve, T., Pihu, T., Prikk, A., Tiikma, T. Experience of Estonian oil shale combustion based on CFB technology at Narva Power Plants. *Oil Shale*, 2005, **22**(4S), 381–398.
7. Neshumayev, D., Ots, A., Parve, T., Pihu, T., Plamus, K., Prikk, A. Combustion of Baltic oil shales in boilers with fluidized bed combustion. *Power Technology and Engineering*, 2011, **44**(5), 382–385.
8. Parve, T., Loosaar, J., Mahhov, M., Konist, A. Emission of fine particulates from oil shale fired large boilers. *Oil Shale*, 2011, **28**(1S), 152–161.
9. Pihu, T., Arro, H., Prikk, A., Rootamm, R., Konist, A. Corrosion of air pre-heater tubes of oil shale CFB boiler. Part I. Dew point of flue gas and low-temperature corrosion. *Oil Shale*, 2009, **26**(1), 5–12.

10. Plamus, K., Ots, A., Pihu, T., Neshumayev, D. Firing Estonian oil shale in CFB boilers – ash balance and behaviour of carbonate minerals. *Oil Shale*, 2011, **28**(1), 58–67.
11. Plamus, K., Soosaar, S., Ots, A., Neshumayev, D. Firing Estonian oil shale of higher quality in CFB boilers – environmental and economic impact. *Oil Shale*, 2011, **28**(1S), 113–126.
12. Suik, H., Pihu, T., Molodtsov, A. Wear of the fuel supply system of CFB boilers. *Oil Shale*, 2008, **25**(2), 209–216.
13. Suik, H., Pihu, T. Warranty reliability of CFB boiler burning oil shale. *Oil Shale*, 2009, **26**(2), 99–107.
14. Suik, H., Pihu, T., Konist, A. Catastrophic wastage of tubes in fluidized bed boiler. *Oil Shale*, 2011, **28**(1S), 162–168.
15. Kartushinsky, A., Siirde, A., Rudi, Ü., Shablinsky, A. Mathematical model of two-phase flows loaded with light and heavy particles to analyze CFB processes. *Oil Shale*, 2011, **28**(1S), 169–180.
16. Ots, A. *Oil Shale Fuel Combustion*. Tallinn, 2006, 833 pp.
17. Pihu, T., Konist, A., Neshumayev, D., Loosaar, J., Siirde, A., Parve, T., Molodtsov, A. Short-term tests on firing oil shale fuel applying low-temperature vortex technology. *Oil Shale*, 2012, **29**(1), 3–17.
18. EVS-EN 12952-15:2003. *Water-Tube Boilers and Auxiliary Installations*. Part 15. Acceptance Tests.
19. Arro, H., Prikk, A., Pihu, T. Calculation of qualitative and quantitative composition of Estonian oil shale and its combustion products. Part 1. Calculation on the basis of heating value. *Fuel*, 2003, **82**(18), 2179–2195.

Received July 4, 2012

PAPER III

SHORT-TERM TESTS ON FIRING OIL SHALE FUEL APPLYING LOW-TEMPERATURE VORTEX TECHNOLOGY

T. PIHU^{(a)*}, A. KONIST^(a), D. NESHUMAYEV^(a),
J. LOOSAAR^(a), A. SIIRDE^(a), T. PARVE^(a), A. MOLODTSOV^(b)

^(a) Department of Thermal Engineering
Tallinn University of Technology
116 Kopli St., Tallinn 11712, Estonia

^(b) Eesti Power Plant
PO Box 140, Narva 21001, Estonia

The present paper provides experimental data from short-term, full-scale experiments of a high-pressure pulverized firing (PF) boiler, TP-67, firing oil shale after a retrofit to use vortex combustion (VC) technology. The essence of VC technology consists of the generation, at a lower part of the furnace, of a circulatory motion of gas relative to the horizontal axis (horizontal vortex) by rearranging the geometry of the combustion air injection and the fuel feeding into the combustion chamber. The tests were conducted at three boiler loads: 50% (160 t/h), 75% (240 t/h) and 100% (320 t/h). During the experiments, fuel samples of air-solids in the conduit and samples of bottom ash and fly ash from inertia dust collectors after the super heater (SH) and economizer (ECO), as well as fly ash from the electrostatic precipitator (ESP) of the first and second fields, were taken from both the left and the right sides of the boiler. The gas analysis was performed at the ESP exit. It was attempted to measure temperature distribution in the combustion chamber. Temperature measurements in the furnace using an infrared thermometer showed that the maximum temperature did not exceed 1150 °C, and there was slight temperature nonuniformity across the combustion chamber. During the tests, the ash distribution at different boiler ash discharge ports was obtained. Analysis of the bottom ash chemical composition showed a considerable increase in the amount of unburned carbon and marcasite S_p . The retrofit of the boiler to use VC technology did not result in a reduction in the amount of SO_2 emissions, indicating an even weaker process of binding sulphur oxides in the furnace as compared to PF.

Introduction

At the present time, more than 90% of the electricity production in Estonia is generated by burning oil shale fuel, and most of this electricity generation is

* Corresponding author: e-mail tpihu@staff.ttu.ee

based on pulverized firing (PF) technology. Some of the characteristics that are attributed to this technology, including temperatures as high as 1350–1400 °C within the combustion chamber, the occurrence of reducing atmosphere zones in the furnace and the fine particle fraction of ground fuel, also significantly characterize the thermal conversion of the mineral part of oil shale, which will eventually lead to intense deposition formation and corrosion of the boiler heat transfer surfaces. Generally, it is possible to decrease the deposition formation and the rate of corrosion of the heat transfer surfaces, therefore improvement of the fuel efficiency, by decreasing the temperature in the combustion chamber, increasing the coarse-ground particle fraction of the fuel and preventing the formation of reducing atmosphere zones in the furnace.

One concept pertaining to combustion technology that makes it possible to decrease the temperatures in the combustion chamber is the low-temperature vortex combustion (VC) method, the basic principles of which were first developed by Leningrad Polytechnical Institute in collaboration with NPO CKTI (formerly Central Boiler and Turbine Institution) [1]. The essence of this combustion technology consists of the generation, at a lower part of the furnace, of a circulatory motion of the gas relative to the horizontal axis (horizontal vortex) by rearranging the geometry of the combustion air injection and the fuel feeding into the combustion chamber. This process allows for a reduction in the maximum temperature level within the furnace, which equalizes the heat flux distribution and increases the heat absorption. Due to multiple circulations of the particles in the furnace, the coarse-ground particle fraction of the fuel could be fed.

The first full-scale experiments on vortex combustion technology using oil shale as fuel were conducted in the early 70s on the medium-pressure boiler BKZ-75-39F at the Ahtme Thermal Power Plant (Estonia) and Slantsy Power Plant (Russia). The main findings have been previously described [1–10]. During the reconstruction of the boilers, the combustion air injection direction of the frontal mounted burners was changed, and the nozzles of the lower forced draft were mounted within the opening of the combustion chamber throat. The grinding fineness of the fuel was increased from $R_{90} = 16.5\text{--}28$ to $R_{90} = 48\text{--}60$. To maintain the temperature in the furnace below 1180 °C, the exceeding of which leads to an intensification of the slagging processes and the formation of tightly bound deposits, a radiant super heater platens was installed in the lower part of the combustion chamber. To reduce the erosive wear of the economizer (ECO) in the flue gas pass after the convective super heater, a specially designed high-temperature ash collector was mounted. The arrangements made during the reconstruction helped to increase the maximum nominal steam capacity from 16.7–18.0 kg/s up to 21.0–21.7 kg/s and to increase the boiler's thermal efficiency (gross) from 86.0–86.5% up to 88.0–90.8% due to the decrease of the flue gas temperature at the boiler outlet. Simultaneously, increases in losses due to enthalpy and unburned carbon in the bottom ash were observed; they were caused by

the increased amount of ash particles captured in the furnace (up to 50%) when using the coarse-ground particle fraction of the fuel. The considerable increase in the content of sulphur, mainly marcasite, in the bottom ash was found to be caused by the occurrence of the reducing atmosphere zones in the furnace.

As described previously [10], a comparative analysis of the chemical composition of the fly ash that was obtained using the different fuel combustion technologies like PF and VC showed that the content of the ash components that are most prone to sulphation, such CaO and MgO, are nearly identical in the fine particle fraction and in the coarse particle fraction. When using VC for firing coarse-ground fuel, no noticeable increase in the relative K₂O content in the fine particle fraction relative to the content in the coarse fraction was observed when the median diameter Δ_s of the fly ash was increased. The ratio of the K₂O in case of the vortex combustion was approximately 2.2 at $\Delta_s = 51 \mu\text{m}$, whereas for PF it reached a value of approximately 3.5–4.1 μm as Δ_s increased up to 26–28 μm . The considerable increase in the chlorine content (Cl = 2.56–3.82%) in the fine fraction of the fly ash using VC was found to be several times higher than the corresponding content (Cl = 0.20–0.50%) [2] using PF. In the opinion of the authors, this difference was caused by changing the atmosphere of the combustion chamber (the occurrence of the reducing atmosphere zones).

Subsequently in 1981, the reconstruction of the high-pressure boiler TP-17 at Balti Power Plant to use VC technology was performed [1]. Experiments showed that during the entire period of the operation of the boiler before the planned overhaul, the gas temperatures along the flue gas path, as well as the steam temperatures, remained stable without the application of heat transfer surface cleaning devices in the furnace and super heater. Intensive deposit formation on the heating surfaces could be explained as follows [1]. It is known that the chemical composition of the ash that forms during oil shale combustion is different for the various ash particle fractional groups; the most chemically active components are contained within the finest ash particle fraction. As VC technology uses coarse-ground fuel and there is strong relationship between fractional compositions of the fuel and the ash formed, there is a decrease in the fraction of particles that contain chemically active components and an increase in the fraction of inert particles that have a destructive effect on deposit formation.

Simultaneously, the coarse particle fraction of the ash, the increased flue gas velocity that occurs with formation along the flue gas pass cross-sections with a highly nonuniform flow and the distribution of the fly-ash particles have significantly intensified the erosive wear process. For example, in the case of the medium-pressure boiler BKZ-75-39F, after 350 h of continuous operation at a mean boiler load of 20.5 kg/s, a magnitude of wear of the economizer tubes of approximately 0.4–0.6 mm was observed.

The present paper provides experimental data from a short-term, full-scale test of a high-pressure boiler, TP-67, firing oil shale after reconstruc-

tion to use VC technology. The implementation of VC technology on high-pressure boiler TP-67 was performed by Polytechenergo Ltd during 2008–2010.

Experimental

The full-scale experiments of the present investigation were carried out on a high-pressure boiler, TP-67, at the Balti Power Plant, which is located in eastern Estonia [11]. The boiler is of a Taganrog boiler-making works (“Krasny Kotelshchik”) design and has been in operation since the 60s. The main parameters of the boiler are as follows: boiler load (live steam) 280 t/h, live steam pressure and temperature – 13.8 MPa and 515 °C, respectively.

The lower heating value (LHV) of oil shale used in the thermal experiments was at approximately 10.77 MJ/kg; the studied oil shale characteristics on an as-received basis are provided in Table 1.

The flue gas analysis performed by the plant personnel from the gas laboratory shortly before the transfer of the boiler to use VC technology showed that the normalized contents (reduced to O₂ = 6%) of the SO₂ and NO_x for the dry gases were approximately 2097 mg/Nm³ and 338 mg/Nm³, respectively.

In the original design, the boiler (see Fig. 1) was equipped with vortex burners that are mounted on the frontal panel in two different row arrangements, with four burners on each row. The fuel is ground by four MMT-1500-2510-735 hammer mills, which have a compact separator of the pulverized fuel at their outlet. In addition to a combustion chamber, the boiler has two vertical flue gas passes in the first downflow, in which the hanging platen super heaters having longitudinal flows of gas are installed. The second rising flue gas pass contains the economizer and the air

Table 1. Studied oil shale characteristics on an “as-received” basis

Parameter	Value, wt%
Carbon, C ^r	25.87
Hydrogen, H ^r	3.34
Oxygen, O ^r	4.76
Nitrogen, N ^r	0.05
Organic sulphur, S _o ^r	0.3
Pyritic sulphur, marcasite, S _p ^r	0.91
Sulphate sulphur, S _s ^r	0.09
Chlorine, Cl	0.14
Mineral carbon dioxide, CO ₂ ^r	12.9
Corrected ash content, A _{co} ^r	36.28
Crystal water, W ^r	0.56
Moisture, W ^r	14.9
Total*	100

* – does not contain sulphate sulphur because it is included in the corrected ash content

preheater. Behind the air preheater, the flue gas pass splits into two channels (channel A, located on the left side of the boiler front, and channel B, located on the right side) that connect the tail of the boiler with two electrostatic precipitators (ESP), the left ESP and the right ESP relative to the front of the boiler. Each ESP is connected to the induced draft fan by two channels (left and right channels, similarly denoted relative to the front of the boiler). A more detailed description, including the design features and thermal characteristics of the considered boiler can be found in [2].

For generation of low-temperature horizontal vortex motion in the combustion chamber, a set of modifications were made. The modifications included replacing the vortex burners that were located at the lower row with direct-flow burners with a downward slope. The opening of the combustion chamber throat along the entire width of the lower forced draft was performed by mounting two-stage deflection-nozzle devices. With the aim of obtaining a coarse-ground fraction of fuel feeding into the lower row of burners, the hammer-mill separator was modified. The forced draft fan capacity was increased by building up the fan wheel blades and installing a more powerful motor.

The tests were conducted at three boiler loads: 50% (160 t/h), 75% (240 t/h) and 100% (320 t/h). The sampling of pulverized fuel from the air-solids conduits supplying fuel to the replaced direct-flow burners of the lower burner row (with a modified solid separator) and to the original vortex burners of the upper row was performed to determine the particle size distribution. The sampling was performed by means of a VTI design sampling device with a cobra-type probe head with an inner diameter of 46 mm. The probe was equipped with a manual system allowing the equalization of the velocities in the channel of the probe and in the pulverized fuel conduit during the sampling (isokinetic sampling). The fuel samples were taken over the cross section of the air-solids conduit at ten points that were derived by dividing the conduit's cross-sectional area into concentric, equal area rings and a central circle.

During the experiments, samples of bottom ash and fly ash from the inertia dust collectors after SH and ECO, as well as from the ESP of the first and second fields, were taken from both the left and the right sides of the boiler. The ash sampling location is shown in Fig. 1. In addition, the isokinetic fly ash samples from the flue gas pass after the AP and before the ESP were obtained. To determine the modified boiler ash balance, the ash mass flow rates in the ash discharge ports were received experimentally. The ash mass flow of the dust collectors located under the SH and ECO were determined by a slurry method that consisted of measuring the time required to fill the calibrated volume by slurry and in the subsequent determination of the slurry mass. The mass flow of the fly ash entering into the ESP was obtained by measuring the fly ash content in the flue gas pass before the ESP; the measurements were performed using an Emes 3866 (VTT-Energy Ltd) according to Finnish standard SFS 3866. The bottom ash flow mass was

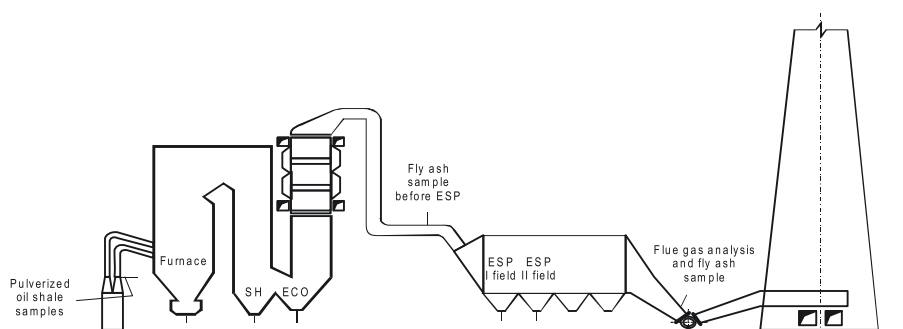


Fig. 1. Sectional side view of the Boiler TP-67.

calculated as the difference between the total ash mass flow entering into the boiler with fuel, which was determined through the indirect heat balance of the boiler, and the total fly ash mass flow.

The gas analysis was performed both in the right flue gas duct at the left ESP exit and in the left flue gas duct at the right ESP exit using the F-TIR type gas analyzer (Gasmeter DX-4000).

During the tests, an attempt was made to measure the temperature distribution in the combustion chamber. The measurements were performed by an infrared thermometer (M90L, Mikroninstrument) operating in the CO_2 absorption band. Prior to these tests, parallel measurements of the flame temperature in the furnace of a boiler that was firing oil shale made with this infrared thermometer and a suction pyrometer have shown that the spectral flame emissivity in the CO_2 absorption band is close to unity.

Results and discussion

Temperature distribution in the furnace

The measurements of the flame temperature in the furnace were performed at five different cross-sections along the height of the boiler (see Figs. 2-4) in the following locations: at 8 m on the left and right sides of the furnace, at 12 m in the left rear corner, at 16 m on the rear wall, at 20 m on the left and right sides and on the center of the frontal wall and at 24 m on the left part of the frontal wall.

The first measurements at full load have shown that the gas temperature in the left upper part of the furnace volume was significantly higher than the corresponding values for other measuring points. The maximum temperature obtained was $1370\text{ }^\circ\text{C}$ and varied within the range from $1270\text{--}1370\text{ }^\circ\text{C}$. A high nonuniformity of the temperature field along the furnace width was observed. In subsequent experiments, after the reconstruction team performed some additional boiler adjustments, the maximum temperature was decreased and no longer exceeded $1150\text{ }^\circ\text{C}$, and the temperature distribution along the furnace cross section was more uniform.

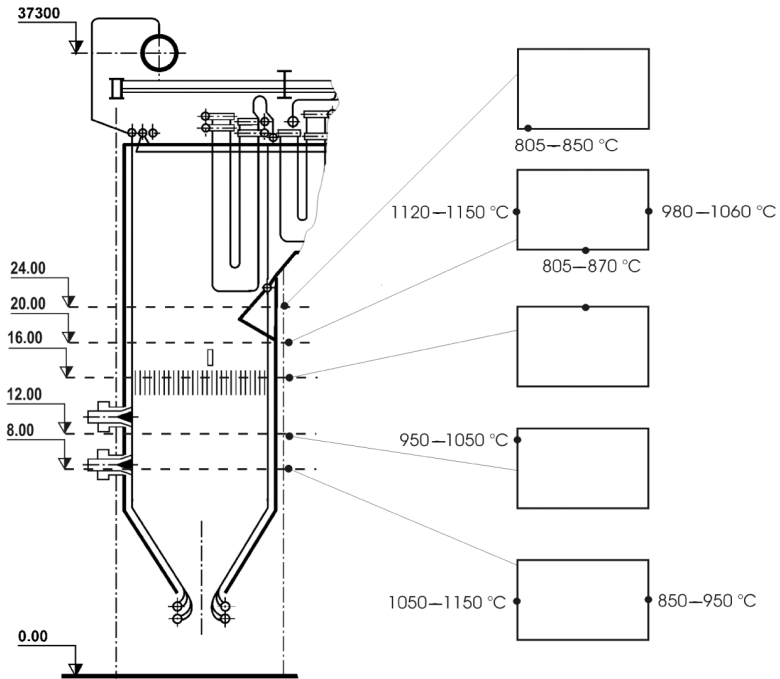


Fig. 2. Temperature distribution in the furnace at 100% boiler load.

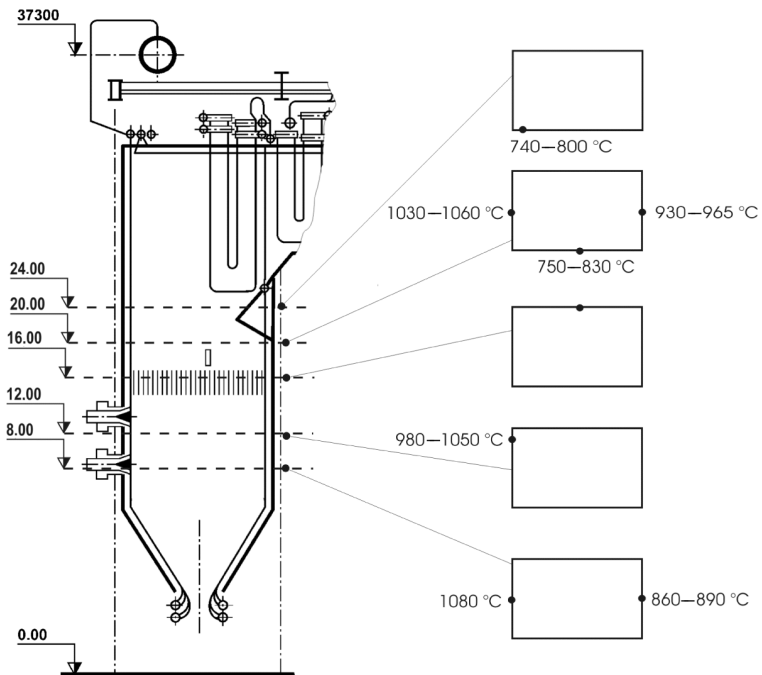


Fig. 3. Temperature distribution in the furnace at 75% boiler load.

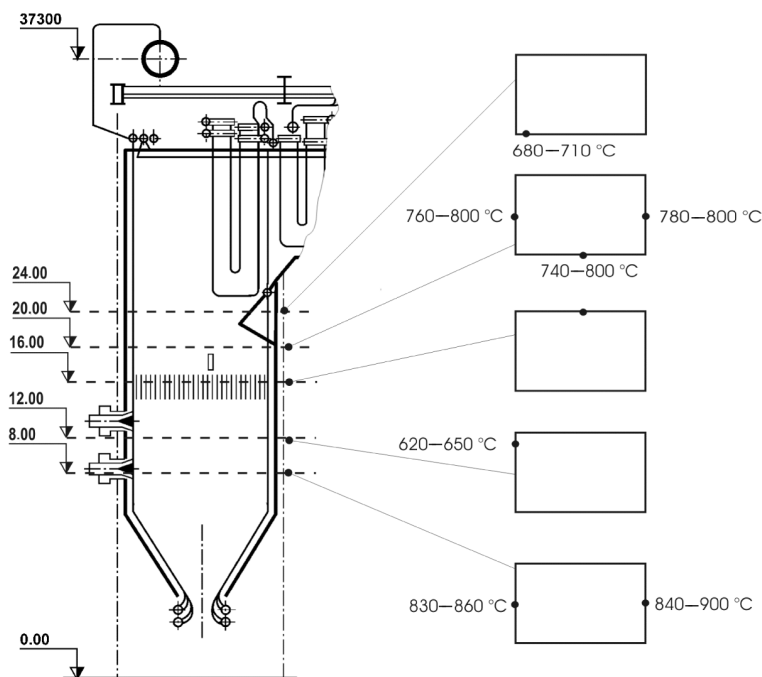


Fig. 4. Temperature distribution in the furnace at 50% boiler load.

Size distribution analysis of fuel/ash and ash mass flow balance

The results of a comparative size distribution analysis of the pulverized fuel after both a modified and an unmodified separator are presented in Table 2. It is clear that there are significant differences in the fuel fractional composition. The median particle diameter of the fuel entering the lower row burners increased by 2.5-fold, and the percentage residue R_{200} on the sieve with a grid spacing of $200\ \mu\text{m}$ increased by approximately 1.7 times, indicating increasing percentages of coarse fuel particles as compared to finer particles.

Firing coarse-ground fuel resulted in changing the fractional composition of the bottom and fly ashes (see Table 3). As compared to the PF technology at a full boiler load (here, as an example, the ash particle fractional composition of the PF boiler TP-101 is used), it can be seen from Table 3 that significant ash particle coarsening occurs in different boiler locations.

Table 2. Fractional composition at 100% boiler load

Parameter	Modified separator	Unmodified separator
Median particle diameter Δ_m , μm	90–200	35–50
Sieve residue R_{90} , %	46–57	32–42
Sieve residue R_{200} , %	34–46	19–29

Table 3. Fractional composition of the ash at different ash discharge ports at 100% boiler load

Parameter	Bottom ash	Super heater	Economizer	ESP 1 field
Median ash particle diameter Δ_m , μm	600–1500	300–380	290–320	25–45*
Sieve residue R_{90} , %	~95*	~95*		15–30
Sieve residue R_{200} , %	80–90	70–80	75–85	3–6
Median diameter (TP-101 boiler) Δ_m , μm	200–300	~180	~95	10–12
Sieve residue (TP-101 boiler) R_{90} , %	~88	~80	~55	
Sieve residue (TP-101 boiler) R_{200} , %	~56	~45	~15	

* – values are obtained by extrapolating

More than a two-fold increase in the median ash particle diameter Δ_m was observed. The residue R_{8000} of bottom ash on the sieve with an aperture of 8000 μm varied within the range from 0.5–4%, depending upon on which side of the boiler furnace the ash sample was obtained from. A relative increase in the coarse fraction and a decrease in the fine fraction of the ash has likely become one of the main factors resulting in the reduction of the rate of deposit formation on heating surfaces. This change has allowed for an increase in the boiler capacity from 290 t/h to 320 t/h. The coarse particle fraction increase with the simultaneous increase of the flue gas pass velocity due to both the increase in the boiler load and the change in the combustion air regime can cause the intensification of the erosive wear process on the heating surfaces; the parts that are most susceptible to wear are the tubes of the ECO.

When reducing the boiler load to the minimum (50% of rated load, 160 t/h), an increase in the median particles diameter Δ_m of the bottom ash and the first fields ESP fly ash was observed (see Table 4). In contrast, a slight decrease in the median diameter of the fly ashes collected from the SH and ECO ducts was found.

The results of the ash balance of the considered reconstructed boiler under a full load (100%, 320 t/h) are depicted in Fig. 5. From Fig. 5, it can be seen that in spite of the coarsening of the ash particles, the share of the ash streams captured in the furnace (bottom ash) was smaller than expected compared to the previously conducted experiments on medium-pressure boilers that were described in Introduction section. The bottom ash stream was found to be approximately 23% of the total ash flow rate. In the absence

Table 4. Fractional composition of the ash at different ash discharge ports at 50% boiler load

Parameter	Bottom ash	Super heater	Economizer	ESP 1 field
Median diameter Δ_m , μm	900–1500	220–270	280–300	90–120
Sieve residue R_{90} , %	~95*	~94*		52–67
Sieve residue R_{200} , %	95–97	60–67	70–78	18–20

* – values are obtained by extrapolating

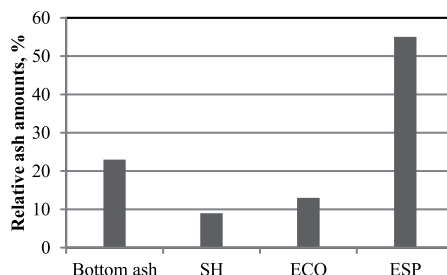


Fig. 5. Ash mass flow rate distribution at different ash discharge ports at 100 % boiler load.

of reliable data in the literature concerning the ash stream distribution at different ash discharge locations of the studied boiler using PF technology, it could be stated on the basis of experimental data that there was a slight decrease in the bottom ash flow rate after the retrofit of the boiler to use VC technology. An even smaller amount of total ash was discharged in the inertia ash collectors located in the SH and ECO ducts: 9% and 13%, respectively. Therefore, the main part of the total ash, approximately 55%, was entrained by the flue gas stream and collected at the ESP.

During the present experiments, an attempt was made to obtain ash amount distributions at different boiler locations at the boiler minimum load (50%, 160 t/h of live steam). Due to inaccuracies in determining the fly ash content entering the ESP at increased gas velocities, these data are not presented here. However, according to these data, an increase was observed in the amounts of bottom ash and fly ash discharged at inertia ash collectors located in the SH and ECO ducts.

Chemical composition of the ash

The results of the chemical analysis of the ash at different discharge locations at a boiler load of 320 t/h (100%) and 160 t/h (50%) are summarized in Tables 5 and 6. Analyzing the chemical composition of the bottom ash when firing oil shale by applying VC technology shows a considerable increase in the amount of unburned carbon, which was caused by the separation of the coarser, unburned particles through the furnace throat opening. A significant increase in the amount of marcasite sulphur S_p in the bottom ash, most probably due to the occurrence of reducing atmosphere zones in combustion chamber, was also observed. The simultaneous maintenance of a lower temperature in the furnace with the feeding of coarse-ground fuel resulted in a lower degree of decomposition of carbonate minerals in the furnace as compared to the PF technology. At a full boiler load, the extent of the carbonate mineral decomposition was approximately $k_{CO_2} = 0.84$.

From Tables 5 and 6, it can be seen that the content of components causing sulphation, such as CaO and Na₂O, in the finer fraction of the ash

Table 5. Chemical composition of the ash at different ash discharge ports at 100% boiler load

Parameter	Bottom ash, right side, wt%	Bottom ash, left side, wt%	Super heater, right side, wt%	Super heater, left side, wt%	Economizer, right side, wt%	Economizer, left side, wt%	ESP 1 field, right side, wt%	ESP 1 field, left side, wt%	ESP 2 field, right side, wt%	ESP 2 field, left side, wt%
CO ₂	21.5–26.5	19.3–14.1	3.6–4.7	3.3–4.3	4.7	2.5–4.0	2.6–2.7	2.0–2.5	2.7	2.5
C _{el}	9.59–10.61	8.00–7.13	0.93–1.23	0.73–1.11	1.21	0.57–1.07	0.64–0.60	0.43–0.45	0.66	0.48
S _{el}	0.78–0.92	0.85–0.78	1.40–1.59	1.56–1.94	1.50	1.49–1.48	2.84–2.35	2.65–2.45	2.47	3.16
SO _{3total}	1.95–2.30	2.13–1.95	3.43–3.63	3.48–3.73	3.75	3.73–3.70	7.1–5.88	6.63–6.13	6.18	7.90
S _s	0.46–0.39	0.52–0.51	1.40–1.56	1.55–1.94	1.52	1.49–1.60	2.75–2.32	2.80–2.42	2.44	2.90
S _p	0.32–0.53	0.33–0.27	0.03	0.01	–	–	0.09–0.03	0.03	0.03	0.26
SiO ₂	14.64–11.22	18.20–18.37	23.72–22.4	24.4–23.0	20.72	22.52–22.17	30.75–29.25	25.77–27.81	24.84	26.58
Fe ₂ O ₃	3.55–3.62	2.49–3.81	5.15–4.56	5.01–4.51	4.56	4.70–4.69	4.47–4.79	4.20–4.66	4.42	4.07
Al ₂ O ₃	4.88–10.40	5.61–4.56	6.48–5.87	6.72–5.77	4.12	4.66–5.12	11.82–7.44	7.31–7.76	5.48	6.56
CaO	52.45–50.32	45.68–54.04	53.21–54.06	51.66–50.79	55.82	55.80–50.89	48.97–43.08	49.32–44.21	50.23	46.07
CaO _{free}	5.57–6.06	8.56–6.67	24.49–24.22	25.08	–	–	19.45–14.62	18.12–15.53	–	–
MgO	2.56–3.86	1.79–3.22	1.51–2.66	3.42–4.11	2.68	3.06–6.72	0.52–4.62	3.06–4.82	2.49	2.09
K ₂ O	0.16–0.14	0.16–0.14	2.08–2.11	2.10–3.64	1.64	1.61–1.8	0.85–3.20	3.03–3.07	2.41	3.27
Na ₂ O	1.27–1.10	1.41–1.72	0.18–0.20	0.18–2.28	0.18	0.16–0.16	0.21–0.20	0.22–0.21	0.18	0.23
Heat loss	25.1–30.5	23.6–20.3	3.8–4.8	3.3–4.7	4.9	2.4–4.3	2.9–2.6	2.1–2.1	2.8	2.3

Table 6. Chemical composition of the ash at different ash discharge ports at 50% boiler load

Parameter	Bottom ash, right side, wt%	Bottom ash, left side, wt%	Super heater, right side, wt%	Super heater, left side, wt%	Economizer, right side, wt%	Economizer, left side, wt%	ESP 1 field, right side, wt%	ESP 1 field, left side, wt%	ESP 2 field, right side, wt%	ESP 2 field, left side, wt%
CO ₂	31.4	30.0	15.1	13.3	15.1	13.4	7.6	6.9	4.5	4.2
C _{el}	17.73	11.99	4.04	3.65	4.17	3.61	2.04	1.81	1.19	1.00
S _{el}	1.17	1.17	1.59	2.10	2.17	1.97	2.59	2.45	2.84	3.0
SO ₃ total	2.93	2.93	3.98	5.26	5.43	4.93	6.48	6.13	7.10	7.50
S _s	0.33	0.50	1.59	2.15	2.12	2.00	2.48	2.40	2.81	2.94
S _p	0.84	0.67	—	—	0.05	—	0.11	0.05	0.03	0.06
SiO ₂	7.95	8.99	14.94	17.23	13.13	13.83	20.55	19.77	27.68	27.61
Fe ₂ O ₃		2.42	3.81	3.97	3.89	3.37	4.24	2.13	4.47	4.63
Al ₂ O ₃		5.47	4.56	4.30	3.66	7.18	4.23	13.09	5.56	5.48
CaO	47.0	50.54	49.86	52.13	50.22	54.11	50.47	63.49	43.38	42.77
CaO _{free}	2.0	5.67	20.92	23.9				23.69		
MgO	2.49	3.70	2.00		4.79	2.59	3.37	4.43	2.73	2.78
K ₂ O	0.85	0.92	1.89	1.34	1.37	1.19	1.55	1.92	2.64	2.91
Na ₂ O	0.19	0.12	0.15	0.13	0.13	0.15	0.13	0.19	0.20	0.21
Heat loss	41.3	34.0	14.7	13.6	15.5	13.3	7.6	6.8	4.6	4.0

($\Delta_m = 25\text{--}40\ \mu\text{m}$, fly ash obtained from the first field of the ESP in the case of VC and from the cyclone of boiler TP-101 in the case of PF) is approximately the same for the VC and PF technologies. However, the content of MgO was found to be somewhat lower (on average 50%), and the content of K₂O was found to be higher (on average 50%) for the VC compared to the PF technology.

Flue gas analysis

The results of the flue gas analysis performed behind the ESP before the induction of a draft fan in two ducts at different boiler loads are presented in Table 7. It can be seen that the retrofit of the boiler to use VC technology did not result in a reduction of SO₂ emissions, indicating an even weaker process of binding sulphur oxides in this furnace compared to the PF. This lack could partially be explained by the following reasons. As the Estonian oil shale in nature is heterogeneous fuel, during the process of oil shale pulverizing and separating, the redistribution of the fuel components by particle fractions occurs: the sulphur (most forms) locates within the finer particle fraction, whereas molecules participating in the process of binding sulphur oxides, i.e., the free lime CaO_{free}, locate within coarser particle fraction. During the fuel particle separation process that occurs in a vortex combustion chamber, the lighter particles, containing mostly the organic components of fuel (organic sulphur in particular), and the finer particles, consisting of the sandy clay part of the fuel (marcasite in particular), are entrained by the gas stream into the direct-flow jet, bypassing the recirculation vortex zone that forms in the lower part of the furnace. As a result, the CaO content decreases in just that zone where the modification of sulphur oxides occurs during combustion. Additionally, the reduction in sulphur capture that occurs by implementing VC is obviously caused by the coarsening of the ash particles, which then have a smaller specific surface area compared to the ash that forms during PF. The specific surface area

Table 7. Emissions of SO₂, NO_x and CO at different boiler loads

Experiment number	Flue duct	Boiler load, t/h	NO _x , mg/Nm ³ (6% O ₂)	SO ₂ , mg/Nm ³ (6% O ₂)	CO, mg/Nm ³ (6% O ₂)
Exp 1	ESP A, right channel	160	312	3585	830
Exp 2	ESP A, right channel	160	455	1707	40.1
Exp 3	ESP A, right channel	160	362	2225	25.5
Exp 4	ESP B, left channel	160	391	1971	26.2
Exp 5	ESP B, left channel	240	384	2314	13.5
Exp 6	ESP A, right channel	240	372	2490	9.9
Exp 7	ESP B, left channel	320	327	3164	0.0
Exp 8	ESP A, right channel	320	336	2715	1.1
Exp 9	ESP A, right channel	320	334	3083	0.2
Exp 10	ESP B, left channel	320	302	3344	0.3

decrease inevitably leads to a decrease in the intensity of the chemical reaction between CaO and SO₂.

The results show that with increasing boiler loads, the SO₂ content was increased and varied within the range from 2715–3344 mg/Nm³ (reduced to 6% of the O₂). The content of the nitrogen oxides NO_x for both combustion technologies at a full boiler load was at approximately the same level. As the boiler load decreases, the content of the NO_x increases.

Conclusions

The present paper provides experimental data from short-term, full-scale experiments after the retrofit of a high-pressure PF boiler TP-67 operating on oil shale, to use VC technology.

The retrofit of the boiler to use VC technology has enabled an increase in the boiler maximum continuous output rate up to 320 t/h.

The temperature measurements, which were performed using an infrared thermometer, show that the maximum temperature across the furnace did not exceed 1150 °C (on the left side of the boiler). Slight temperature nonuniformity across the combustion chamber was observed, and the temperature difference between the left and right sides did not exceed 100–150 °C.

The firing the coarse-ground fuel resulted in the changing of the fractional composition of the bottom and fly ash, and more than a two-fold increase in the median ash particles diameter Δ_m was observed. The residue R₈₀₀₀ of bottom ash on the sieve with an aperture of 8000 μm varied within the range of 0.5–4%, depending on which side of the boiler the ash sample was obtained from. When reducing the boiler load to the minimum (50% of rated load, 160 t/h), an increase in the median particle diameter Δ_m of the bottom ash and the first fields ESP fly ash was observed. In contrast, a slight decrease in the median diameter of the fly ash collected from the SH and ECO ducts was also found.

During the tests, the distribution of the amount of ash at different boiler locations was experimentally obtained. The bottom ash stream was found to be approximately 23% of the total ash flow rate. Smaller amounts of total ash were discharged in inertia ash collectors located in the SH and ECO ducts (9% and 13%, respectively). Therefore, the main part of the total ash, approximately 55%, was entrained by the flue gas stream and collected at the ESP.

Analysis of the bottom ash chemical composition has shown the considerable increase in the amounts of unburned carbon and marcasite S_p. At a full boiler load, the extent of carbonate mineral decomposition in the furnace was approximately $k_{CO_2} = 0.84$.

The retrofit of the boiler to use VC technology did not result in the reduction of SO₂ emissions, indicating an even weaker process of binding sulphur oxides in the furnace compared to the PF technology. The SO₂

content normalized to $O_2 = 6\%$ during the experiments at a full boiler load varied within the range of 2715–3344 mg/Nm³, exceeding emissions of SO₂ for the existing PF technology and indicating an even weaker process of binding sulphur oxides in the furnace.

REFERENCES

1. *Rundygin, Y.* Low-Temperature Firing of Oil Shale. – Leningrad: Energoizdat, 1987 [in Russian].
2. *Ots, A.* Oil Shale Fuel Combustion. – Tallinn: Eesti Energia AS, 2006, 833 pp.
3. *Ots, A., Prikk, A., Arro, H., Rundygin, Y., Konovich, M.* An investigation of fly-ash chemical composition in vortical burning of oil-shale // Transactions of Tallinn Polytechnical Institute. 1977. Series A, No. 416. P. 91–100 [in Russian].
4. *Ots, A., Prikk, A., Arro, H., Rundygin, Y., Konovich, M.* An investigation of oil-shale mineral matter conversion in vortical burning // Transactions of Tallinn Polytechnical Institute. 1977. Series A, No. 416. P. 79–84 [in Russian].
5. *Ots, A., Prikk, A., Arro, H., Rundygin, Y., Konovich, M.* Fly-ash grain composition in vortical burning of oil-shale // Transactions of Tallinn Polytechnical Institute. 1977. Series A, No. 416. P. 85–90 [in Russian].
6. *Ots, A., Prikk, A., Arro, H., Rundygin, Y., Konovich, M., Schuchkin, I.* The nature of ash deposits on the tubes of convective super-heater in vortical burning of oil-shale // Transactions of Tallinn Polytechnical Institute. 1977. Series A, No. 416. P. 109–116 [in Russian].
7. *Pomerantsev, V., Rundygin, Y., Konovich, M., Lysakov, I., Marjamchik, M., Ots, A., Arro, H., Prikk, A.* Study and improvement of low-temperature vortex firing of oil shale in medium-pressure boilers // Transactions of Tallinn Polytechnical Institute. 1977. Series A, No. 416. P. 65–78 [in Russian].
8. *Prikk, A., Ingermann, K., Touart, R., Rundygin, Y.* Wastage of screen-super heater tubes in the low-temperature vortical furnace by water soot-blowing // Transactions of Tallinn Polytechnical Institute. 1980. Series A, No. 483. P. 99–107 [in Russian].
9. *Prikk, A., Shchuchkin, I.* Ash wearing of water-economizer tubes of boiler BKZ-75-39-F with vortex furnace arrangement // Transactions of Tallinn Polytechnical Institute. 1981. Series A, No. 502. P. 19–28 [in Russian].
10. *Ots, A., Prikk, A., Arro, H., Rundygin, Y., Konovich, M.* On the nature of ash deposits on furnace platens in vortex firing of oil shale // Transactions of Tallinn Polytechnical Institute. 1977. series A, No. 416. P. 101–108 [in Russian].
11. *Pihu, T., Arro, H., Prikk, A., Neshumayev, D., Loosaar, J., Parve, T., Konist, A., Rootamm, R., Nuutre, M., Aluvee, R.* Boiler No. 26 thermal test at Balti Power Plant. – Research report of TUT, 2010. 80 pp [in Estonian].

Received May 18, 2011

PAPER IV

EMISSION OF FINE PARTICULATES FROM OIL SHALE FIRED LARGE BOILERS

T. PARVE*, J. LOOSAAR, M. MAHHOV, A. KONIST

Department of Thermal Engineering, Tallinn University of Technology
116 Kopli St., Tallinn 11712, Estonia

Emissions of fine particulates of grade PM_{2.5} and PM₁₀ from different oil shale (OS) power plant (PP) boilers were studied. Pulverized (PF) and circulating fluidized-bed (CFB) boilers burning oil shale, biomass and retort gas were investigated. Particle emissions from OS boilers were found to be very fine. Over 90% of emitted particulate matter was in the size range of PM₁₀ and 40-60% under the size of 2.5 μm. Distribution of fine particles by size was found to be depending on OS firing mode (PF or CFB). At CFB firing mode the share of the finest fraction PM_{2.5} was higher than that at PF firing mode. The distribution varied at the same type of different PF boilers, depending on the efficiency of boiler flue gas cleaning system and value of total suspended particulates' emission (TSP).

Introduction

According to different studies [1] fine particulates (PM_{2.5} and PM₁₀) in the ambient air present serious health risk due to their ability to pass through the human respiratory organs directly to the lungs or even blood. Harmfulness of the fine particulates is caused by different hazard compounds (heavy metals, carcinogenic compounds, etc.) integrated into particles.

Different sources [2] confirm a significant correlation between PM level in the ambient air and mortality.

Another important feature, making fine particles an attractive research subject, is their transboundary effect – the ability to spread on long distances. Beside motor vehicles and local pollution sources, far large-scale combustion utilities (stationary emission sources) are playing important role in the quality of the ambient air.

Despite renovated electrostatic precipitators (ESP), PP combusting Estonian OS are still remarkable emitters of solid particulates (about 6240 tons in 2009/2010) [3], size distribution of these emissions was unknown until lately.

From beginning of 2008 relevant investigations at different OS fired boilers were started, the results of which are now reported.

* Corresponding author: e-mail tparve@sti.ttu.ee

Experimental

Sampling method

The sampling method is based on the principle of impaction. The method is designed for stack measurements at stationary emission sources. The method allows gravimetric determination of concentrations of PM10 and PM2.5 emissions.

PM concentrations were measured with Johnas II cascade impactor. The standards CEN 13284-1 and VDI 2066 were followed [4, 5].

PM10 and PM2.5 mass concentrations are determined by size-selective separation of gas-borne particles basing on different inertia of particles. Flue gas is isokinetically sucked into the cascade impactor. The impactor separates particles above a specific aerodynamic diameter. The aerosol is accelerated in a nozzle and then deflected by 90°. Particles with greater aerodynamic diameters are not able to follow the flow lines of the gas due the mass inertia. They are separated on the collection plate. During sampling the particles are divided into three fractions with aerodynamic diameters greater than 10 µm, between 10 µm and 2.5 µm, and smaller than 2.5 µm.

In-stack sampling was provided isokinetically from the one point of the flue gas duct, usually before the flue gas fan, where flue gas temperatures remain in the limits of 140–200 °C (Fig. 1). The one-point sampling was reasonable because of relatively high TSP concentrations and therefore limited time of sampling. The sampling point location was chosen from the most homogeneous region of the velocity field based on grid measurement

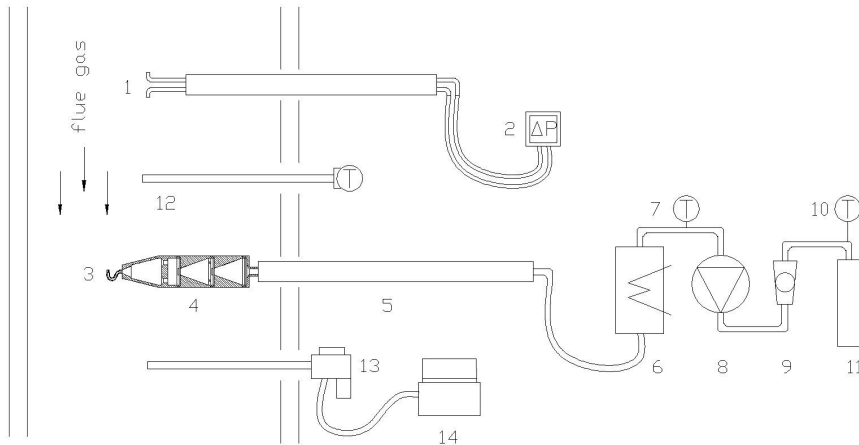


Fig. 1. General measuring setup.

1 – S-type Pitot tube, 2 – differential manometer, 3 – nozzle, 4 – Johnas II cascade impactor, 5 – heated sample probe, 6 – condensator, 7 – thermometer, 8 – pump, 9 – flow meter, 10 – thermometer, 11 – O₂ analyzer, 12 – thermocouple, 13 – gas analysis probe, 14 – FTIR gas analyser.

of flue gas velocities at the cross section (Fig. 2). A suitable nozzle diameter (usually 6–7 mm) of the probe and suction speed were chosen according to the flue gas velocity and isokinetic sampling presumption.

Sampled flue gas amounts (dry) varied from 0.5 to 0.8 Nm³ and sampling times were from 20 to 40 minutes. The blank test, including the whole procedure without real sampling, was carried out for each test series.

Filters

To avoid chemical effects from acidic components of flue gas micro-quartz fibre filters Munktell type MK360 were used for sampling. The grade MK360 filters ability of catching 0.3 µm particles is better than 99.998%.

Preparation of filter sets was carried out at the laboratory. Filters were heated up to 160 °C for the removal of organic impurities at first. Before and after the test the filters together with holders were dried at 105 °C. After drying, filters were stored in desiccator for over 12 hours, until stable weight. Initial and final weighing of the filters was done at micro-analytical balance with the accuracy of 0.1 mg (readability – 0.01 mg).

Test objects and targets

The general target of the measurements was to determine emission factors of fine particulates, since only partial data about OS PM emissions was available [6]. The PM_{2.5} and PM₁₀ emission factors were needed for the emission reports of PP and also for the National Emission Inventory (NEI).

Another interest was to find out how the fuel type, the power unit construction and operation mode affect emission of fine particles. Therefore the tests were carried out at different types of OS-fired boilers with addition of woody biomass and the retort gas from the OS processing factory.

Most of the tests were carried through on PF boilers type TP 101 of Eesti PP. The influence of OS and biomass (BM) co-firing on fine PM emissions was studied at Sillamäe PP at PF boilers type TP 35 [7]. Average furnace temperatures at OS CFB and PF boilers are usually in the range of 800 °C and 1400 °C, respectively.

Results and discussion

Reproducibility test was arranged at one of PF boilers to control the reliability of the sampling method, operator skills and influence of possible fluctuations in boiler run (Fig. 2). Single-point sampling was repeated in similar way from the same point of flue gas duct.

At first velocity field was determined at the sampling cross section and then the sampling point location was chosen (Fig. 3).

The results of the test revealed good concurrence, and standard deviation of the repeated measurements remained below 5% in the case of size

fractions below 10 μm . Because of relatively low concentration of larger particles ($>10 \mu\text{m}$), the variation of results was higher, below 10% in that case.

An overview of the results of all tests at Narva PP boilers is given in Fig. 4.

A quite clear correlation between TSP value and size distribution of particulates can be seen in the diagram. The proportion of larger particles

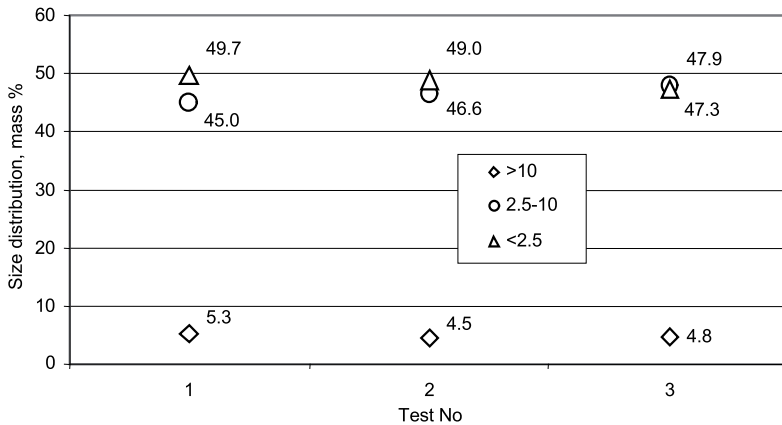


Fig. 2. Reproducibility test at PF boiler TP101 No 7B, ESP D.

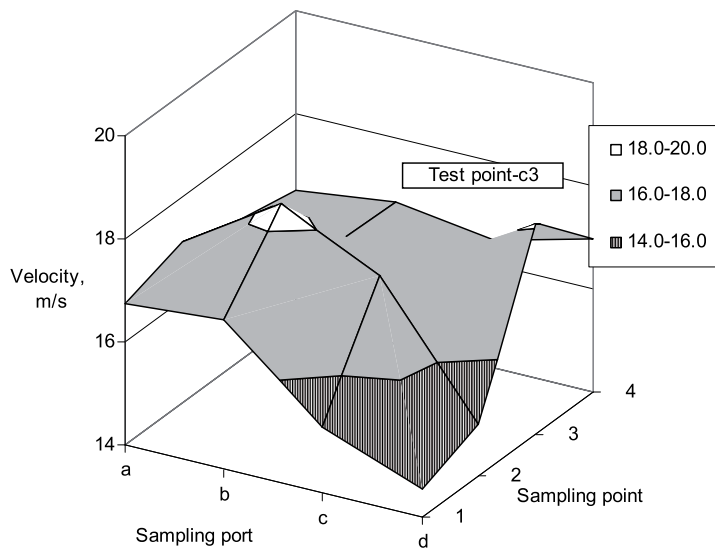


Fig. 3. Flue gas velocity field and the test point location during reproducibility test.

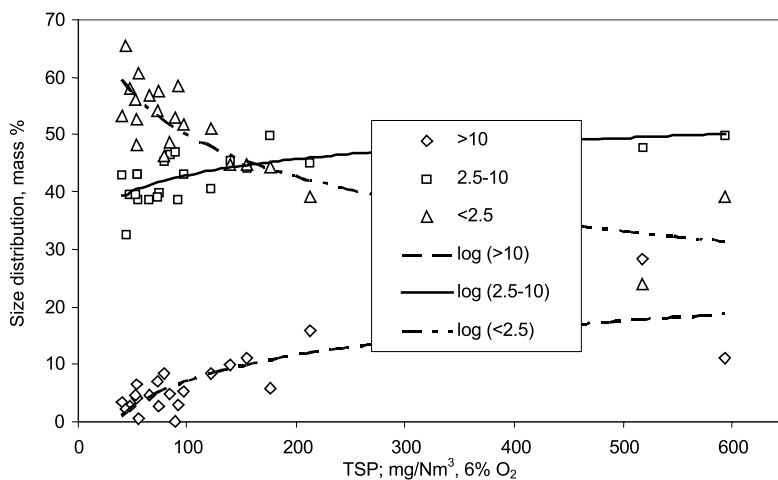


Fig. 4. Size distribution (by mass) of the emission of TSP from Estonian OS fired boilers.

increases concurrently with TSP emission. At usual TSP emission rates ($\sim 200 \text{ mg/Nm}^3$) the mass of fractions PM10 and PM2.5 is 90% and 45%, respectively. At lower TSP concentrations ($<100 \text{ mg/Nm}^3$), the share of PM10 increases exponentially to 95% and that of PM2.5 to 50%.

In addition to the impactor measurements after the ESP collection of solid particles, at the inlet of one CFB boiler ESP was provided. Particle size distribution of the collected sample was analysed using the method of laser diffraction/scattering and sample dry dispersion. As a result data based on comparison of size distribution of fly ash particles at the inlet and outlet of ESP and relative cleaning efficiency of ESP are presented in Table 1 [8].

The trends of particle size distribution in Fig. 4 and PM concentrations at the inlet and outlet of ESP (Table 1) show that electrostatic precipitators most efficiently clean flue gases from larger OS fly ash particles. ESP efficiency at cleaning flue gas flow from particles of the size $>10 \mu\text{m}$ is 63 times higher than from particles $<2.5 \mu\text{m}$.

Tests at two different CFB boilers showed little variations ($<5\%$) in size distribution of the finest part (PM2.5) of TSP emissions. These differences remained in the limits of uncertainty according to repeatability test and can

Tab. 1. Solid particulates at inlet and outlet of ESP of CFB boiler

Sampling location	Unit	Particle size, μm			Total
		<2.5	2.5–10	>10	
ESP inlet	$\text{g/Nm}^3, 6\% \text{ O}_2$	7.8	22.5	29.8	60.1
ESP outlet	$\text{mg/Nm}^3, 6\% \text{ O}_2$	21.3	17.1	1.3	39.7
Efficiency of ESP	%	99.9726	99.9924	99.9996	99.9934

be caused by fluctuations of boilers operation, fuel supply and feeding. The tested CFB boilers are of the same type, but they are located at different power stations.

Comparison of size distribution of TSP emissions from PF (TP101) and CFB boilers reveals that the mass share of fine particles (PM_{2.5}) is about 10% higher in the case of CFB boiler (Fig. 5). Combustion conditions in CFB and PF furnaces, temperature distribution and residence times in gas passes are very different. At PF boilers also ESP-s with lower efficiency are used resulting in more large particulates at the ESP outlet and lower mass share of PM_{2.5} fraction.

Changes in PF boiler load and co-firing of OS with retort gas (share of gas <10% of thermal capacity) have little effect on size distribution of TSP emissions (Figures 6, 7).

TSP emission value itself is lower at co-firing with retort gas, because of lower ash load to the boiler.

In the case of lower boiler loads the velocities of flue gases remain almost the same, and smaller ash amounts in boiler do not have any significant effect on TSP emissions. The PF boilers are equipped with old fashioned fuel/air control system with limited possibilities to regulate combustion (uncontrolled air penetration).

TSP emissions and their size distribution at co-firing of Estonian OS and BM as sawdust was investigated at the boiler TP35 equipped with three-field ESPs of Sillamäe PP.

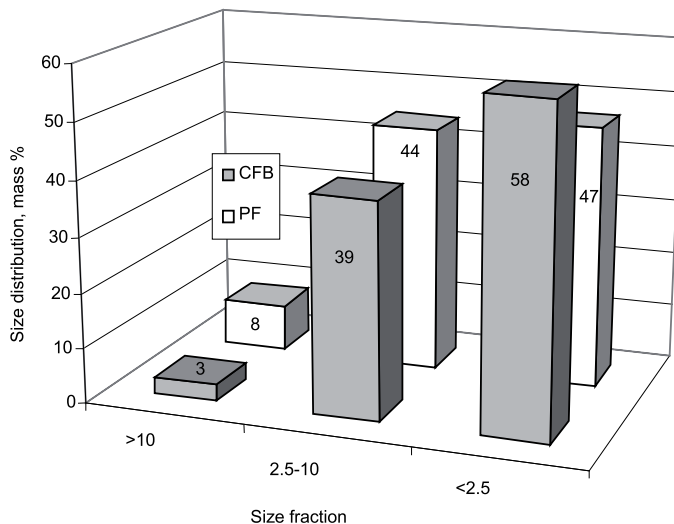


Fig. 5. Size distribution of solid particulates emission - CFB versus PF boilers.

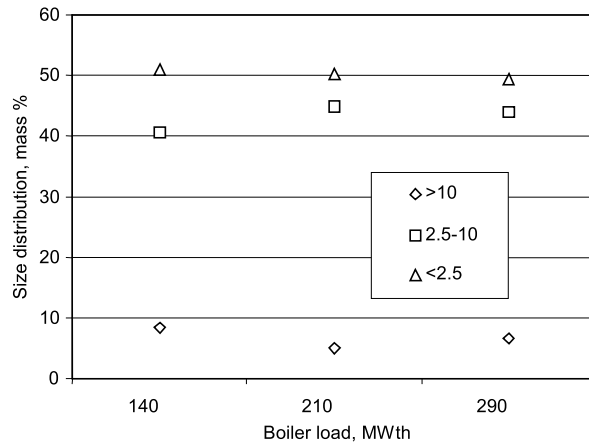


Fig. 6. Particle size distribution of TSP emission at PF boiler different loads.

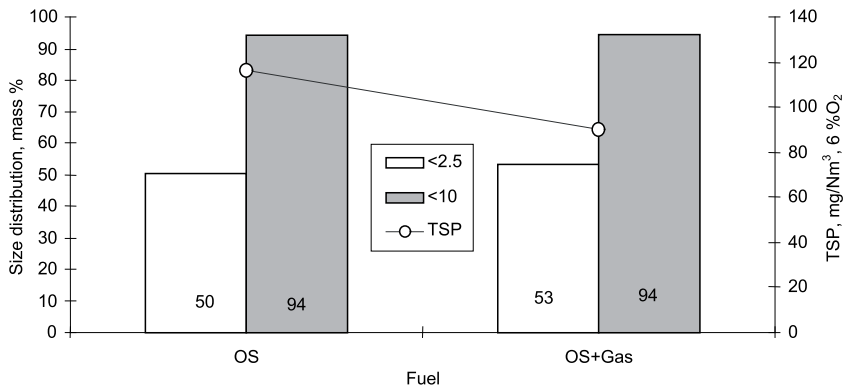


Fig. 7. PM2.5 and PM10 of PF boiler at OS and retort gas co-firing.

Measurements were made at combustion of four different fuels: pure OS; three mixtures of OS with woody BM, with the mass share of BM of 5, 10 and 15 per cent, respectively. From the results of these tests (Fig. 8) follows that the emission of TSP decreases with the increase of the share of BM, the fuel with less ash content. The average ash content of the fuel as received was 43% for OS (815 °C) and 2.8% for BM (550 °C).

Size distribution of the emitted solid particles is quite similar for all cases (Fig. 8). Majority of the particles mass (50–55%) remains between sizes of 2.5 and 10 μm , the share of particles below 2.5 μm is the next in the row (35–40%). The share of the largest particles (>10 μm) is the smallest (10–15%). The trend of the slight fall of the PM2.5 fraction with addition of BM was noticed.

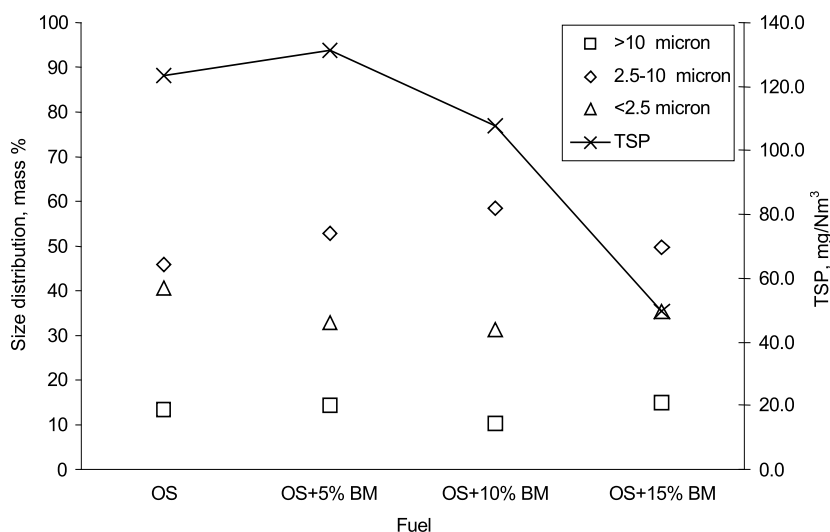


Fig. 8. Emission and size distribution of solid particles at OS and BM co-firing.

As a result a conclusion about similar size distribution of emission of solid particulates from PF boilers TP35 and TP 101 with the same TSP value can be drawn.

Comparison of emissions factors of fine particles of OS and solid fuels used in RAINS model is given in Table 2 [7, 9, 10]. Certainly the factors depend on combustion conditions also in the case of other solid fuels, and presented in Table 2 figures are the averages of very different data. In that sense Table 2 is having only an illustrating purpose.

It follows from Table 2 that PM_{2.5} emissions at OS firing are higher than at coal firing, remaining at the same level with the waste fuel, but are much lower than those for biomass. Emission of PM₁₀ at OS firing is high and at the same level at co-firing with biomass.

Tab. 2. Size distribution of solid particulate emissions at different fuels firing, mass %

Solid fuel	Particle size fraction			
	PM _{2.5}	2.5–10 μm	PM ₁₀	>10 μm
Coal	13	39	52	48
Derived coal	30	40	70	30
Biomass	93	3	96	4
Waste	60	30	90	10
Oil shale (PF)	30–59	40–50	80–95	5–20
Oil shale (CFB)	55–65	33–43	96–98	2–4

Conclusions

- Particle emissions from OS-fired large boilers are relatively fine – the share of PM_{2.5} is between 50–60% and that of PM₁₀ more than 90% in the case of usual TSP values (~200 mg/Nm³).
- Decrease in TSP value involves a relative increase in the finest fraction (PM_{2.5}) and decrease in the coarsest fraction (>10 μm). The share of intermediate fraction (2.5–10 μm) stays almost unchanged.
- ESP cleans flue gas from particles over 10 μm more efficiently than from particles under 2.5 μm.
- Mass percentage of PM₁₀ is the same for PF and CFB boilers but percentage of PM_{2.5} is higher for CFB boilers.
- Co-firing Estonian OS and fuels with lower ash content (BM and retort gas) results in lower TSP emission, but does not change relative shares of PM_{2.5} and PM₁₀.
- PM_{2.5} and PM₁₀ total emissions from large OS boilers can be estimated based on regular TSP emission measurements of separate boilers and relevant mass shares of fractions.

Acknowledgements

Authors express their gratitude to Estonian Environmental Investment Centre (KIK), to Eesti Energia Narva Power Plants Ltd. and Sillamäe Power Plant Ltd. for the financial support and technical assistance of carrying out firing tests.

REFERENCES

1. Health risks of particulate matter from long-range transboundary air pollution. Joint WHO/Convention Task Force on the Health Aspects of Air Pollution.
2. Health aspects of air pollution with particulate matter, ozone and nitrogen dioxide. Report on a WHO working group. Copenhagen, WHO Regional Office for Europe, 2003 (document EUR/03/5042688). Available from: <http://www.euro.who.int/document/e79097.pdf>, accessed 1 October 2005.
3. Environmental Report of Eesti Energia Ltd. Available from: <https://www.energia.ee/en/investor/start>.
4. CEN 13284-1 Stationary source emissions – Determination of low range mass concentration of dust – Part 1: Manual gravimetric method.
5. Guideline VDI 2066 Part 10. Particulate matter measurement – Dust measurement in flowing gases – Measurement of PM₁₀ and PM_{2.5} emissions at stationary sources by impaction method.
6. *Loosaar, J., Parve, T., Konist, A.* Environmental Impact of Estonian Oil Shale CFB Firing // Proceedings of the 20th International Conference on Fluidized Bed Combustion: 20th International Conference on Fluidized Bed Combustion,

- China, Xi'an, May 18–21, 2009 / Yue, G., Zhang, H., Zhao, C., Luo, Z. (eds.). China: Tsinghua University Press/Springer, 2009. P. 422–428.
7. Determination of solid particulates $PM_{2.5}$ and PM_{10} in flue gases from oil shale boilers at Narva Power Plants Ltd. TTU TED Reports, 1998–2010.
 8. *Hotta, A., Parkkonen, R., Hiltunen, M., Arro, H., Loosaar, J., Parve, T., Pihu, T., Prikk, A., Tiikma, T.* Experience of Estonian oil shale combustion based on CFB technology at Narva Power Plants // Oil Shale. 2005. Vol. 22, No. 4S. P. 381–398.
 9. *Sippula, O., Hokkinen, J., Puustinen, H., Yli-Pirilä, P., Jokiniemi, J.* Fine Particle Emissions from Biomass and Heavy Fuel Oil Combustion without Effective Filtration (BIOPOR). – VTT Technical Research Centre of Finland, University of Kuopio, 2007.
 10. Fuel combustion in stationary sources. Emission factors for solid fuels. Available from: <http://www.iiasa.ac.at/~rains/PM/docs/documentation.html> .

Received December 3, 2010

PAPER V

ENVIRONMENTAL IMPACT OF ESTONIAN OIL SHALE CFB FIRING

J. Loosaar, T. Parve, A. Konist

*Department of Thermal Engineering, Tallinn University of Technology,
Kopli 116, 11712, Tallinn, Estonia*

Abstract: Oil shale based power production has been the basement of Estonia's energetical independency and economy for over 60 years. At the same time oil shale power plants emissions still give the biggest share of Estonian stationary source pollution, having significant impact to the environment. Thanks to the introduction of oil shale large scale CFB firing, reduction of the total environmental impact was achieved in last years.

Detailed information about emissions from CFB power units was collected during several research projects in last years. The paper reviews this new data and compares it with former information. Analysis and estimation of changes of charges of all main polluting components at CFB firing compared to former pulverized firing (PF) are presented. It concerns mass balance of trace metals in initial fuel and in formed ash, emissions of PCDD/F, PCB, PAH, PM_{2.5/10}, plus conventional air emissions as NO_x, SO₂, CO₂, CO, HCl, TSP.

It was found out, that the relative share of very small (<2,5 µm) particulates is higher in case of oil shale CFB firing, what could be explained with very efficient milling effect of relatively soft minerals of oil shale at CFB furnace.

In relation of emission studies also mass distribution of CFB boiler ash between different separation points along the flue gas duct (ash mass balance) was determined and analyses of sampled ashes were provided.

This information is important from the point of view of better understanding of thermochemical processes and emission formation in CFB boiler, wider reuse of the ashes of CFB unit.

Keywords: oil shale, CFB, emission, ash, PM_{2.5}

INTRODUCTION

After the start up of new CFB boilers different tests and measurements were carried out at different oil shale fired boilers during last two years. At Narva power plants two types of boilers were tested – pulverized fired (PF) TP 101 and Foster Wheeler 215 MWe CFB boilers. Technical specifications and descriptions of these boilers can be found in Ots (2006) and Hotta et al. (2005).

Most of tests were provided only at CFB boilers, since there was a lack of information about these boilers emissions. Beside the measurement of ordinary air emissions with FTIR spectrometer (SO₂, NO_x, N₂O etc.) samples for the determination PAH, PCDD/F, trace metals were collected following respective standards - CEN 1948:1999, parts 1-3; CEN 14385:2004. Quantitative determinations of PCDD/PCDF, PCB, PAH and HM were provided at laboratory of Ecochem a.s. in Prague by using ICP-MS, ICP-OES, HRGC/HRMS and AAS.

Fine particulates emissions (PM_{2.5/10}) emissions were measured at both type of boilers, because no former data about these emissions from oil shale fired boilers exist. At the same time high health risks related to fine particulates in air are well known and more strict demands on control and reduction of this emissions are introduced nowadays. PM_{2.5/10} emissions were determined with Johnas II type cascade impactor system from Paul Gothe GmbH. At sampling standards CEN 13284-1 and VDI 2066 were followed. Sampling was provided to the circular 50 mm quartz fibre filters type MK 360 of Munktell (catching efficiency of 99.998 % at cutsize of 0.3 µm). The sampling was provided from one point of the flue gas cross section, which was choosed based on flue gas velocity field determination beforehand for the whole cross section.

For the verification of total solid particles (TSP) concentration measured with cascade impactor from one point, parallel measurements of TSP from the 16 points of the whole cross section were provided.

RESULTS

Ash balance

Ash content of Estonian oil shale is very high (~ 50 %). During oil shale combustion ash is removed from several (8) ports along the gas duct. For the material balance of ash and its components ash flows from these ports were measured and respective ash samples were analysed for the components under interest.

In the CFB boiler the most of ash (~50 %) is removed by the I field of ESP. The share of the bottom ash is the next in the order, forming 37.4 % and 29.3 % of the total ash amount in firing conventional (8.5 MJ/kg) and

enriched (11.5 MJ/kg) oil shale fuels respectively (Fig. 1)



Fig.1 Relative distribution of CFB boiler ash flow, mass percents.

(a) Conventional oil shale fuel; (b) Enriched oil shale fuel

Trace metals emission and distribution

During tests and samplings, directed for the determination of specific pollutants, on-line monitoring of flue gases main components and boiler (power unit) basic operation parameters for background information was carefully provided. Results of monitoring of traditional gaseous pollutants at CFB boiler for CO, N₂O, NO, NO_x, SO₂, HCl, CO₂, TSP (total solid particles) remain in the same range as detected already during previous tests and published in (Hotta A. et al., 2005).

Determination of trace elements in the flue gases of CFB unit gave expected result. Comparing with former similar tests at PF units (Aunela L. et al., 1995, 1998; Pets L. et al., 1995), the emissions were much lower (Table 1). First of all it is explained with the effect of much more efficient ESP-s installed at CFB units, which decreased trace element release with solid particles for about two orders. Because of similar temperature distribution at the tail of the CFB boiler emission of trace elements in gaseous phase remain at the same level as in case of PF.

Much lower (over 10 times) result of Hg content in flue gases determined in case of CFB boiler was unexpected. At flue gas temperature (~160°C) most of Hg should be in gaseous phase and the results in case of CFB and PF should be comparable. Because of very low concentrations the measurement error can be the reason of this discrepancy.

Elements relative enrichment factors (by (Meij R, 1994) calculated on the basis of new data are also different from the former results (Aunela-Tapola L. et al., 1998), which could be explained with changes in fly ash size distribution. As usual, enrichment is taking place towards finer ashes. Enrichment factor is highest for the Cd as it was also for PF ashes Oil shale power plants are firing about 13 million tons of oil shale per year. As a result 5-6 million tons of ash is formed, which is mostly (> 90 %) landfilled at ash fields.

Table 1 Trace metals emission and distribution at oil shale CFB firing

Element	Dry flue gas, μg/m ³ O ₂ =6 %	Emission factor, mg/GJ	Relative enrichment factor of TSP	
			versus total ash of CFB	versus oil shale at PF
Al	1675	639	1.4	0.2
As	3.7	1.4	2.0	0.4
Ba	11.2	4.3	1.9	0.4
Cd	1.4	0.5	37.7	5.7
Co	1.4	0.5	0.9	0.6
Cr	5.5	2.1	1.6	1.2
Cu	11.2	4.3	2.4	1.3
Hg	0.2	0.07	n.m.	0.02
Mn	13.9	5.3	0.5	0.3
Mo	0.5	0.2	0.02	0.01
Ni	2.9	1.1	11.3	1.2
Pb	3.8	1.4	0.9	0.5
Se	<1,7	0.6	9.4	0.9

Continued

Element	Dry flue gas, $\mu\text{g}/\text{m}^3$ $\text{O}_2=6\%$	Emission factor, mg/GJ	Relative enrichment factor of TSP	
			versus total ash of CFB	versus oil shale at PF
Sn	<3,5	1.3	1.3	n.m.
Sr	17.4	6.6	1.1	0.1
Ta	<1,4	0.5	15.1	n.m.
Ti	51.1	19.5	4.0	0.8
Tl	<1,3	0.5	4.3	2.1
U	1.2	0.5	0.8	0.3
V	4.1	1.5	13.7	0.6
Zn	27.6	10.5	1.7	0.3
Zr	1.9	0.7	1.8	n.m.

Fortunately trace metal concentrations in landfilled ash are in average at the same level of their content in the ground.

From that point of view oil shale ash utilization e.g. in agriculture for the acidic soil neutralization should not do any harm. On the contrary, trace metals leaching by highly alkaline water, circulating in closed ash removal system and at ash fields, is potential hazard to the surrounding environment because of unbalanced water evaporation and pre-cipitation at Estonian climate conditions.

During last years significant effort has been made to minimize the water amount in ash removal system to minimize the risk of release of ash removal system water to the nature.

Table 2 Trace metals in landfilled total ash of CFB unit

Component	Content mg/kg	Component	Content mg/kg	Component	Content mg/kg
Al	19000	Mn	460	Ta	<0,5
As	7.4	Mo	4.5	Ti	180
Ba	73	Ni	3.0	Tl	0.4
Cd	0.1	Pb	33	U	2.3
Co	4.2	Se	<1,0	V	2.9
Cr	25	Sn	1.5	Zn	31
Cu	8.0	Sr	190	Zr	7.5

The balance of nine trace metals (regularly reported components) in fired fuel and in collected from the boiler gas passes ashes, calculated to the fuel dry matter, is presented on Figure 2.

Difference of the heights of column pairs reflects the error made on ash flow measurements and the sampled fuel or ash analyses of the certain trace element. In case of Hg the difference can be explained by the share of gas phase emission.

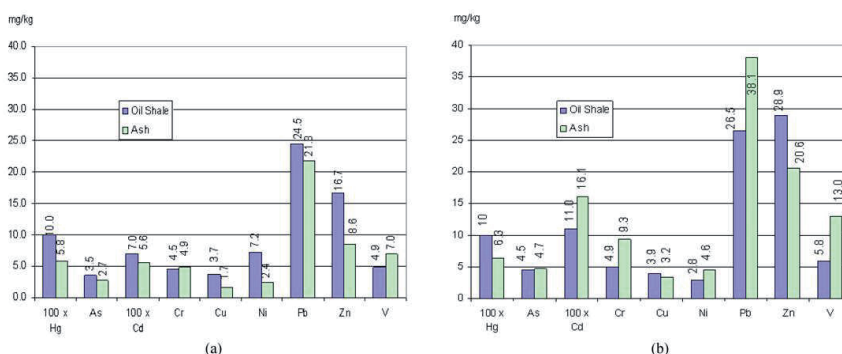


Fig.2 Trace metals balance – inserted fuel versus collected ash in mg to kg of fuel dry matter
(a) Conventional oil shale fuel; (b) Enriched oil shale fuel

Particulate matter PM 2,5/10 emissions

Impactor measurements at several PF boilers and at CFB unit (two boilers) were provided to find out emissions of fine particles to air and get more information about emitted solid particles size distribution. The information is needed for the purpose of emission inventory and for planning measures of reduction of fine particles emissions.

In all cases the main part of the collected samples (>80 %) consisted from fine particles below 10 μm (Fig.3). The relative content of PM₁₀ was higher in case of CFB boiler. Also the share of very fine particles with the size below 2.5 μm (PM_{2.5}) was higher in CFB boiler emissions. This result can be explained at first with different construction of ESP at CFB (4 fields) and PF (3 fields) units, but can be also the result of very efficient milling effect of CFB furnace.

At this point also other factors following from oil shale firing mode (PF or CFB) and probably resulting to ESP efficiency should be mentioned (Hotta, A. et.al.,2005):

- Different ash load at the inlet of ESP – at PF about 1,5 times higher than at CFB;
- Very different shape of fly ash particles, especially fine ones (Fig. 3);
- Very different flue gas composition – in case of PF SO₂ about 1000 and NO_x about 1.5 times higher.

TSP absolute emissions from CFB and PF boilers differ several times, depending on ESP construction, condition and operating parameters. TSP concentrations at CFB unit are mainly below 50 mg/Nm³. In case of PF units variation of TSP values is much higher, remaining in the range of 100 – 450 mg/Nm³.

From the comparison of the results of tests with varying operating parameters and efficiency of ESP next conclusions can be made.

Higher TSP concentrations at PF boilers flue gases correspond to higher shares of particulates with size over 10 μm . E.g. at concentration 450 mg/Nm³ the share of particulates >10 μm is about 30 % and PM_{2.5} decreases to 22 %. It means, that the share of PM₁₀ is remaining almost the same as it is in lower TSP concentrations. Described behaviour of changes in particle size distribution of emitted solid particles proves, that ESP is more efficient in catching particles with size over 10 μm (Table 3).

It is interesting to mention, that the relative share of particles with size between 2.5 and 10 μm remains approximately to the level of 50 % in all tests, not depending on factors mentioned before.

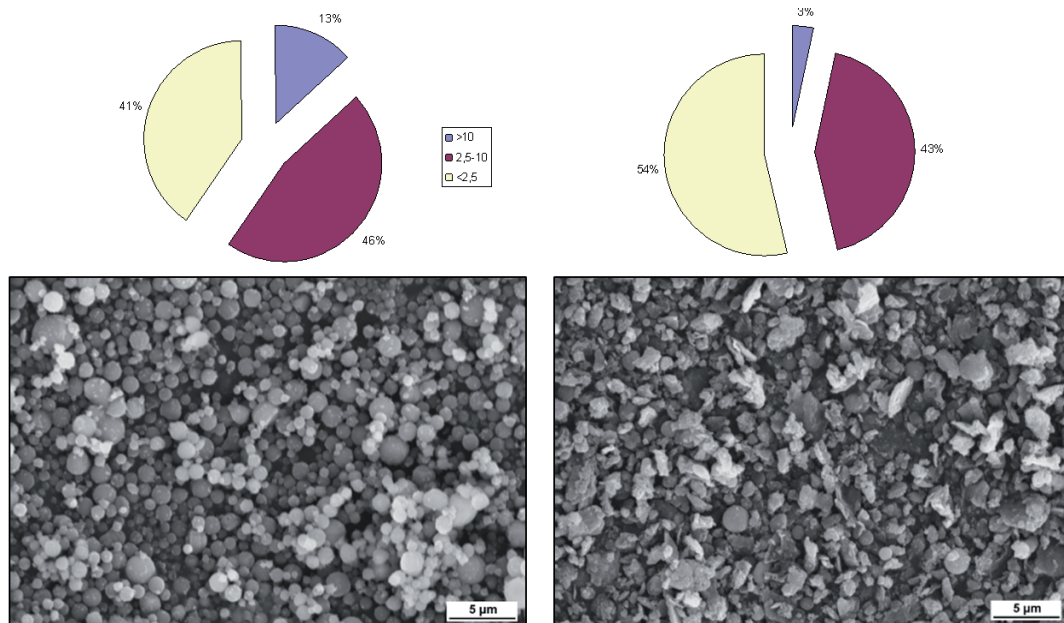


Fig.3 Size(μm) distribution(in mass per cents) and the view of emitted to air solid particles (PM_{2,5}) from oil shale boilers
PF –pulverized firing ; CFB – circulated fluidized bed firing

Significant influence of oil shale firing mode to the shape of fine ash particles can be easily noticed from the SEM pictures of PM_{2.5} fractions at oil shale PF and CFB combustion (Figure 3). The ash particles from PF (> 1400 °C) are overburnt and nicely round. Thanks to the much lower furnace temperatures of CFB boiler (<850 °C) ash particles are having irregular shape.

Table 3 Particles distribution in fly ash of oil shale fired CFB boiler before and after ESP

Sampling location	Unit	Particle size			Total
		<2.5	2.5 - 10	> 10	
ESP inlet	g/Nm ³ , 6 % O ₂	7.77	22.45	29.76	59.9
ESP inlet	%	13.0	37.5	49.7	100.0
ESP outlet	mg/Nm ³ 6 % O ₂	21.3	17.1	1.3	39.7
ESP outlet	%	53.5	43.1	3.4	100
Efficiency of ESP	%	99.9726	99.9924	99.9996	99.9934

PAH and dioxines

Priority PAH (EPA-16) contents at CFB unit flue gases (Table 4) were much lower than at oil shale PF boilers, which is probably the result of much higher residence time of fuel particles and combustion products at high temperature zone. E.g. at CFB benzo(a)pyrene content remain below 11 ng/Nm³ (6 % O₂) comparing with concentrations 32-89 ng/Nm³ measured at PF boilers (Loosaar et al. 1982, Aunela L. et al., 1995). Similar was the result in case of PAH concentrations at landfilled total ash (Table 4).

Table 4 PAH in flue gases and in total ash of CFB boiler

	Flue gas ng/Nm ³	Total ash mg/kg
Naphtalene	1784	0.3
Acenaphtylene	<1487	<0,25
Acenaphtene	<60	0.046
Fluorene	<23	0.084
Phenanthrene	<283	0.23
Anthracene	<23	<0,020
Fluoranthene	<11	<0,080
Pyrene	18	0.077
Benzo(a)anthracene	<11	<0,020
Chrysene	<11	<0,037
Benzo(b)fluoranthene	<11	<0,020
Benzo(k)fluoranthene	<11	<0,0070
Benzo(a)pyrene	<11	<0,010
Dibenzo(a,h)anthracene	<11	<0,010
Benzo(g,h,i)perylene	<11	<0,017
Indeno(1,2,3-cd)pyrene	<11	<0,034
PAH sum		0.74

When concentration of benzo(a)pyrene in bottom ash of PF boiler was ~230 ng/kg (Loosaar et al. 1982, Aunela L. et al., 1995), then the same number for CFB boiler is <10 ng/kg.

The same conclusion about lower PAH concentrations at oil shale CFB firing comparing with traditional PF, only based on investigations of ESP ashes, is drawn by other researchers (Kirso U. et al., 2005).

Determination of dioxins and furans in emitted by CFB boiler flue gases gave very positive and similar to former results on PF boilers of oil shale (table 5). Measured concentrations were very low and the estimated maximum hazard equivalent of these emissions (I-TEQ 1.472 pg/Nm³ at 6 % O₂) was almost 70 times lower than the emission limit to the waste incineration plants - 0.1 ng/Nm³ at 6 % O₂ (DIRECTIVE 2000/76/EC). Very low concentrations of PCDD/F were also found in the landfilled summary ash.

Table 5 PCDD/F and PCB from oil shale combustion at Narva PP

Parameter	Unit	CFB boiler	PF boiler (Schleicher et al.,2005)
<i>Total ash</i>			
I-TEQ for PCDD/F lowerbound	µg/ton of oil shale	0.000	
I-TEQ for PCDD/F upperbound *	µg/ton of oil shale	8.381	0.0 - 0.49
Landfilled PCDD/F in 2006, max possible	g	12.0	1.6
I-TEQ for PCB lowerbound	µg/ton of oil shale	0.774	
I-TEQ for PCB upperbound	µg/ton of oil shale	6.416	
Landfilled PCB in 2006, max possible	g	9.2	
<i>Flue gas</i>			
I-TEQ for PCDD/F lowerbound	pg/Nm ³ (6 % O ₂)	0.699	
I-TEQ for PCDD/F upperbound	pg/Nm ³ (6 % O ₂)	1.472	3.144 -5.878
Air emissions of PCDD/F in 2006, max possible	g	0.015	0.139
I-TEQ for PCB lowerbound	pg/Nm ³ (6 % O ₂)	0.280	
I-TEQ for PCB upperbound	pg/Nm ³ (6 % O ₂)	0.360	
Air emissions of PCB in 2006, max possible	g	0.004	

Lowerbound and upperbound are levels defined in Directive 2002/69/EC and 2002/70/EC

* calculated based on detection limit values - all contents remain below detection limits (in average - 3 ng/kg)

CONCLUSIONS

With introduction of CFB firing at Estonian oil shale power plants environmental impact of oil shale power production decreased significantly, considering not only conventional air pollutants, but also trace metals, PAH and dioxins/furans.

Toxic compounds low content is not limiting possible utilization of CFB ash in agriculture and industry.

Relative enrichment of trace metals towards smaller ash fractions (flying ash versus landfilled total ash) takes place like it also was found out in former studies.

PAH concentrations in the flue gas of CFB boiler are at least several times lower than in PF boilers. Benzo(a)pyrene content remain below 11 ng/Nm³ (6 % O₂) at CFB firing. PCDD/F and PCB air emissions of oil shale firing CFB boilers are very low and remain below 20 mg per year.

PM₁₀ relative content in emissions of oil shale boilers (PF and CFB) is significant, forming over 80 % of TSP. PM_{2.5} share from TSP is higher in case of CFB boiler exceeding 50 %. Absolute values are lower for the CFB boilers.

The share of solid particles with size over 10 µm tends to increase in correlation with TSP content. It proves that ESP is more efficient in catching larger particles.

ACKNOWLEDGEMENTS

The authors are grateful for financial support and co-operation of this work by Narva Power Plants Ltd. and Estonian Environmental Research Centre.

REFERENCES

- Aunela, L., Häsänen, E., Kinnunen V., Larjava K., Mehtonen A., Salmikangas T., Leskela J., Loosaar J.: Emissions from Estonian oil shale power plants, *Oil Shale*, V 12, No 2, 1995, pp. 165-178.
- Aunela-Tapola, L. et al.: Trace metal emissions from Estonian oil shale fired power plant, *Fuel Processing Technology*, No 57, 1998, pp. 1-24.
- Loosaar, J. et al.: Release of toxic and carcinogenic compounds during the burning of Estonian oil shale in industrial boilers (in Russian), *Transactions of Tallinn Polytechnic Institute*, No 522, 1982, pp. 59-71.
- Hotta, A., Parkkonen, R., Hiltunen, M., Arro, H., Loosaar, J., Parve, T., Pihu, T., Prik, A., Tiikma, T.: Experience of Estonian oil shale combustion based on CFB technology at Narva Power Plants, *Oil Shale*, V 22, No 4S, 2005, pp. 369-381.
- Kirso, U., Laja, M., Urb, G.: Polycyclic aromatic hydrocarbons (PAH) in ash fractions of oil shale combustion: fluidized bed versus pulverized firing, *Oil Shale*, V 22, No 4S, 2005, pp. 537-547.
- Schleicher, O., Roots, O., Jensen, A. A., Hermann, A., Tordik, A.: Dioxin emission from two oil shale fired power plants in Estonia, *Oil Shale*, V 22, No 4S, 2005, pp. 563-571.

- Pets, L., Vaganov, P., Rongsheng, Z.: A comparative study of remobilization of trace elements during combustion of oil shale and coal at power plants, *Oil Shale*, V 12, No 2, 1995, pp. 129-145.
- Ots, A: Oil shale fuel combustion, Eesti Energia AS, Tallinn, 2006, pp. 61-64.
- Meij, R.: Trace element behavior in coal-fired power plants, *Fuel Processing Technology*, No 39, 1994, pp. 199-217.
- DIRECTIVE 2000/76/EC OF THE EUROPEAN PARLIAMENT AND OF THE COUNCIL, of 4 December 2000 on the incineration of waste

PAPER VI

COMPARISON OF ASH FROM PF AND CFB BOILERS AND BEHAVIOUR OF ASH IN ASH FIELDS

H. Arro, T. Pihu, A. Prikk, R. Rootamm, A. Konist

*Department of Thermal Engineering, Tallinn University of Technology,
116 Kopli St., 11712 Tallinn, Estonia*

Abstract: Over 90% of electricity produced in Estonia is made by power plants firing local oil shale and 25% of the boilers are of the circulating fluidised bed (CFB) variety. In 2007 approximately 6.5 million tons of ash was acquired as a byproduct of using oil shale for energy production. Approximately 1.5 million tons of that was ash from CFB boilers. Such ash is deposited in ash fields by means of hydro ash removal.

Ash field material properties have undergone changes as a result of CFB ash deposition – the ash field surface is not stabilising, the ash is not becoming petrified and is unsuitable for building dams needed for the hydro technology application.

The analytical research was dedicated to determining the reasons for this different ash field behaviour of ash from CFB and pulverised firing (PF) boilers based on changes of ash properties. Comparative CFB and PF ash studies were conducted: chemical analysis, surveys with X-ray diffractometers (XRD) and scanning electron microscopes (SEM), study of binding properties. Bottom and electrostatic precipitator ash was scrutinised, with its typical rougher and finer particles, accordingly. Such ash types comprise the predominant current ash deposit content in ash fields. The ash samples were taken from boilers of the Balti Power Plant.

The Estonian oil shale mineral part consists mainly of the following minerals: calcite 44.0%, dolomite 19.5%, quartz 8.7%, orthoclase 10.5%, hydromuscovite 8.6%. These minerals comprise 91.3% of the mineral part and it should be noted that 63.5% of that are minerals in the carbonaceous part and 27.8% – in the terrigenous part. When oil shale is fired, thermal decomposition of these minerals occur into simpler compounds, coupled with volatilisation of some compounds and formation of novel minerals, and there are changes in the mineral phase state as well. The ash binding properties and behaviour in ash fields depend on these changes, the extent of which is determined by the firing temperature in the boiler furnace.

The comparative studies indicate that the introduction of the CFB method of firing has caused several important changes in the mineralogical composition and properties of oil shale ash. The reason behind this is that the CFB boiler furnace firing temperature is approximately 600°C lower than in the PF counterpart, resulting in weaker fuel mineral decomposition and lower novel mineral formation intensity during combustion. The ash solidification tendency is in this instance substantially less than that observed in PF ash. The compressive strength of the electrostatic precipitator ash test samples from CFB boilers was 4.4 N/mm²; from PF boilers – 15.3 N/mm², the corresponding specific surface area: 4 533-9 806 cm²/g and 707-3 966 cm²/g.

The obtained data confirms the need to alter the ash storage technology.

Keywords: estonian oil shale ash, pulverised firing, circulating fluidised bed combustion

INTRODUCTION

The essential change in properties of ash field material while the CFB oil shale ash is stored, caused the demand to analyze the different behavior of stored PF and CFB ashes. The chemistry and mineralogy of CFB coal ashes and the behavior of coal ash-water system while deposited are thoroughly investigated (Anthony et al., 2002; Anthony et al., 2003).

The properties of PF ashes stored at ash fields are earlier investigated (Arro et al., 2002; Kespre, 2004). The change in properties of moistened PF ashes in laboratory conditions are also investigated (Kuusik et al., 2004). The results of XRD analyses show at X-ray spectra the peaks belonging to the portlandite, α -quartz, calcite and ettringite. The ash field material contains also in small extents: several silicates, Ca-aluminates and other minerals.

The short overview about behavior of fuel minerals in combustion process and formation of novel minerals and binding properties of ash is given below (Butt et al., 1967; Boikova, 1974; Budnikov et al., 1971).

Carbonate minerals. The decomposition processes start at temperatures below 800°C and depend on CO₂ partial pressure in flue gas. Formed (CaO, MgO ja FeO) stay in ash free oxides and CO₂ volatilize. Decomposition of dolomite (CaMg(CO₃)₂) occurs in two steps: Mg(CO₃) decompose at lower temperatures and

Ca(CO₃) at higher temperatures. The extent of carbonate decomposition (ECD) k_{CO_2} is 0.97 in PF boilers, and 0.60 in CFB boilers because of lower temperatures in furnace (Arro et al., 2006).

Quartz (SiO₂) does not decompose in furnace processes, but may undergo polymorphic changes in crystal structure – β -quartz changes to the α -quartz at 573°C. SiO₂ mainly appears in oil shale ash in form of α -quartz.

Orthoclase (K₂O·Al₂O₃·6SiO₂) changes to the sanidine at ~900°C, in decomposition process it forms leucite (K₂O·Al₂O₃·4SiO₂), while SiO₂ separates in form of amorphous SiO₂ or cristobalite. The presence of lime accelerates the thermal decomposition of orthoclase.

Micas are presented in oil shale as muscovite. At 120°C, absorbed water and, between 450 and 700°C, crystal water are released. In the temperature range 850 to 1,200°C (depending on the composition of micas), novel crystals are formed. Between 1,000 and 1,300°C, the liquid phase begins. At higher temperatures, corundum (Al₂O₃), mullite (3Al₂O₃·2SiO₂), and glassy substance form.

Novel minerals and binding properties of ash. One of more active oil shale mineral part decomposition component is CaO, which reacts with SiO₂ and other minerals decomposition components.

The binding properties of ash are basically caused by β -2CaO·SiO₂ and CaO, but also Ca, Al, Fe ja SiO₂ classy phase content in ash (~30%). In addition, the non soluble residue of ash in hydrochloric acid contains compounds having no binding properties, but in presence of Ca(OH)₂ and water behave like binding material.

The hardening process of ash containing free CaO is associated with formation of CaCO₃. The CaO having contact with water (hydration) gives the Ca(OH)₂ and reaction with CO₂ from air gives CaCO₃.

The other binding materials in ash have water binding properties while petrified (hydro binding materials). These materials may petrify having no contact with air, also under the water.

The slackening factor of ash minerals hydration is high content of Ca(OH)₂ and CaSO₄ in water, which is specific to the ash transport water (Kespre, 2004).

The differences in CFB and PF ash properties are investigated earlier (Kuusik et al, 2005). The methods used to determine ash properties were chemical analyses, XRD, SEM and BET method for determination of the specific surface area (SSA).

The ash properties and behavior at ash fields has been changed because of low combustion temperatures in CFB boiler (~600°C lower comparing PF). Formation of novel minerals with binding properties in CFB ash is much lower comparing to PF ash – solidification is low.

Because of lower temperatures compare to PF boilers, presumably the fuel minerals decomposition and novel minerals formation proceeds at lower rate in CFB boilers. Presumably the CFB ash contains less β -2CaO·SiO₂, also CaO in free form and less classy phase. Lower activity of CFB ash might be the main reason for inefficient solidification processes in ash fields.

MATERIALS AND METHODS

The ash samples were taken from boiler ash flows at nominal load: PF boiler – furnace, superheater, economizer, cyclone, ESP fields (I – IV); CFB boiler – bottom ash, FB heat exchanger of ash, superheater, economizer, air preheater, ESP fields (I – IV).

The furnace/bottom- and ESP I field ashes were chosen as main investigation objects, as they represent 80 – 85% of whole ash stored on ash fields and these are also coarse and fine ash fractions. The composition and properties of the rest ashes are between these two ash types mentioned before. The relative amount of these ashes is small and their role is not decisive in ash solidification process on ash field.

Following investigation methods were used: chemical analysis, X-ray diffractometry, scanning electron microscopy, determination of binding properties and specific surface area.

In XRD analysis the following parameters were used: step size 0.04°, time per step 5.0 s, tube current 40mA, tube voltage 40kV, 2 θ 20-40°. In data processing the software package *DIFFRAC plus* was used. In crystal phase identification the software package *Powder Diffraction Database – 2 (PDF-2)* was used.

In furnace/bottom ash XRD and SEM analyses the ash with dimension <500 μ m was used. The larger particles were separated by sieving. It was presumed that the large ash particles behave like filler in ash mortar.

To investigate the binding properties and solidification kinetics of ashes, the cubes with dimensions 40 × 40 × 40mm³ were made from the paste-water mix. The compressive strength of specimens was determined after 7, 14, 21, 28 and 56 days ageing in humid environment.

Ash specimen's bulking (volume stableness) was determined using Le Chatelier cylinders. The expansion of petrified specimens was measured in water and in humid environment up to 28 days.

Specific surface area of ash was determined using Blaine method.

RESULTES AND DISCUSSION

Chemical analysis

The CO₂ content and heating residue was determined in ash samples. As the PF and CFB boiler ashes were investigated earlier (Arro et al., 2005), these results can be used in this investigation to figure out the differences in ash composition from different combustion technologies. The chemical analyses data of bottom- and ESP I field ashes were represented in Table 1.

Table 1 Chemical analyze of CFB- ja PF-ashes, %

Description	Bottom ash		Ash from EP field I	
	PF-boiler	CFB-boiler	PF-boiler	CFB-boiler
Chemical analyse				
SiO ₂	18.90	11.26	22.79	38.58
Fe ₂ O ₃	5.28	3.12	4.11	4.88
Al ₂ O ₃	4.59	4.38	10.45	11.86
CaO	55.35	48.90	39.60	27.98
CaO _v	26.63	13.88	14.75	8.36
MgO	7.77	6.37	4.69	4.53
K ₂ O	1.36	1.15	4.58	4.47
Na ₂ O	0.12	0.10	0.13	0.24
SO ₃ total	2.43	13.88	7.65	4.10
CO ₂	2.70	11.90	1.91	5.28
Calculated extent of carbonates decomposition				
CO ₂ CaO	43.09	38.07	30.83	21.78
CO ₂ MgO	8.20	6.72	4.95	4.78
CO ₂ total	51.29	44.79	35.78	26.56
k _{CO2}	0.95	0.73	0.95	0.80
Distribution of CaO between ash minerals				
CaO _{carb}	3.44	15.15	2.43	6.72
CaO _{sulf}	1.70	9.72	5.36	2.87
CaO _{free}	26.63	13.88	14.75	8.36
∑CaO _{carb+sulf+free}	31.77	38.75	22.54	17.95
CaO _{tm}	23.58	10.15	17.06	10.03

In calculations of extent of carbonates decomposition (k_{CO_2}) proceeded from fact, that in oil shale 99.2% from CaO and 96.7% from MgO are in composition of CaCO₃ and MgCO₃ respectively (Arro et al., 2006). On base of CaO and MgO content in ash it is possible to calculate CO₂ content in initial fuel. The content of Fe₂CO₃ is frivolous (Ots, 2006) and may be not excepted here. To estimate the formation of novel minerals in combustion process the distribution of CaO in ash minerals – CaO_{carb} and CaO_{sulf} are given in Table 1. Adding CaO_{free} (free lime) to them and subtracting acquired sum $\sum CaO_{carb+sulf+free}$ from overall CaO content, the result shows the portion of CaO bonded into the novel minerals – CaO_{tm}.

Comparing the ashes from different combustion technologies, proceeding from factors influenced the ash binding properties, significantly different ECD and CO₂ free lime content in PF and CFB ash samples can be observed. There is also significant difference in CaO content which bound into several novel minerals. The CaO_{tm} content in PF ashes is significantly higher than in CFB ashes. At considerably higher furnace temperatures approximately more than two times of CaO bound into different ash minerals. The novel minerals are mainly with binding properties.

On the basis of chemical analysis the PF ashes are significantly active in binding processes compare to CFB ashes.

X-ray diffractometry (XRD) analysis

To estimate the influence of furnace processes of different combustion technologies to the mineral content of ash, the content of components in crystal phase in ash samples were determined by XRD analyses.

On the basis of X-ray spectra the main minerals in ash samples are: α -quartz (SiO₂), free lime (CaO),

calcite (CaCO_3), anhydrite (CaSO_4) and periclase (MgO). Low intensity peaks in X-ray spectra refer to the content of different Ca-silicates, aluminates and ferrites.

Bottom ash (Fig. 1). The peaks in X-ray spectra of CFB ash are more intensive compare to PF ash. Because of lower furnace temperatures the binding of SiO_2 and CaO into novel minerals proceeded on lower rate than in PF boiler. The binding decreases CaO and SiO_2 content in sample and intensity of peaks. The content of CaSO_4 ja CaCO_3 in CFB ash is higher compare to PF ash.

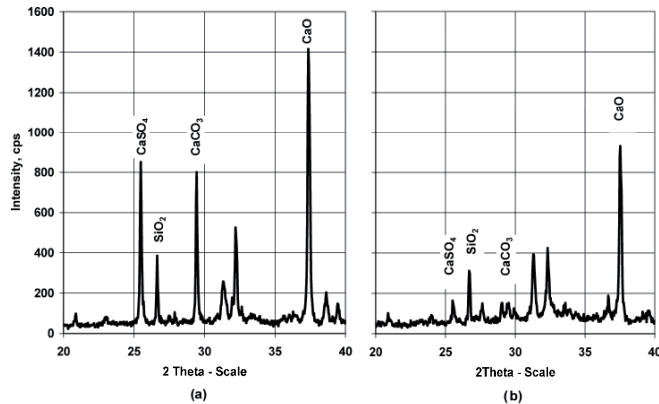


Fig. 1 XRD of bottom/furnace ashes. (a) CFB-boiler, (b) PF-boiler

ESP ash (Fig. 2). The peaks in X-ray spectra show that content of SiO_2 in form of α -quartz in CFB ash is substantially higher than in PF boiler ash. The free lime content in PF boiler ash is significantly higher compare to PF boiler ash.

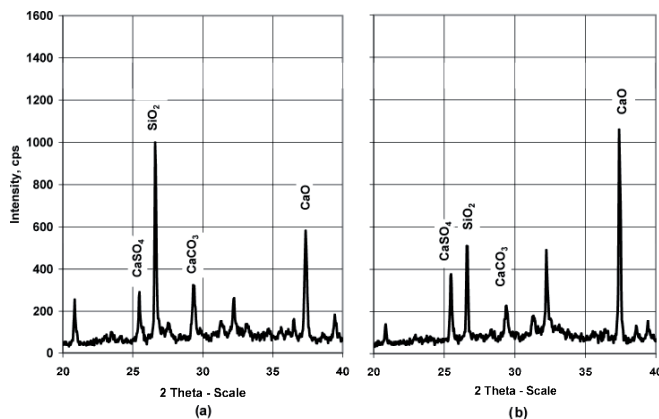


Fig. 2 XRD of ESP first field ashes. (a) CFB-boiler, (b) PF-boiler

Specific surface area of ash (blaine method)

The specific surface area (SSA) of CFB boiler ESP ashes is substantially bigger than PF boiler ashes – $4\,533\text{--}9\,806\text{ cm}^2/\text{g}$ and $707\text{--}3\,966\text{ cm}^2/\text{g}$ correspondingly. The SSA of powder-like materials with same density depends of material fineness and shape as well. Finer material has bigger the SSA. It explains why the ESP last fields' ashes have bigger SSA. The SSA is smaller when the particles are regular shape (spherical).

Ash binding properties

Ash specimen's bulking (volume stableness), compressive strength and solidification kinetics were measured. The specimens were made of ash and water, without adding any filler. This method was chosen due to the interest of ash behavior in ash field. In comparison the binding activity of ash mortar were also determined.

The solidification data show that the specimens made of PF boiler ESP ash and cyclone ash expand in

water and in humid air a lot more than specimens made of CFB boiler ESP ash. The bottom ashes from CFB and PF boilers have no significant difference. During the test of solidification in water almost all the specimens resolved in water except specimens made of CFB boiler ESP ash, which stood the test for 28 days. Their bulking (expansion) did not exceed 3 mm in water and 2 mm in humid air. At the same time specimens made of PF boiler ESP ash and cyclone ash expanded 9 mm and 15 mm.

Data of ash solidification kinetics and compressive strength show that almost all specimens that were put into water resolved. Strength properties were only received from specimens that were petrified in humid air. The obtained data show that CFB and PF boiler bottom ash binding properties are significantly low (compressive strength after 56 days were only 1.9 N/mm² and 1.8 N/mm²). The difference between CFB and PF boiler ESP ash compressive strength is approximately three times (4.4 N/mm² and 15.3 N/mm² accordingly).

Solidification kinetics is described with compressive strength change in time (Fig. 3).

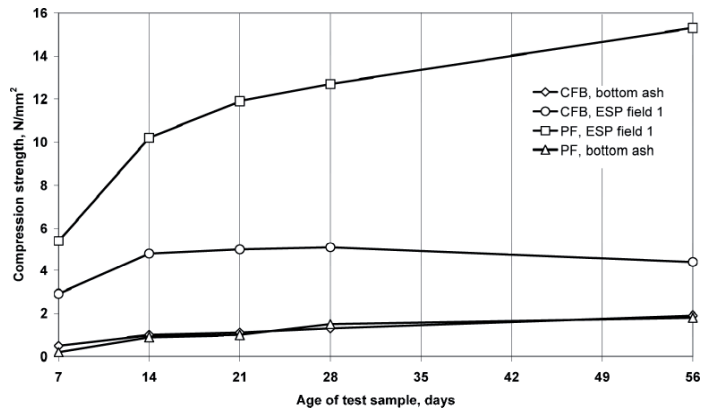


Fig. 3 Solidification kinetics of CFB and PF ash specimens

The CFB boiler ESP ash reaches the maximum compressive strength in 14 days. From there the compressive strength increase is extremely slow. The compressive strength of PF boiler ESP ash does not stabilize even in 56 days and continues increasing.

Better binding properties of PF boiler ESP ash are also seen on 28 day old specimens that are made of ash mortar. Even though the compressive strength difference between CFB and PF boiler ESP ashes is not as big they are for specimens that are made of ash only.

The test results allow to state that the main binder in ash solidification process in ash fields is ESP ash. Moreover, comparing binding properties of PF and CFB boiler ESP ashes, the first one is significantly better. The binding properties of PF and CFB boiler bottom ashes are relatively low and similar.

Scanning electron microscopy of ash

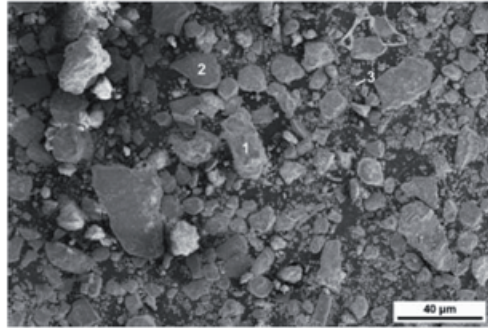
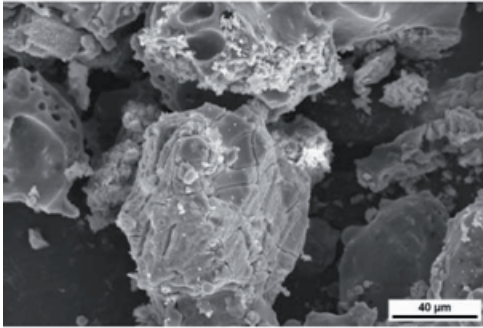
The results of SEM analyses with CFB and PF boiler ashes confirm previous research results with other methods.

Attached four photos in couple indicate expressively that CFB and PF boiler ash particles differ from each other substantially. CFB boiler ash particles have irregular shape; the percentage of melted spherical particles is irrelevant even in finest fractions of the ESP ash. In PF boiler ash the majority of particles have melted to sphere and their relative importance grows when it becomes finer. This confirms that in PF boiler (furnace temperature above 1400°C) the minerals decomposition process and formation of novel minerals takes place in relatively higher rate than in CFB boiler (furnace temperature around 800°C).

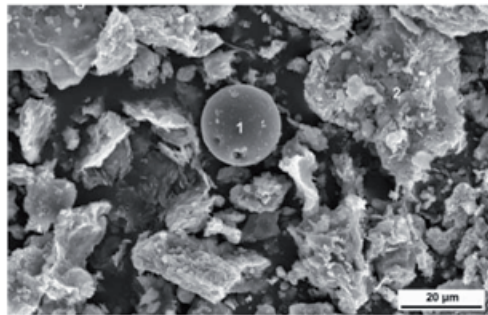
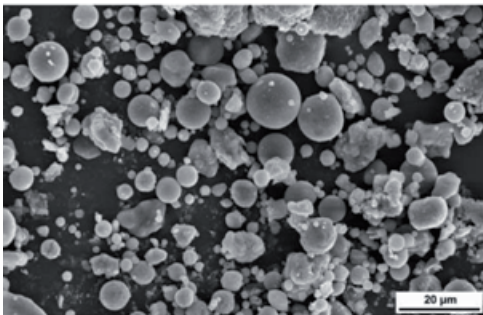
Last couple of photos illustrates the finest ash which has passed the ESP (particle size below 2.5 μm).

PF-BOILER

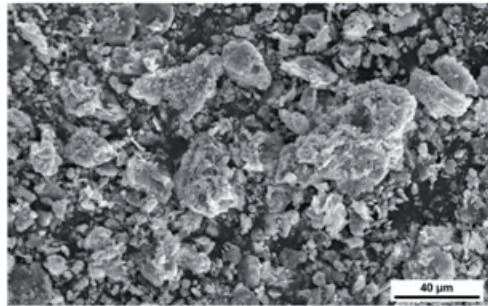
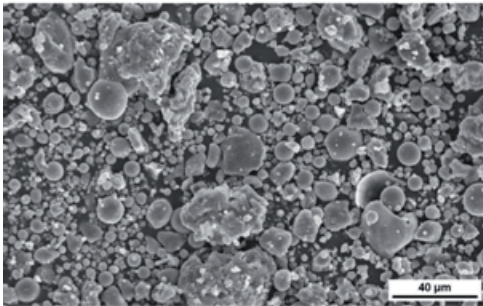
CFB-BOILER



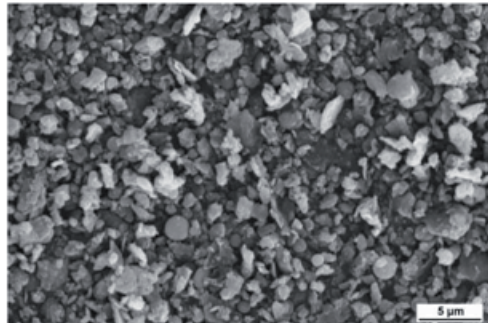
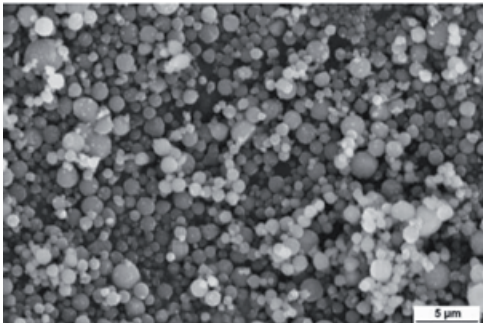
Bottom ash , ×500



ESP field I, ×1000



ESP field II, ×500



Ash sample after ESP, ×3000

CONCLUSIONS

Submitted data about behaviour of oil shale fuel minerals in combustion process and research works that have been done, indicate that CFB burning technology cause a lot of changes in oil shale ash mineralogical composition and properties. Reason for this is significantly lower burning temperature, which therefore cause lower fuel minerals decomposition and novel minerals formation. Ash is formed with the lowest binding properties and the solidification tendency in ash field is significantly lower than it is for PF boiler ash.

Research results raise a number of points, which determine the oil shale ash solidification tendency in ash field:

(1) The main binding material is ESP ash, which properties determine the solidification tendency and strength of ash field material.

(2) According to chemical analysis the free lime content in CFB boiler ESP and bottom ashes is twice lower from PF boiler ash.

(3) The most of CaO in PF ash is bonded into novel minerals than in CFB ash. As the novel minerals have binding properties, then the PF ash is more active in binding processes than CFB ash.

(4) Ash specimen XRD analyses show that PF boiler ESP ash contains more free lime and novel minerals than CFB boiler ESP ash.

(5) The comparison of specific surface area shows deeper thermal treatment of PF ash. The large specific surface area of CFB ESP ash show that the ash particles are not melted in burning process. Melting of ash particles generate classy phase which is active binder.

(6) Whole picture of ash binding properties is given by ash sample solidification kinetics, which shows that PF boiler ESP ash as binder is a lot better than CFB boiler ash and PF boiler bottom ash. PF boiler cyclone ash specimen compressive strength gains almost the strength of CFB boilers ESP ash specimen compressive strength within 56 days.

Above mentioned facts are confirmed by SEM analysis. SEM photos show that PF boiler ash has passed a lot deeper thermal processing than CFB boiler ash.

REFERENCES

- Anthony E.J., Bulewicz E.M., Dudek K., Kozak A. The long term behaviour of CFBC ash–water systems. *Waste Management* 22 (2002) pp. 99–111.
- Anthony E.J., Berry E.E., Blondin J., Bulewicz E.M., Burwell S. Advanced ash management technologies for CFBC ash. *Waste Management* 23 (2003) pp. 503–516.
- Arro, H., Prikk, A., Pihu T. et al. Research of Balti Power Plant's ash fields. Research report, Tallinn University of Technology (TUT), 2002, 84 p. In Estonian.
- Arro, H., Prikk, A., Pihu T. et al. Results of investigations related to CFB boilers and ash fields (2004-2005). Research report, TUT, 2005, 41 p. In Estonian.
- Arro, H., Prikk, A., Pihu T. CO₂ emission from CFB boilers of oil shale power plants. Research report, TUT, 2006, 18 p. In Estonian.
- Arro, H., Prikk, A., Pihu, T. Calculation of CO₂ emission from CFB boilers of oil shale power plants. // *Oil Shale*, 2006, Vol. 23. No. 4 Special, pp. 356-365.
- Boikova, A. Solid solutions of cement minerals. Leningrad, 1974, 100 p. In Russian.
- Budnikov, P., Ginstling, A. Reactions in mixtures of solid materials. Moscow, 1971, 488 p. In Russian.
- Butt, Y., Timashev, V. Portland Cement clinker. Moscow, 1967, 304 p. In Russian.
- Kespre, T. Mineralogy of Eesti Power Plant's oil shale ash plateau sediments. Master's degree thesis. Tartu University, Tartu, 2004, 46 p. In Estonian.
- Kuusik, R., Paat, A., Veskimäe, H., Uibu, M., Transformations in oil shale ash at wet deposition. // *Oil Shale*, 2004, Vol. 21. No. 1, pp. 27-42.
- Kuusik, R., Uibu, M., Kirsimäe, K. Characterization of oil shale ashes formed at industrial-scale CFBC boilers. // *Oil Shale*, 2005, Vol. 22. No. 4 Special, pp. 407-419.
- Ots, A. *Oil Shale Fuel Combustion*. Tallinn, 2006, 833 p.

CURRICULUM VITAE

1. Personal data

Name Alar Konist
Date and place of birth 06.05.1985, Vinni
Citizenship Estonian
Marital status Cohabiting

2. Contact information

Address Ehitajate tee 5, 19086 Tallinn, Estonia
Phone +372 56 480 478
E-mail alar.konist@ttu.ee

3. Education

Educational institution	Graduation year	Education
Tallinn University of Technology	2009	master`s degree
Tallinn University of Technology	2008	bachelor`s degree
Rakvere Secondary School	2004	secondary education

4. Language skills

Language	Level
Estonian	native language C2
English	fluent C1
Russian	average B2
Finnish	basic skills A2

5. Professional employment

Period	Organisation	Position
2009-present	Tallinn University of Technology, Department of Thermal Engineering	research scientist
2006-2009	Tallinn University of Technology, Department of Thermal Engineering	engineer

6. Special courses

Period	Educational or other organisation
2010	Internal quality control management in universities – special course organized by SA Archimedes
2009	Energy Auditing for Buildings – special course organized by Tallinn University of Technology Open University

7. Scientific work

Investigation of boiler heating surfaces fouling at Tallinn Powerplant;

Shale oil and power cogeneration process modeling;

Reduction of CO₂ emission of CFB boiler by enrichment of combustion air with oxygen;

Oil shale power plants operational problems related to thermal engineering and environment protection.

8. Defended theses

Carbon Dioxide binding in ash fields. Master of Science thesis, TUT, Tallinn, 2008;

Usage and composition of biofuels. Bachelor thesis, TUT, Tallinn, 2007.

9. Main areas of scientific work

Natural sciences and engineering, energetic research

10. Other research projects

Subject	Nr of Project	Financing source	Duration
Sustainable utilization of energy resources and process improvement in combustion facilities	SF0140024s07	Estonian Ministry of Education and Research	1.01.2007-31.12.2012
Reduction of CO ₂ emission of CFB boiler by enrichment of combustion air with oxygen	AR12003	National R&D program „Energy Technology Program,“ SA Archimedes	1.01.2012-31.12.2014

ELULOOKIRJELDUS

1. Isikuandmed

Ees- ja perekonnanimi Alar Konist
Sünniaeg ja -koht 06.05.1985, Vinni
Kodakondsus Eesti
Perekonnaseis vabaabielus

2. Kontaktandmed

Address Ehitajate tee 5, 19086 Tallinn, Eesti
Telefon +372 56 480 478
E-posti aadress alar.konist@ttu.ee

3. Hariduskäik

Õppeasutus	Lõpetamise aeg	Haridus
Tallinna Tehnikaülikool	2009	tehnikateaduste magistrikraad
Tallinna Tehnikaülikool	2008	bakalaureusekraad
Rakvere Gümnaasium	2004	keskharidus

4. Keelteoskus

Keel	Tase
Eesti keel	emakeel C2
Inglise keel	kõrgtase C1
Vene keel	kesktase B2
Soome keel	algtase A2

5. Teenistuskäik

Töötamise aeg	Tööandja nimetus	Ametikoht
2009-käesoleva ajani	Tallinna Tehnikaülikool, Soojustehnika instituut	teadur
2006-2009	Tallinna Tehnikaülikool, Soojustehnika instituut	insener

6. Täiendusõpe

Õppimise aeg	Täiendusõppe läbiviija nimetus
2010	Kõrgkooli sisemise kvaliteedikindlustamise protsess – SA Archimedes
2009	Hoonete energeetiline auditeerimine – TTÜ avatud ülikool

7. Teadustegevus

Energiaressursside säästlik kasutamine ja protsesside täiustamine põletusseadmetes;

Katla küttepindade saastumise põhjuste väljaselgitamine ja meetmete kavandamine saastumise vähendamiseks Tallinna Elektri jaamas;

Põlevkiviõli ja elektrienergia koostootmise mudelleerimine;

CO₂ heitme vähendamine põlemisõhu hapnikurikkamaks muutmisega keevkihtkatlas;

Põlevkivielektri jaamade käiduga seotud soojustehniliste ja keskkonnavalaste probleemide lahendamine

8. Kaitstud lõputööd

Süsinikdioksiidi tagasisidumine tuhaväljadel. TM väitekiri, TTÜ, Tallinn, 2008.

Biokütuste koostis ja kasutamine. Bakalaureusetöö, TTÜ, Tallinn, 2007.

9. Teadustöö põhisuunad

Loodusteadused ja tehnika, energeetikaalased uuringud – T140.

10. Teadusprojektid

Teema	Projekti number	Finantsallikas	Kestus
Energiaressursside säästlik kasutamine ja protsesside täiustamine põletusseadmetes	SF0140024s07	HM sihtfinantseerimine	1.01.2007-31.12.2012
CO ₂ heitme vähendamine põlemisõhu hapnikurikkamaks muutmisega keevkihtkatlas	AR12003	RP "Energiatehnoloogia T&A toetamine," SA Archimedes	1.01.2012-31.12.2014

**DISSERTATIONS DEFENDED AT
TALLINN UNIVERSITY OF TECHNOLOGY ON
MECHANICAL ENGINEERING**

1. **Jakob Kübarsepp**. Steel-Bonded Hardmetals. 1992.
2. **Jakub Kõo**. Determination of Residual Stresses in Coatings & Coated Parts. 1994.
3. **Mart Tamre**. Tribocharacteristics of Journal Bearings Unlocated Axis. 1995.
4. **Paul Kallas**. Abrasive Erosion of Powder Materials. 1996.
5. **Jüri Pirso**. Titanium and Chromium Carbide Based Cermets. 1996.
6. **Heinrich Reshetnyak**. Hard Metals Serviceability in Sheet Metal Forming Operations. 1996.
7. **Arvi Kruusing**. Magnetic Microdevices and Their Fabrication methods. 1997.
8. **Roberto Carmona Davila**. Some Contributions to the Quality Control in Motor Car Industry. 1999.
9. **Harri Annuka**. Characterization and Application of TiC-Based Iron Alloys Bonded Cermets. 1999.
10. **Irina Hussainova**. Investigation of Particle-Wall Collision and Erosion Prediction. 1999.
11. **Edi Kulderknup**. Reliability and Uncertainty of Quality Measurement. 2000.
12. **Vitali Podgurski**. Laser Ablation and Thermal Evaporation of Thin Films and Structures. 2001.
13. **Igor Penkov**. Strength Investigation of Threaded Joints Under Static and Dynamic Loading. 2001.
14. **Martin Eerme**. Structural Modelling of Engineering Products and Realisation of Computer-Based Environment for Product Development. 2001.
15. **Toivo Tähemaa**. Assurance of Synergy and Competitive Dependability at Non-Safety-Critical Mechatronics Systems design. 2002.
16. **Jüri Resev**. Virtual Differential as Torque Distribution Control Unit in Automotive Propulsion Systems. 2002.
17. **Toomas Pihl**. Powder Coatings for Abrasive Wear. 2002.
18. **Sergei Letunovitš**. Tribology of Fine-Grained Cermets. 2003.
19. **Tatyana Karaulova**. Development of the Modelling Tool for the Analysis of the Production Process and its Entities for the SME. 2004.
20. **Grigori Nekrassov**. Development of an Intelligent Integrated Environment for Computer. 2004.
21. **Sergei Zimakov**. Novel Wear Resistant WC-Based Thermal Sprayed Coatings. 2004.
22. **Irina Preis**. Fatigue Performance and Mechanical Reliability of Cemented Carbides. 2004.
23. **Medhat Hussainov**. Effect of Solid Particles on Turbulence of Gas in Two-Phase Flows. 2005.

24. **Frid Kaljas**. Synergy-Based Approach to Design of the Interdisciplinary Systems. 2005.
25. **Dmitri Neshumayev**. Experimental and Numerical Investigation of Combined Heat Transfer Enhancement Technique in Gas-Heated Channels. 2005.
26. **Renno Veinthal**. Characterization and Modelling of Erosion Wear of Powder Composite Materials and Coatings. 2005.
27. **Sergei Tisler**. Deposition of Solid Particles from Aerosol Flow in Laminar Flat-Plate Boundary Layer. 2006.
28. **Tauno Otto**. Models for Monitoring of Technological Processes and Production Systems. 2006.
29. **Maksim Antonov**. Assessment of Cermets Performance in Aggressive Media. 2006.
30. **Tatjana Barashkova**. Research of the Effect of Correlation at the Measurement of Alternating Voltage. 2006.
31. **Jaan Kers**. Recycling of Composite Plastics. 2006.
32. **Raivo Sell**. Model Based Mechatronic Systems Modeling Methodology in Conceptual Design Stage. 2007.
33. **Hans Rämmal**. Experimental Methods for Sound Propagation Studies in Automotive Duct Systems. 2007.
34. **Meelis Pohlak**. Rapid Prototyping of Sheet Metal Components with Incremental Sheet Forming Technology. 2007.
35. **Priidu Peetsalu**. Microstructural Aspects of Thermal Sprayed WC-Co Coatings and Ni-Cr Coated Steels. 2007.
36. **Lauri Kollo**. Sinter/HIP Technology of TiC-Based Cermets. 2007.
37. **Andrei Dedov**. Assessment of Metal Condition and Remaining Life of In-service Power Plant Components Operating at High Temperature. 2007.
38. **Fjodor Sergejev**. Investigation of the Fatigue Mechanics Aspects of PM Hardmetals and Cermets. 2007.
39. **Eduard Ševtšenko**. Intelligent Decision Support System for the Network of Collaborative SME-s. 2007.
40. **Rünno Lumiste**. Networks and Innovation in Machinery and Electronics Industry and Enterprises (Estonian Case Studies). 2008.
41. **Kristo Karjust**. Integrated Product Development and Production Technology of Large Composite Plastic Products. 2008.
42. **Mart Saarna**. Fatigue Characteristics of PM Steels. 2008.
43. **Eduard Kimmari**. Exothermically Synthesized B₄C-Al Composites for Dry Sliding. 2008.
44. **Indrek Abiline**. Calibration Methods of Coating Thickness Gauges. 2008.
45. **Tiit Hindreus**. Synergy-Based Approach to Quality Assurance. 2009.
46. **Karl Raba**. Uncertainty Focused Product Improvement Models. 2009.
47. **Riho Tarbe**. Abrasive Impact Wear: Tester, Wear and Grindability Studies. 2009.
48. **Kristjan Juhani**. Reactive Sintered Chromium and Titanium Carbide-Based Cermets. 2009.

49. **Nadežda Dementjeva**. Energy Planning Model Analysis and Their Adaptability for Estonian Energy Sector. 2009.
50. **Igor Krupenski**. Numerical Simulation of Two-Phase Turbulent Flows in Ash Circulating Fluidized Bed. 2010.
51. **Aleksandr Hlebnikov**. The Analysis of Efficiency and Optimization of District Heating Networks in Estonia. 2010.
52. **Andres Petritšenko**. Vibration of Ladder Frames. 2010.
53. **Renee Joost**. Novel Methods for Hardmetal Production and Recycling. 2010.
54. **Andre Gregor**. Hard PVD Coatings for Tooling. 2010.
55. **Tõnu Roosaar**. Wear Performance of WC- and TiC-Based Ceramic-Metallic Composites. 2010.
56. **Alina Sivitski**. Sliding Wear of PVD Hard Coatings: Fatigue and Measurement Aspects. 2010.
57. **Sergei Kramanenko**. Fractal Approach for Multiple Project Management in Manufacturing Enterprises. 2010.
58. **Eduard Latõsov**. Model for the Analysis of Combined Heat and Power Production. 2011.
59. **Jürgen Riim**. Calibration Methods of Coating Thickness Standards. 2011.
60. **Andrei Surzhenkov**. Duplex Treatment of Steel Surface. 2011.
61. **Steffen Dahms**. Diffusion Welding of Different Materials. 2011.
62. **Birthe Matsi**. Research of Innovation Capacity Monitoring Methodology for Engineering Industry. 2011.
63. **Peeter Ross**. Data Sharing and Shared Workflow in Medical Imaging. 2011.
64. **Siim Link**. Reactivity of Woody and Herbaceous Biomass Chars. 2011.
65. **Kristjan Plamus**. The Impact of Oil Shale Calorific Value on CFB Boiler Thermal Efficiency and Environment. 2012.
66. **Aleksei Tšinjan**. Performance of Tool Materials in Blanking. 2012.
67. **Martinš Sarkans**. Synergy Deployment at Early Evaluation of Modularity of the Multi-Agent Production Systems. 2012.
68. **Sven Seiler**. Laboratory as a Service – A Holistic Framework for Remote and Virtual Labs. 2012.
69. **Tarmo Velsker**. Design Optimization of Steel and Glass Structures. 2012.
70. **Madis Tiik**. Access Rights and Organizational Management in Implementation of Estonian Electronic Health Record System. 2012.
71. **Marina Kostina**. Reliability Management of Manufacturing Processes in Machinery Enterprises. 2012.
72. **Robert Hudjakov**. Long-Range Navigation for Unmanned Off-Road Ground Vehicle. 2012.